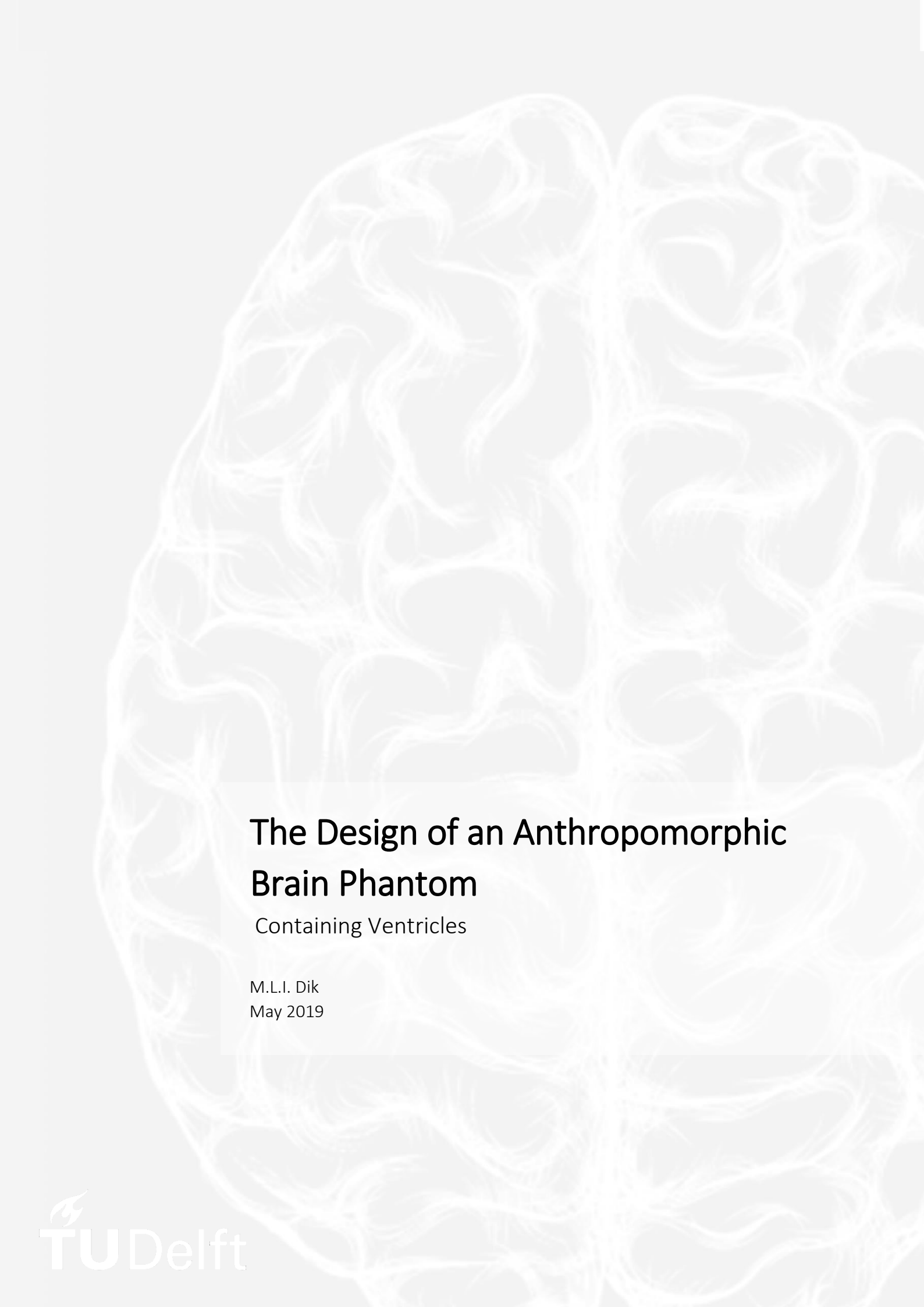

The Design of an Anthropomorphic Brain Phantom

Containing Ventricles

M.L.I. Dik

May 2019

TU Delft

The Design of an Anthropomorphic Brain Phantom

Containing Ventricles

By

M.L.I. Dik

In partial fulfilment of the requirements for the degree of

Master of Science
in Biomedical Engineering

at the Delft University of Technology
to be defended publicly on May 17th 2019.

Supervisor:	Dr. J.J. van den Dobbelsteen	TU Delft
	Prof. Dr B.H.W. Hendriks	Philips
Thesis committee:	Dr. J.J. van den Dobbelsteen	TU Delft
	Prof. Dr B.H.W. Hendriks	Philips
	M. de Vries	TU Delft
	N. Sarkalkan	TU Delft

Delft University of Technology and Philips Healthcare

TU Delft

PREFACE

During the past year, I have been working on my master thesis project concerning the development of a brain phantom containing ventricles. With this master thesis project, I will conclude the master Biomedical Engineering at the TU Delft. The project was performed in collaboration with the research department of Philips Healthcare in Best, the Netherlands. The goal of this project was to develop an anthropomorphic brain phantom that contains the ventricles, the cavities in the brain. The steps taken to achieve this goal are described in this thesis.

This project would not have been possible without the people from both Philips and the TU Delft, who helped me throughout this project. I owe special thanks to Benno Hendriks and Marco Lai from Philips for helping me with my project and providing the opportunity to make use of the facilities from Philips.

From the TU Delft, I owe special thanks to Jan van Frankenhuyzen, who offered me great help and insights during the project. He was always there for me to think about the possibilities and to experiment with the 3D printers.

I would also like to thank my supervisor John van den Dobbelsteen from the TU Delft for the freedom to explore my own creativity and ideas, but was always there for feedback and guidance in the project, to help me back on the right track.

Furthermore, I would like to thank my lab partners who shared this whole journey with me and supported me through ups and downs and providing the occasional distraction from work.

Last but not least I would like to thank my family and friends for their support and motivation not only during my graduation project but also during my time as a student in Delft.

M.L.I. Dik
Delft, May 2019

SUMMARY

Brain, outside the body, will decay quickly, causing ex vivo studies to be difficult. Having a phantom model has a great beneficial value for numerous reasons. Phantoms are, among others, used in research centres, to validate new equipment, to develop biomechanical models or to test new treatment methods. They are representations of organs or tissues made from tissues that mimicking the desired properties of the organ.

This thesis research is performed in collaboration with Philips Healthcare research department. They benefit from having a brain phantom for the development of a new endoscopic tool that incorporates virtual reality images in the view. Existing phantoms are usually expensive and are not meant for destruction by needle interventions or endoscopic interventions, or are a very rough representation of reality. For this study, it was the aim to develop an anthropomorphic brain phantom containing the hollow space of the ventricles of the brain, with the correct mechanical and optical characteristics.

From a digital 3D mesh brain, moulds were made to assess different ways to produce a brain phantom with ventricles. From literature, the tissue mimicking material (TMM) PVA was selected to use for the production of the phantom. After evaluation of the different approaches to fabricate a phantom, it was decided to produce the hollow spaces of the ventricles by using 3D printed soluble PVA, to be removed out of the model after casting. This was done by 3D printing a brain mould in which a 3D printed PVA ventricle could be inserted. A solution of 6% PVA as tissue mimicking material was used.

After the mould and production principle of the model was finalized, the imaging part was assessed. In order for the phantom to be used in CT imaging, barium sulphate was added to the PVA solution as a contrast enhancing material. Two phantoms were made with 1% and 2% barium sulphate. Finally, to assess the shape and the quality of the ventricles in the phantom, the phantom was scanned with a CT scan at Philips Healthcare in Best, the Netherlands. The CT files were evaluated using RadiAnt and 3D slicer to assess the ventricular shape and position. 3D slicer was also used to segment the ventricle shape out of the designed models to compare with the originally developed ventricle structure.

This study functions as a proof of concept for the development of a PVA brain phantom containing ventricles produced with 3D printed soluble PVA. All in all, the overall evaluation of the prototypes have shown to be promising models for the development of a brain phantom using PVA and ‘homemade’ fabrication techniques. The use of 3D printed soluble PVA is a novelty in this field of application. It makes the design easy to develop and easily adjusted to patient-specific cases as personalized models can be made.

CONTENTS

LIST OF FIGURES

LIST OF TABLES

LIST OF ACRONYMS

CNS	central nervous system
CSF	cerebrospinal fluid
CT	computed tomography
DTI	diffusion tensor imaging
DWI	diffusion-weighted imaging
ETV	endoscopic third ventriculostomy
EVD	external ventricular drain
FTC	freeze-thaw-cycle
HU	Hounsfield units
MRI	magnetic resonance imaging
MRS	magnetic resonance spectroscopy
PLA	polylactic acid
PVA	polyvinyl alcohol
PVC	polyvinyl chloride
TBI	traumatic brain injury
VR	virtual reality

1. INTRODUCTION

1.1. RATIONALE

Brain, outside the body, will decay quickly, causing ex vivo studies to be difficult. Having a phantom model has a great beneficial value for numerous reasons. Phantoms are, among others, used in research centres, to validate new equipment, to develop biomechanical models or to test new treatment methods. They are representations of organs or tissues made from tissues that mimic the desired properties of the organ. There is a great variety of tissue-mimicking materials (TMMs) for the desired function of the phantom. Phantoms are also a common way to study the interactions between needles and tissue [1]. Moreover, in a clinical setting, phantoms are widely used for clinical training or surgical planning.

Surgeons require a sufficient amount of training in order to obtain high standards to perform complex tasks. Cadaveric training is often used and is thought to be the golden standard in order to practice on the right technical proficiency, as cadaveric training provides the right details on anatomical structures, proportions, positions and consistencies. However, the use of human specimen often leads to ethical issues, as well as the problem with preservation of the specimen [2]. Concerning soft tissue, sometimes animal models are used, as for some organs, animal models resemble human anatomy, yet these solutions are not without drawbacks and ethical issues [3].

New technical surgical developments are emerging, to assist surgeons in diagnosis and planning, such as realistic and detailed digital 3D images. In virtual reality (VR) techniques researchers aim to find appropriate mathematical models of the mechanical properties of the brain for computer simulations of neurological procedures, which can be used for operation planning systems, and calibration of robotic devices to perform minimally invasive brain surgery. Though there is still a need for surgical training phantoms as these new digital developments lack haptic and tactile realism and as multiple studies have shown that not having satisfactory tactile feedback can have a negative effect on the training progress. If a model does not have the right mechanical properties, the trainees may apply higher force than needed, which could increase the risk of causing damage or traumatic injuries when going into a real surgery [3]–[7].

The human brain is a complex organ with deep fissures and sulci over its surface as well as complex shapes in it's interior such as the with cerebral spinal fluid (CSF) filled ventricles. Currently used phantoms are very expensive and not intended for invasive procedures, or bear only the gross anatomy of the cerebrum and do not include the complex structure of the ventricles [8].

1.2. PROBLEM DEFINITION AND OBJECTIVE

This thesis research is performed in collaboration with Philips Healthcare research department. They benefit from having a good brain phantom for the development of a new endoscopic tool that incorporates virtual reality images in the view. A brain phantom will help test and validate this tool. Next to that, a brain phantom can also be used for medical education of surgeons in training to practice in a zero-risk environment. A brain phantom can also be used for surgical planning in order to optimize the surgical procedure and minimize operation time, morbidity and even mortality. Physical phantoms can also be used for communication before and during surgery between surgeons and OR staff, or facilitate a clear explanation of the procedure to patients and relatives.

Existing phantoms are usually expensive and are not meant for destruction by needle interventions or endoscopic interventions, or are a very rough representation of reality. Based on the current limitations with existing phantom models and previously performed researches regarding the development of brain phantoms and brain tissue-mimicking materials, the aim of this research is:

To develop an anthropomorphic brain phantom containing the ventricles of the brain, with the correct mechanical and optical characteristics.

This research aim is in line with the request initiated by Philips. To assess this research aim, it will be divided into 2 subgoals:

Evaluate different production principles and materials to produce a hollow space of the ventricles in a brain model.

During this research, different production principles for the development of a model with a hollow space, representing the ventricles, will be assessed. For this development, tissue mimicking materials (TMMs) will be selected from literature. Leading to the most suitable phantom material and production method.

Evaluate the models by assessing the X-ray characteristics of the material to validate for X-ray/CT use.

In order to be able to use the phantom for radiology, the imaging characteristics of the phantom should be assessed.

The initial objective of this project is to find a material that mimics brain tissue in a healthy state, with healthy ventricles. The main focus will be the development of the hollow spaces of the ventricles.

1.3. APPROACH

In order to reach this goal the following steps will be taken (see figure 1):

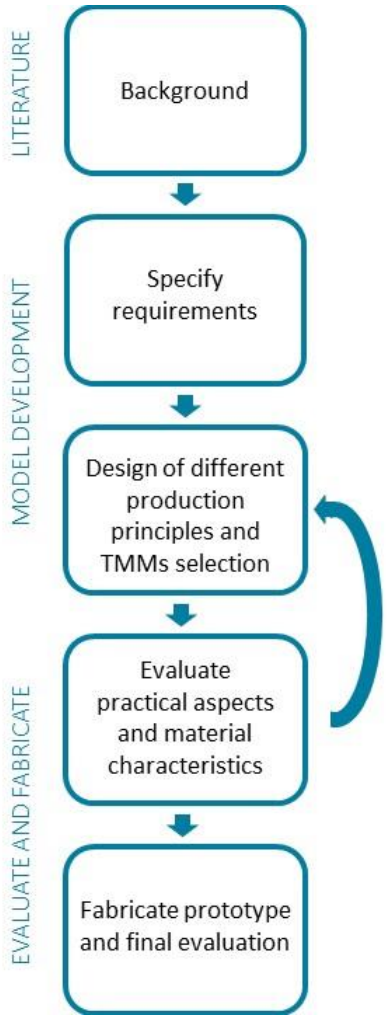

FIGURE 1 - APPROACH

Before designing a brain phantom, a literature study was performed in order to obtain the necessary knowledge about the brain and its anatomy, the anatomy of the ventricles, diseases and treatment. Also, tissue mimicking materials frequently used for mimicking brain tissue were evaluated.

Based on findings in literature and the desires of Philips Healthcare, the requirements and wishes for the development of the brain phantom were set up.

During the model development stage, different production principles have to be assessed in order to create a brain phantom with a hollow space inside representing the ventricles. Based on findings in literature, the specified requirements and practical aspects of different TMMs, a material will be selected for the phantom. In this stage different combinations will be tried out and assessed on their quality in order to create a good model. This is an iterative process so different steps will have to be taken in order to find the most beneficial production principle for the creation of a brain phantom containing ventricles. After finding a good principle for producing the hollow spaces, the imaging characteristics will be assessed, to optimize the final design.

At the end of the project, a final model of the brain will be set up which will be evaluated. The contrast in the images will be analysed and the image quality and segmentation of the ventricles will be assessed.

1.4. THESIS ORGANISATION

This thesis is organized in the following way:

Chapter 2 shows the theoretical background needed for this research. It is divided into different subsections and provides information about the brain and its anatomy, the ventricles, brain tissue characteristics and tissue mimicking materials (TMMs). Also, common brain complications and their treatment will be discussed. Lastly, some of the characteristics of brain phantoms will be presented.

Chapter 3 describes the design of the brain phantom, based on the design criteria that followed from a literature search, the selection of the suitable production principle and TMMs for further investigation based on the selected criteria and promising results.

Chapter 4 is about the iterations of the phantom and the production to be able to set up the final design for evaluation.

Chapter 5 provides the evaluation of the developed brain phantom on its imaging characteristics, and the overall quality of the models and images and segmentation of the ventricles is assessed.

Chapter 6 and 7 contain the overall discussion of the results of the project and describe the limitations of the current research and the recommendations for further future research, to finalize with the overall conclusion.

2. BACKGROUND

At the beginning of this master thesis project, a literature study was done in order to obtain the necessary knowledge about the brain and its anatomy, diseases and treatment and tissue mimicking materials. In this chapter, the important background information will be presented.

In section 2.1 the anatomy and the features of the brain will be presented. The next section will discuss common complications with the brain and the ventricles followed by their usual treatment methods. In section 2.3 and 2.4 the mechanical and imaging characteristics and the tissue mimicking materials (TMMs) and phantom characteristics will we presented.

2.1. BRAIN

2.1.1. FUNCTION

The brain is a part of the central nervous system (CNS), together with the spinal cord, and can be seen as the command centre of the nervous system. The brain has a sensory and motor control function, as it receives senses from sensory organs and sends commands to the muscles and is thus of major importance in the quality of life.

The sensory nervous system is responsible for the reception and processing of sensory triggers. The sensory information is received through the cranial nerves and transported to the brain via tracts in the spinal cord [9]. The motor control system of the brain causes the generation and the control of movement. Movements are generated from the brain, through the nerves to motor neurons in the body, where the movement will be provoked [10].

2.1.2. ANATOMY

The adult human brain weighs about 1,5 kilograms and makes up about 2 per cent of the human's total body weight. The average volume of the human brain is of 1274 cm^3 and 1131 cm^3 for men and women respectively women [11]. The brain consists of the cerebrum, the brainstem and the cerebellum. The brain is protected by the skull and it floats in the skull, cushioned by cerebrospinal fluid.

The cerebrum is the largest part of the brain and consists of two cerebral hemispheres. The outer parts of the hemispheres, the grey matter, are called the cerebral cortex and consist of cortical layers of neurons. Both hemispheres are divided into four lobes. The outer layer of the hemispheres, the cerebral cortex, consist of grey matter which covers the underlying core of white matter. This white matter containing the brainstem and behind the brainstem sits the cerebellum or little brain. The brainstem starts in the midbrain area of the cerebrum and connects to the spinal cord. The brainstem consists of the midbrain, the pons and the medulla oblongata and connects the brain with the spinal cord. Each hemisphere is divided into four lobes, containing the frontal, temporal, parietal and occipital lobe. The cerebrum, brainstem, cerebellum and spinal cord are covered by three different protective membranes. These membranes are called meninges. Between the cerebrum and the brainstem, the thalamus and hypothalamus are located (see figure 2).

A network of billions of nerves leads messages back and forth between the brain and the rest of the body. The brain is primarily constructed by different types of neurons, glial cells, neural stem cells and blood vessels. The different types of neurons include interneurons, pyramidal cells, motor neurons and cerebellar Purkinje cells. It is estimated that the human brain contains about 85 billion neurons of which 16 billion are located in the cerebral cortex and the other 69 billion are located in the cerebellum [12], [13].

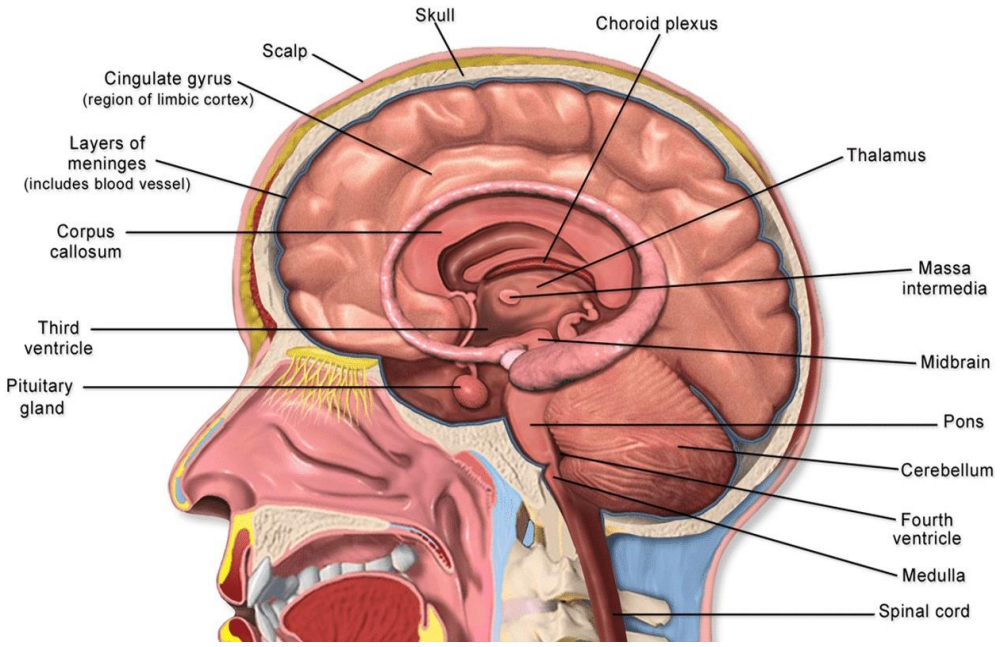

FIGURE 2 - MIDSAGITTAL SECTION OF THE BRAIN

2.1.3. VENTRICLES

The ventricular system of the brain is composed of four interconnected cavities located within the brain, the ventricles. The ventricles are there for the production, transport and removal of cerebrospinal fluid (CSF). They consist of two lateral ventricles, the third ventricle, the cerebral aqueduct and the fourth ventricle (see figure 3). The left and right ventricle are the largest of the ventricles and are situated within their respective hemisphere of the cerebrum. The lateral ventricles are connected to the third ventricle, which is located between the right and left thalamus. The third ventricle is connected to the fourth ventricle, which is the last in the ventricular system. The fourth ventricle receives CSF from the third ventricle via the cerebral aqueduct and can pass it into the central canal of the spinal cord [14], [15], [16].

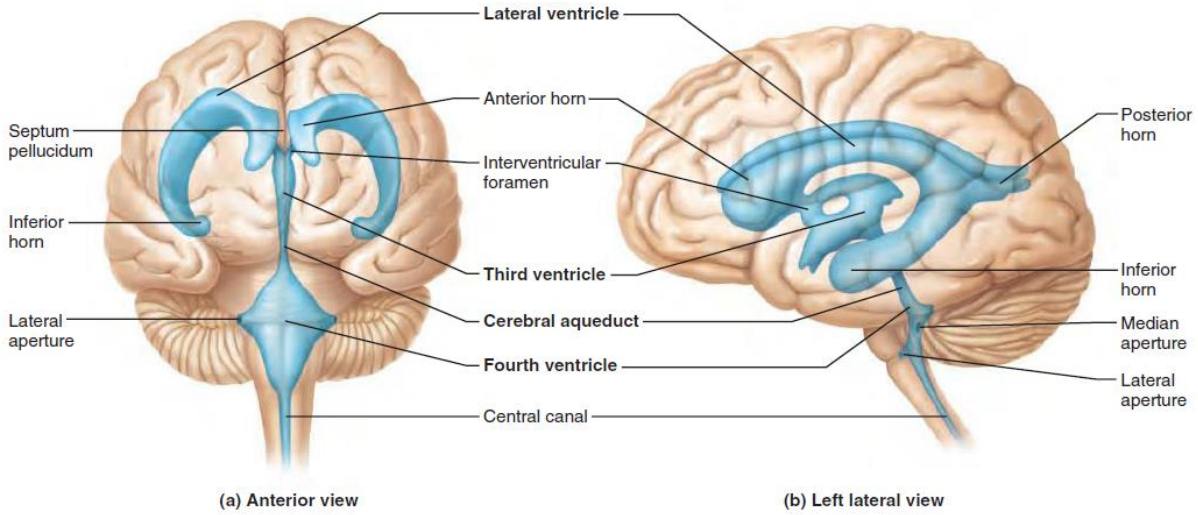

FIGURE 3 - VENTRICLES OF THE BRAIN (A) ANTERIOR VIEW (B) LEFT LATERAL VIEW [16].

2.1.4. CEREBROSPINAL FLUID

Cerebrospinal fluid is a filtrate of plasma which bathes and cushions the brain and the spinal cord. CSF serves as protection, buoyancy and chemical stability. It functions as a liquid cushion and prevents the brain from collapsing under its own weight. It also keeps the brain clean and healthy as it transports and maintains necessary nutrition's and chemical signals, like hormones, in the brain and eliminates harmful substances. As mentioned in section 2.1.3, CSF is produced in the ventricles and flows through and around the brain and spinal cord and is eventually absorbed into the bloodstream. Figure 4 shows the circulation of the CSF. The direction of the flow is indicated by arrows starting in the choroid plexus, located in the ventricle, indicated by the number 1 in the figure. The choroid plexuses are also responsible for the removal of waste product in de CSF.

CSF is constantly in motion as the figure illustrates, the CSF flows from the choroid plexus (number 1) through the ventricles via the apertures (number 2) of the fourth ventricle to the subarachnoid space (number 3). The CSF eventually enters the bloodstream via the arachnoid villi number 4). On average an adult houses a total volume of 150 ml of CSF and produces about 500 ml per day [16].

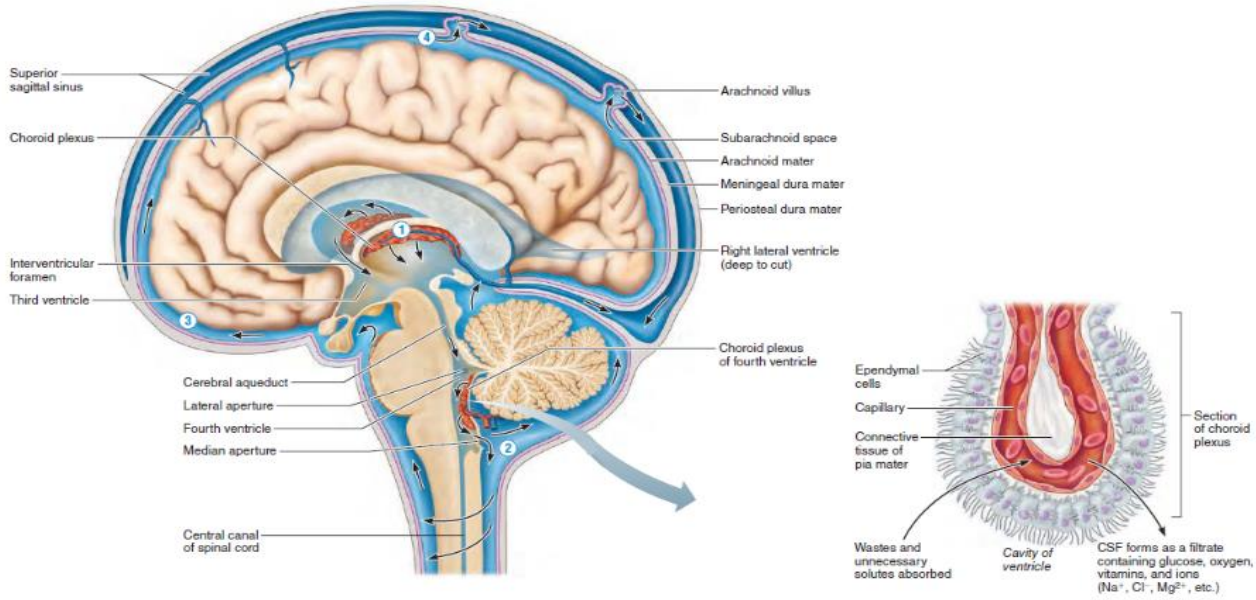

FIGURE 4 - FORMATION, LOCATION AND CIRCULATION OF CEREBROSPINAL FLUID

2.2. NEUROLOGICAL CONDITIONS AND TREATMENT

The brain is a very delicate yet vital organ. Small defects in the brain can have severe consequences on a patients mental and physical state. Abnormalities can occur due to birth defects, disease, injuries, etc. Some complications require neurosurgery in order to cure a patient. This section describes diagnostic techniques, the most common brain complications and treatment.

2.2.1. PREOPERATIVE TECHNIQUES

Before any surgery can take place, it needs to be well prepared and the surgeon needs to plan the procedure. All the steps of the surgery and the route inside the brain have to be thought through. Preoperative planning can be based on 2D images or on 3D models, created from preoperative techniques like CT and MRI. Preoperative planning assesses the optimal surgical route and evaluates the safety of the determined route [17].

The frequent used preoperative techniques for diagnosis and surgical planning will be described below.

Computed Tomography (CT)

Computed tomography is an imaging technique that makes detailed pictures of areas inside the body. This is done by taking X-rays that create cross-sectional images of a full picture of your brain. The X-rays are absorbed in different ways by different tissue types, resulting in an image with information about the anatomy or complications [18]. Sometimes an iodine-based dye is injected into a vein to make the tissue show up more clearly in the image.

Non-Enhanced CT (NECT) is the first type of CT scans used when a patient shows neurological signs or symptoms because it is easily obtained, well tolerated and can directly show emergency cases with life-threatening situations [19].

Magnetic Resonance Imaging

Magnetic resonance imaging (MRI) uses a powerful magnetic field, radio waves and a computer to generate cross-sectional images of the structures within the brain. MRI scans provide a detailed picture of the brain and can be used both preoperatively as intraoperative. Two basic types of MRI images that are used are T1 weighted image and T2 weighted image.

T1 weighted image (T1WI) and T2 weighted image (T2WI) are the basic pulse sequences in MRI. An MRI pulse sequence refers to the set of changing magnetic gradients. On T1 images fat is white, on T2 images both fat and water show up white.

Diffusion-weighted magnetic resonance imaging (DWI or DW-MRI) is a special technique of MRI. With software, images are generated using the diffusion of water molecules, which generates contrast in MR images [20]. MRI DWI measures the random motion of the water molecules in the tissue. Tissue cellularity and the presence of cell membrane, intact or damaged, influences the level of diffusion of the water molecules, which can be quantitatively assessed by the apparent diffusion coefficient (ADC) value [21]. ADC is calculated from the outcomes of the MRI DWI data and is a way to measure the magnitude of diffusion of the water molecules in different kinds of tissue [22]. If MRI DWI measurements show low signal intensity, this indicates a high apparent diffusion coefficient [23].

Diffusion tensor imaging (DTI) is a specific kind of DWI. It is an advanced MR technique that makes it possible to estimate the location, orientation and anisotropy of the brain's white matter tracts. With DTI the movement of water molecules is described by using two metrics, mean diffusivity (MD) for the magnitude of water diffusion and fractional anisotropy (FA) for measuring the direction of the water diffusion [24]. It is used to construct white matter tractography in the brain in a highly detailed way [25].

Tractography, also known as fibre tracking is a technique that uses diffusion tensor to track the whole length of the fibre. Measurements begin in the start region of interest, which is usually manually defined and is tracked along the length of the fibre in the same main diffusion direction as the previous voxel. The most tracked fibre bundle is the corticospinal tract but fibre tracking can also be used to track most of the brains white matter tracts.

Magnetic Resonance Spectroscopy

Magnetic resonance spectroscopy (MRS) is performed with the same machine that is used for conventional MRI measurements and is used to complement magnetic resonance imaging. MR Spectroscopy measures changes in the metabolism of brain tumours, strokes, seizure disorders, Alzheimer's disease, depression and other brain conditions. Spectroscopy is used to further define the tumour type and determine the aggressiveness of the tumour. It can also be used to distinguish between tumour recurrence and radiation necrosis [26], [27].

Ultrasound

Ultrasound (US) imaging techniques use a probe that sends ultrasound pulses into the tissue. The generated soundwaves have a frequency greater than 20 kHz. Different tissues reflect the sound waves in varying ways and the echoes are used to create images.

2.2.2. MINIMALLY INVASIVE NEUROSURGERY

Brain surgery should be as minimally invasive as possible as the brain is a very delicate organ with a lot of vital structures packed in a tight space together. Open brain surgery is also performed but minimally invasive brain surgery is preferred as it reduces hospital and recovery time and results in smaller scars and less pain. A minimally invasive procedure uses only small cuts to gain access to the surgical location and requires an endoscope. Two types of frequently performed minimally invasive neurosurgeries are intracranial surgery and endonasal surgery. Intracranial surgery requires small openings in the skull through which the instruments are introduced. In endonasal neurosurgery, the instruments get access to the brain through the nose.

During these procedures, it is very important for the surgeon to know where the surgical location is and where the surgical instruments are in proportion to that. More about the so-called neuronavigation can be found in section 2.2.3. neuronavigation and brain shift.

2.2.3. NEURONAVIGATION AND BRAIN SHIFT

Neuronavigation based on preoperative imaging data is widely used for image guidance in neurosurgery, to assist the surgeon with the procedure. In section 2.2.1. the preoperative techniques for assessing the brain are described. Of these techniques, MRI and CT are the preferred techniques for neuronavigation at the moment [28].

Unfortunately, brain movement during surgery invalidates the patient-to-images registration so it affects the reliability of the preoperative images for intraoperative surgical guidance. This brain movement, known as brain shift, means that the brain deforms intraoperatively due to a wide variety of causes related to physiological, chemical and physical factors [29], [30].

2.2.4. NEUROLOGICAL CONDITIONS

The most common brain defects that require neurosurgery along with the proportion they occupy of the global neurosurgical need are listed in table 1 [31], [32].

TABLE 1 -ESTIMATED WORLDWIDE NUMBER OF CASES REQUIRING NEUROSURGICAL INTERVENTIONS

Neurological condition	Number of cases per year	The proportion of cases per year (%)
Traumatic brain injury	6,160,814	44.7
Stroke	2,760,403	20
Epilepsy	1,413,624	10.3
Hydrocephalus	971,317	7
Infections	969,001	7
Brain tumour	735,180	5.3
Traumatic spinal injury	399,606	2.9
Vascular anomalies	311,407	2.3
Neural tube defect	35,622	0.3
Spinal tumour	17,840	0.1
Total	13,786,823	

Some of these brain conditions can be treated using an endoscope during surgery. Interesting and relevant for this research are tumours and hydrocephalus. These two conditions will be briefly described below.

Brain Tumours
A brain tumour is the abnormal growth of cells within the brain. There is a great variety in different brain tumours types, grades and the location where they occur. There can be made a distinction in malignant or cancerous tumours and benign tumours. Depending on the tumour type, location and grade, sometimes endoscopic surgery, biopsy or resection of the tumour are possible. Neurological symptoms of brain tumours may include headache, seizure, syncope, focal neurological deficit or papilledema [19].

Hydrocephalus
Hydrocephalus is a condition in which an excessive amount of CSF is produced or built up within the ventricles of the brain, causing the ventricles to enlarge. The enlargement of the ventricles can lead to increased intracranial pressure, which in some cases can be life-threatening. It can develop for various reasons and can be divided into four types. It can occur due to excess production of CSF, impaired reabsorption of CSF into the bloodstream or blockage in the ventricular system that causes CSF to accumulate. It is mainly classified as being communicating or non-communicating. Communicating hydrocephalus does not involve a blockage in the ventricular system. Non-communicating hydrocephalus does involve a blockage of the ventricular system and is the most common cause of

hydrocephalus. It can be present at birth or develop later in life. This condition often occurs in children with an overall incidence of 1.1 per 1000 infants [33].

Hydrocephalus is usually treated by placing a shunt or by endoscopic third ventriculostomy, to drain the excess CSF.

2.2.5. ENDOSCOPIC INTERVENTIONS

Some of the neurological conditions described in section 2.2.3. can be treated by endoscopic interventions. In endoscopic minimally invasive neurosurgery, the surgery is performed via the nose or small openings in the skull. Endoscopic neurosurgery includes among others, endoscopic third ventriculostomy and endoscopic tumour resection. Endoscopic Third Ventriculostomy is the most common procedure for the treatment of hydrocephalus [34].

2.2.6. TRAINING FOR SURGERY

To be able to perform a complex surgical procedure, a new surgeon requires a sufficient amount of training. Training programs are needed to train new surgeons. These programs are experience based and often make use of human or animal cadavers or sometimes even real patients in an operating room. Practising on cadavers offers a risk-free training environment, though it comes with different complications. Human and animal cadavers are expensive, come with ethical concerns and degrade rather quick, causing the mechanical properties to change [5]

The last couple of years there has been a shift towards simulation-based training, which is a great alternative as it enables trainees to practice in a safe environment, provides more room for mistakes and usually offers immediate feedback. There has been great growth in the development of virtual reality (VR) training platforms, which are reusable and often measure the performance level of the trainee. Virtual endoscopy is the name of VR-based simulation focused on endoscopy. It is used for training purposes in neurosurgery for endoscopic third ventriculostomy, endonasal surgery and the evaluation of pathologies in cerebral blood vessels [35]. The downside of these VR training is that simulators lack realising force, tactile and visual feedback [6]. Having unrealistic feedback during training can result in complications during real surgeries. Besides that, these systems often come at high costs [36].

So although VR-based simulators are an interesting development, the systems are currently unrealistic due to the previously mentioned reasons. Another alternative for training is phantoms. Phantoms can be used to familiarize the new surgeon with operation techniques, instruments and endoscopes while training hand-eye coordination.

It was found that training with a real simulator or synthetic model has a great beneficial value compared with VR-simulation training, especially when it comes to neurosurgical training. Surgeons that are trained with phantoms have superior skills in guiding needle position and other clinical procedures [37].

2.3. BRAIN TISSUE CHARACTERISTICS

2.3.1. MECHANICAL

Mechanical properties of brain tissue fall under the category of soft tissues, like kidneys and the liver. Insights in the mechanical characteristics of these soft tissues help to provide information about the biological processes, such as mechanotransduction but are also needed to develop robot-aided surgical tools and virtual reality techniques in order to obtain a realistic haptic experience.

Though brain tissue falls under the soft biological tissues, it is quite different from other soft tissues as its microstructure is not dominated by collagen and elastin fibres. This results in different strain-stiffening behaviour compared to other soft tissues [38], [39].

Many studies performed in the mechanical properties of brain tissue, were focussed on developing a digital model. In vitro researchers extensively asses the brain tissue characteristics under different shear, compression and tension stresses, which offers a lot of knowledge about the mechanical characteristics and behaviour of the brain [40]–[43].

Mechanical Characterization Brain

Brain tissue exhibits nonlinear elastic behaviour, which means that the material stress does not linearly increase with strain. With this nonlinear elastic behaviour, the soft tissue of the brain is therefore denoted as viscoelastic. This viscoelastic material is time and history-dependent meaning that it exhibits different behaviour under different conditions. Viscoelastic materials are also found to possess the characteristics of stress-relaxation (decreasing stress during constant strain), creep (increase in strain during constant stress), strain rate dependency and hysteresis (energy dissipation during loading and unloading) [43].

Researches show that the human brain presents non-linear elastic mechanical behaviour as well as rate-dependent characteristics, which means that the stiffness of the tissue is dependent on the strain/displacement rate [44], [45]. This is due to the interaction between the cerebrospinal fluid (CSF) and the brain tissue which has a viscoelastic behaviour [46]. This is the reason that the brain deforms differently during different rates of impact, ranging from brain shift phenomena (slow rate) to trauma (fast rate) [47].

White and grey matter

As mentioned in section 2.1.2. the human brain is composed of an outer layer of grey matter and an inner core of the white matter. A study by Budday et al. looked at the mechanical properties of grey and white matter brain tissue by indentation. This research concluded that white matter was stiffer than grey matter as white matter, with an average modulus of 1.895kPa±0.592kPa, was on average 39% stiffer than grey matter, $p<0.01$, with an average modulus of 1.389kPa±0.289kPa. The study also showed that white matter displayed larger regional variations and showed to be more viscous than grey matter as it responded less rapidly to mechanical loading [44], [48].

2.3.2. OPTICAL

Regarding the brain, different imaging principles like ultrasound, MRI or CT imaging are used, see section 2.2.2. These methods are used for diagnostic purposes as well as to plan the procedure. For this study, we will look at the X-ray/CT characteristics of the brain tissue.

A CT scan of the head gives an image of different shades of grey. Different features can be identified based on these shades depending on the radiodensity of the feature. The pixels of the image is displayed according to the mean attenuation of the tissues ranging on a scale from -1024 (least attenuation) to +3071 (most attenuation) on the Hounsfield scale. Lower attenuation appears darker on a CT image. Air

has an attenuation of -1000 Hounsfield units (HU), CSF 5 HU, brain tissue ranges generally between 30 to 40 HU and cranial bone can reach 2000 HU. CT images of the brain are usually viewed on a window ranging from 0 HU to 80 HU [49], [50].

Healthy brain

The figure below shows an image of a healthy brain by a CT scan (see figure 5). White matter is slightly darker than the grey matter. Overall you can see the sulci, and the ventricles of the brain very clearly as they turn up darker on a CT scan.

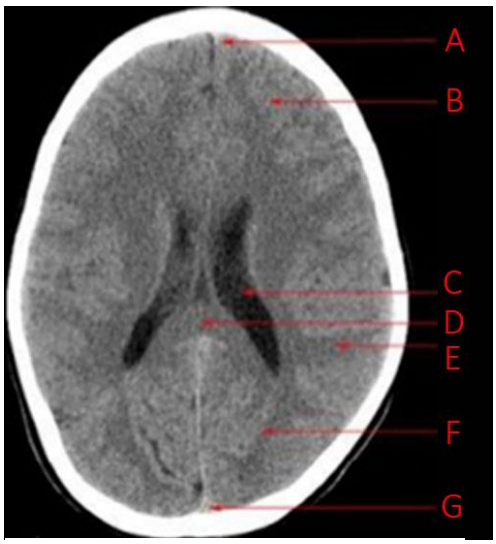

The ventricles are clearly visible and are not dilated. A healthy brain is symmetrical, the ventricular septum is on the midline and is not shifted from right to left.

A. Falx Cerebri
B. Frontal Lobe
C. Body of the lateral ventricle
D. Splenium of the corpus callosum.
E. Parietal Lobe
F. Occipital Lobe
G. Superior Sagittal Sinus

FIGURE 5 - CT IMAGE OF A HEALTHY BRAIN

Diseased brain

Deviations in the CT images can indicate complications. Hypodense (dark) structures can indicate edema and infarction, hyperdense (bright) structures indicate calcification and haemorrhage. Tumours can be detected as they might cause anatomical distortion or swelling, or by surrounding edema.

Brain Tumours

Brain tumours come in numerous forms and sizes, see section 2.2.4., and are sometimes more difficult to see on a CT scan, depending on the type and location. The images below show a tumour on a CT scan, see figure 6.

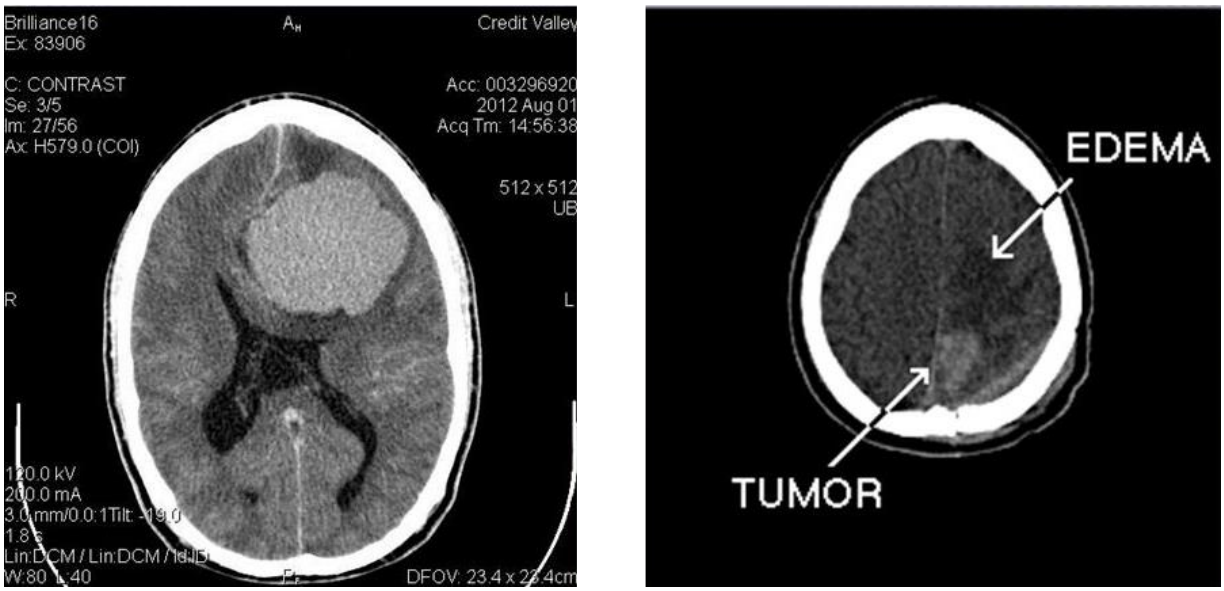

FIGURE 6 - CT SCAN, CLEARLY SHOWING A TUMOUR ABOUT THE SIZE OF A LEMON

Hydrocephalus

Hydrocephalus, as mentioned in section 2.2.4., is a condition in which an excessive amount of CSF is produced or built up within the ventricles of the brain, causing the ventricles to enlarge. Figure 7 shows a brain with hydrocephalus. Hydrocephalus is clearly visible on a CT scan as the lateral and third ventricle are enlarged, indicated by the letter B in the figure.

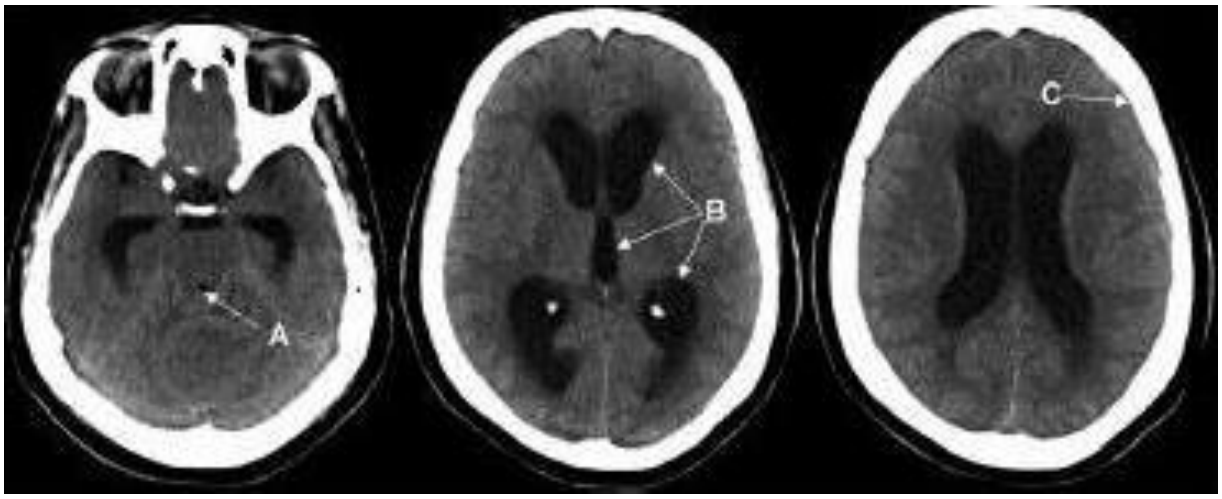

FIGURE 7 - CT SCAN OF A PATIENT WITH HYDROCEPHALUS.

2.4. BRAIN TISSUE MIMICKING MATERIALS

Phantoms and tissue mimicking materials are found to be very useful as they are able to accurately mimic the mechanical and optical characteristics of the desired native tissue. In this chapter, the frequently used materials for mimicking brain tissue are discussed.

2.4.1. POLYMERS

Tissue mimicking materials are usually made from polymers from biological origin or synthesized from monomers by polymerization reactions. Polymers are an interesting category of material for phantoms as polymers are easily available and have a wide range of desirable properties [51]. Polymer structures can be linear, branched or crosslinked, see figure 8 [52].

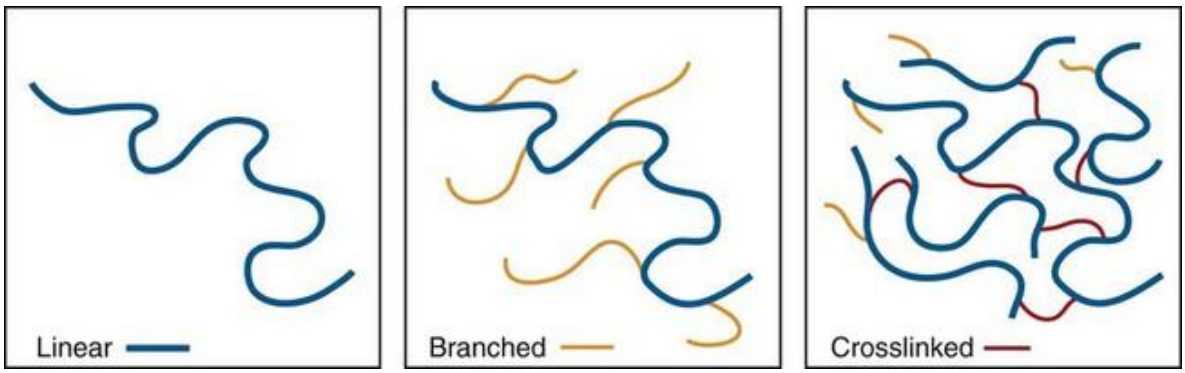

FIGURE 8 - SCHEMATIC DIAGRAMS OF LINEAR, BRANCHED AND CROSSLINKED POLYMERS

Crosslinking happens by physical interaction between the molecules and can be stimulated by the addition of a crosslinking agent. The amount of crosslinks influences the mechanical characteristics of the material. More crosslinks result in a decrease of elasticity and an increase of strength [53].

The degree of polymerization indicates the number of linked monomers and is an important indication of mechanical strength. The higher the polymerization, the higher the mechanical strength. Polymers can be the main component of the TMM or function as a cross-linked polymeric framework which has the capacity to hold water within its porous structure. These polymers are known as hydrogels [51]. The figure below shows the general subdivisions of polymers that are widely used as TMM's, see figure 9. Polyvinylchloride, polyvinyl alcohol, gelatine and agar were described in literature to have promising properties for mimicking brain tissue [7], [54]–[56].

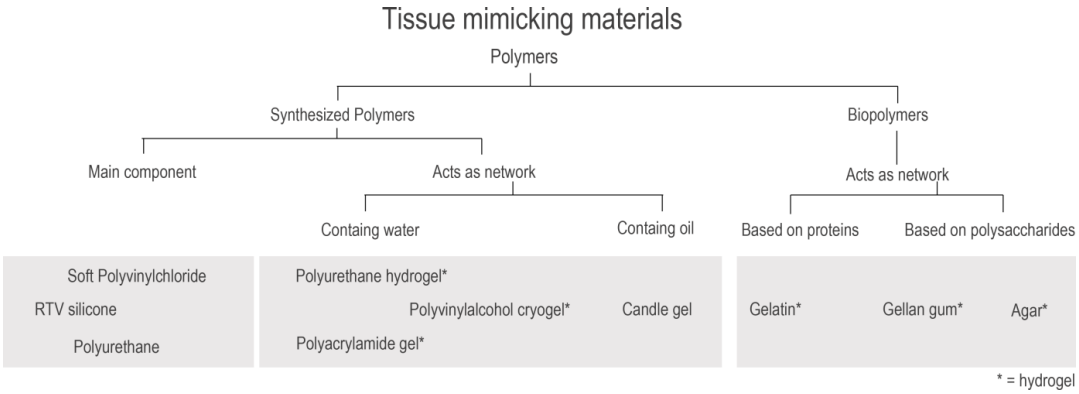

FIGURE 9 - POLYMERS USED AS TISSUE MIMICKING MATERIALS

2.5. PHANTOM CHARACTERISTICS

In the previous section, different materials for the mimicking of brain tissue are mentioned. The material used depends on the desired properties and applications of a phantom. Depending on the desired application, some properties are more important than others, see figure 10.

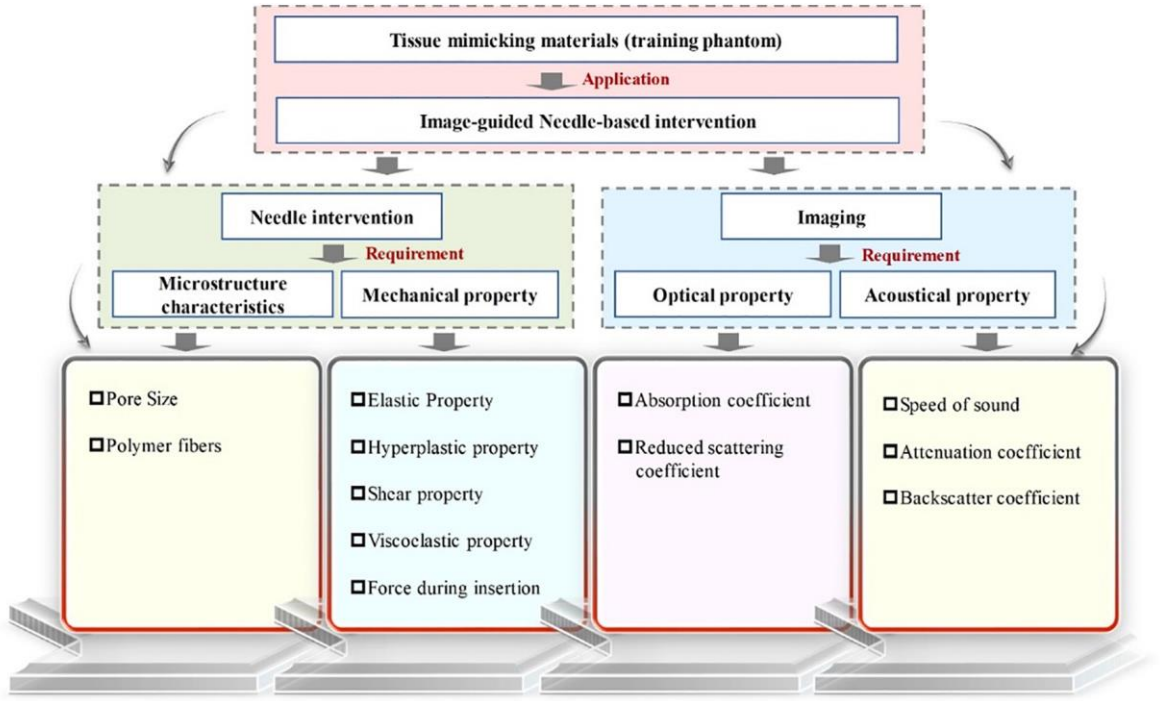

FIGURE 10 - THE FRAMEWORK OF THE REVIEW CONTENT SHOWING THE CONNECTION OF THE MICROSTRUCTURE CHARACTERISTICS, MECHANICAL PROPERTIES, OPTICAL PROPERTIES, AND ACOUSTICAL PROPERTIES OF THE TISSUE MIMICKING MATERIALS IN THE IMAGE-GUIDED NEEDLE-BASED INTERVENTION.

Depending on the application of the phantom, different properties are taken into account. For example, for standardization and comparison of imaging systems, the mechanical properties are not that important.

2.5.1. TYPES OF ADDITIVES IN TISSUE MIMICKING MATERIALS

TMMs come in a wide range of shapes and characteristics which mimics the desired properties. However, usually, there are different needs for a specific characteristic of the desired tissue mimicking organ or application. Additives can be used to change the characteristics of the base material.

Adjustments of characteristics usually focus on the imaging section, The parameters of the material can be adjusted to change the absorption, attenuation and backscattering coefficient which results in changes in the imaging of the material [57], [58].

TMMs are not always visible for imaging in US, MRI and CT so additives are needed with the base material to create sufficient contrast. To increase backscattering of sound waves in US imaging, talcum powder can be mixed with the base solution. For increasing phantom contrast in CT, barium sulphate ($BaSO_4$)is often used. Great concentrations of barium sulphate can influence MRI imaging, but usually, only small concentrations of barium sulphate are required. Therefore copper sulphate ($CuSO_4$) is used to enhance the signal in T1 weighted images [8], [59], [60].

3. DESIGN OF BRAIN PHANTOM

In this chapter, the development and the production of the brain phantom will be described. First, a list of requirements and wishes was set up, after which the initial brainstorm and development took place.

3.1. INTRODUCTION

There are different kinds of brain phantoms with different applications. Depending on the application of the phantom, different properties are taken into account.

Existing phantoms are often expensive or are simplified models and lack anatomical structures, like the ventricles and basal ganglia. This thesis focusses only on the ventricles of the brain and will not incorporate other anatomical structures. Structures like cranial nerves, trigeminal nerves, blood vessels are all neglected for this research. A study by Budday et al. stated there is a difference in mechanical properties of grey and white matter, but as it was found that this is only a small difference, therefore it was neglected [44]. Also, differences in mechanical and optical characteristics of the brain stem are simplified. This thesis only focuses on the design of the brain phantom with the implementation of the hollow spaces of the brain representing the ventricles. Next to that, the brain phantom will be made from a material that mimics the mechanical properties of the brain tissue and it has to comply with CT imaging. The exactly defined design criteria will be listed in the next section.

3.2. DESIGN CRITERIA

Based on findings in literature and the desires of Philips Healthcare, the following design criteria were set up:

The phantom should resemble the anatomy of the human brain containing the ventricles of which the lateral ventricles and third ventricle have to be visible and it would be nice if the fourth ventricle is also visible according to the request from Philips Healthcare. The phantom should be made from a material with similar mechanical properties as real brain tissue and has to be suitable for X-Ray and CT imaging. The phantom should be suitable for fabrication by simple techniques such as casting or 3D printing, in order to make a home-made brain phantom containing ventricles possible. This will enhance the accessibility to cost-efficient and customizable phantoms. Finally, it is important that the is structurally stable at room temperature and it is desired that the phantom is usable for a couple of months, so the TMM should not spoil after a few days/weeks.

To conclude:

- Must see lateral ventricles and third ventricle
- Easy to manufacture
- Similar mechanical characteristics to brain tissue
- Suitable for X-Ray and CT imaging
- The phantom needs to be structurally stable and usable at room temperature.
- Shelf life of 6 months

3.3. MODELS

This chapter describes the development of the brain model, from the initial brainstorms to develop the cavities within a solid shape, to the production of the first phantom materials. In the end, different production principles will be evaluated for further development of a brain phantom, and to evaluate the use for X-ray/CT scanning.

3.3.1. BRAINSTORM

The development of a brain phantom containing the cavities of the ventricles started with an extensive brainstorm to assess the different possibilities. The following varieties were classified:

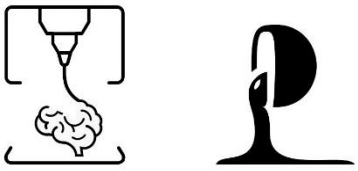

For the idea generation, production by 3D printing and casting were taken into account, as it was required that the model should be able to be easily produced by casing or 3D printing.

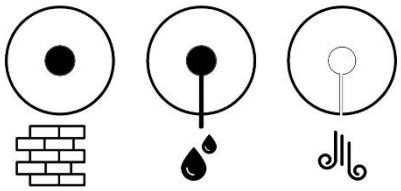

From the brainstorm session 3 possible principles of creating a hollow space where identified (icons on the left, from left to right; solid, liquid and air). Using a solid part that can be removed later, have a solid part that can be solved and having a membrane filled with air that can be removed.

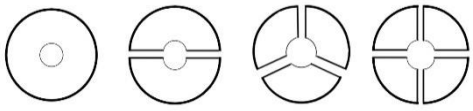

It was also evaluated from how many parts the model would be created. So how many parts the actual model is made from, that have to be assembled to make one brain model and how many parts are needed for the production.

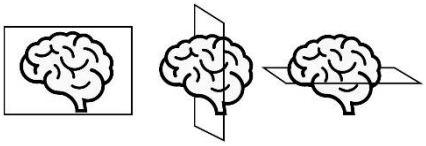

The orientation of the moulds. For casting at least 2 mould parts are needed to be able to remove the casted model from the mould. The moulds can split in the sagittal, coronal and horizontal plane.

3.3.2. IDEA GENERATION

These varieties were summarized in one morphological chart which resulted in a couple of possible concepts. Some of the concepts had to be excluded due to limitations in time and fabrication opportunities. Ideas such as using a membrane in the shape of the ventricles that can be used as an insert in the brain model, or a ventricle balloon shape to be deflated after production might still be

auspicious concepts for the development for the brain phantom with ventricles, but these ideas were excluded for this study. Ideas that required 3D printing of the phantom were also excluded as 3D printing of soft materials is not yet possible, this category was opt-out and the model will be cast.

From all these concepts, a few of the categories were selected for further evaluation, to assess the possibilities of the development of the brain phantom.

3.3.3. CONCEPTS

From the morphological chart, three concepts were selected to further investigate for the developments of the brain phantom.

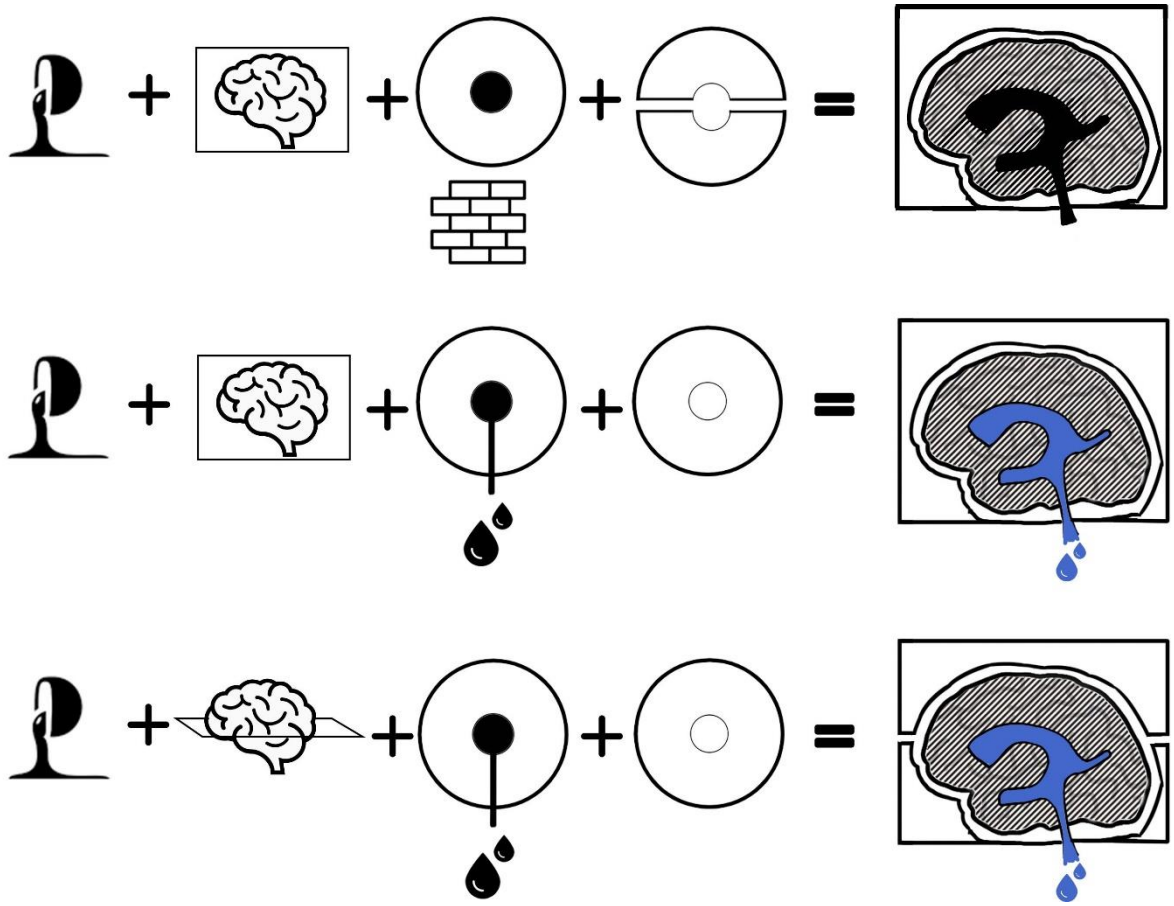

Now for these concepts, the moulds and the ventricle model have to be developed, which is done in the following section. All the moulds will be made from two parts. The first two concepts are both split in the sagittal direction, so for this concept, only one mould has to be developed to be used in two different ways.

3.3.4. BRAIN MOULDS DEVELOPMENT

The mould for the brain phantom was based on a predeveloped, polygonal surface mesh, digital brain model. This 3D model was obtained from Sketchfab and used to create the different mould designs from. The link to this 3D brain model download can be found in Appendix A. This mesh shape was used to subtract from a rectangular shape, creating a 'negative' shape of the brain in a square shape. This process is visualized in figure 11. Starting with the positive brain shape, going to a square with a negative brain shape.

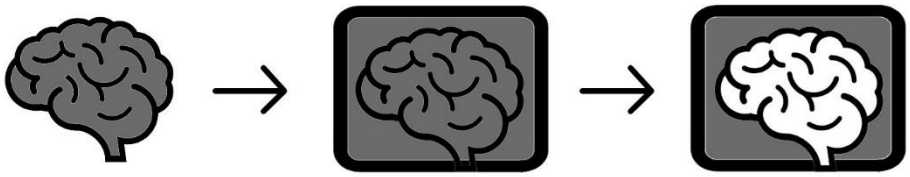

FIGURE 11 - BASIC PRINCIPLE MOULD DEVELOPMENT

For the different production principles of the brain phantom, two different kinds of moulds could be used. One split in the sagittal direction and the other one in the horizontal direction of the brain. These mould shapes form the basis for the development of the different concepts of productions of the phantom.

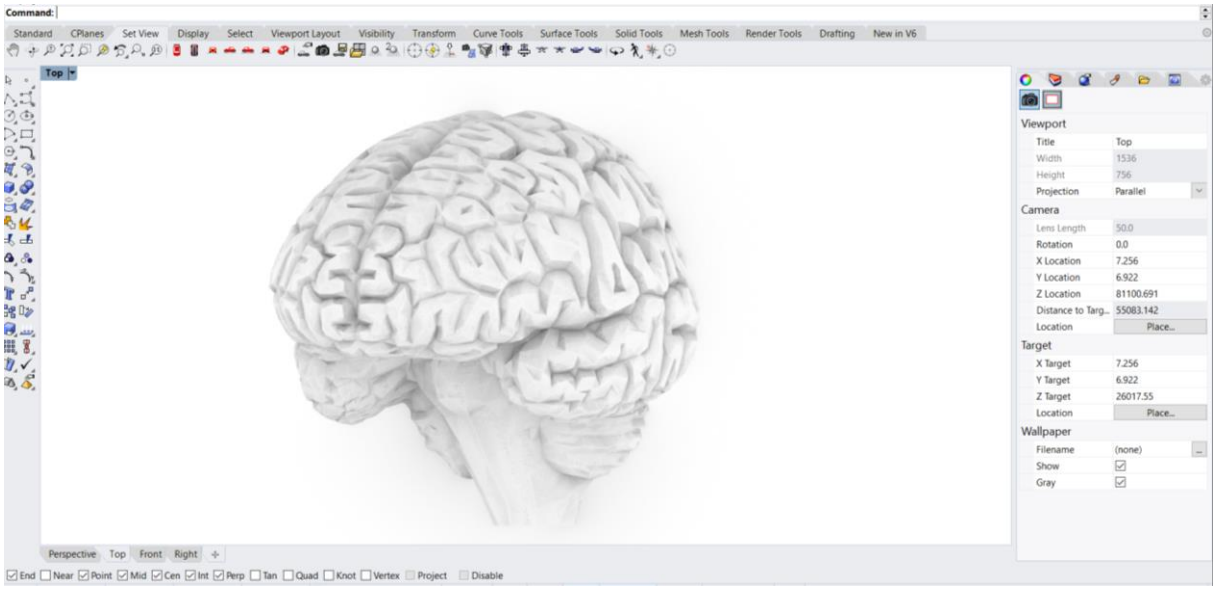

FIGURE 12 - ORIGINAL DOWNLOADED 3D BRAIN MODEL (RESIZED TO MATCH THE AVERAGE BRAIN SIZE)

In the original downloaded 3D brain model, small adjustments were done to make it match the average brain size (12 x 12 x 16 cm). The rectangular box that was placed around it to extract the positive brain shape from has a size of 17 x 13 x 13 cm so that the wall thickness at every outer point of the brain has at least a wall thickness of 0.5 cm.

Mould A:

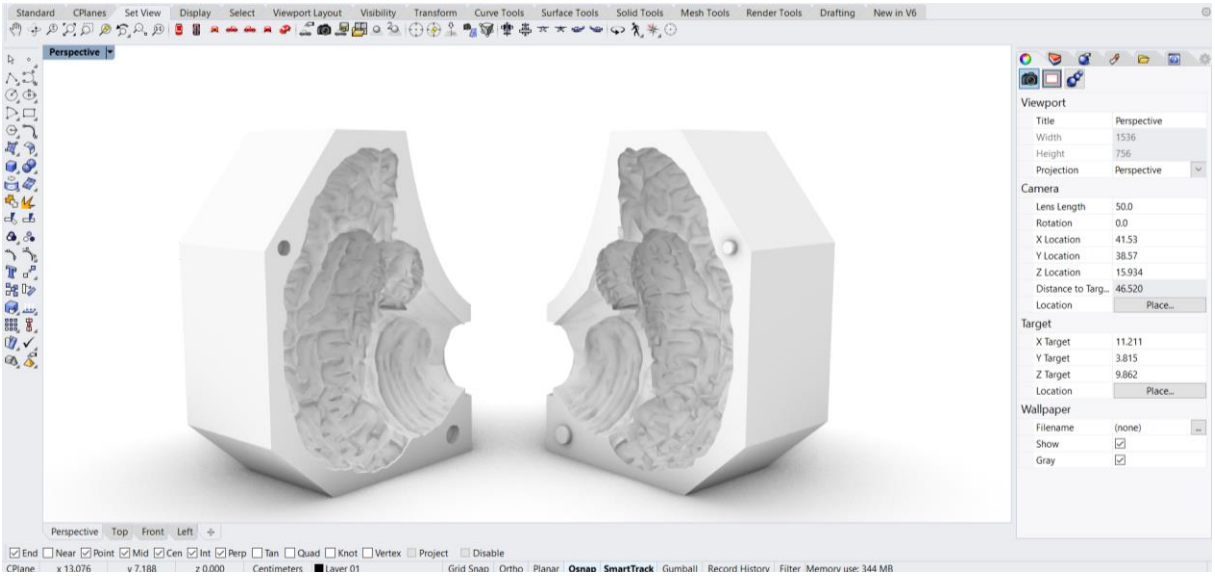

FIGURE 13 - SCREENSHOT FROM RHINO - MOULD A

*Note: For the mould split in the sagittal, the brain shape had to be adjusted a bit in order for the brain model to be able to get out of the mould. To achieve this, the temporal lobe of the brain model was extended.

Mould B:

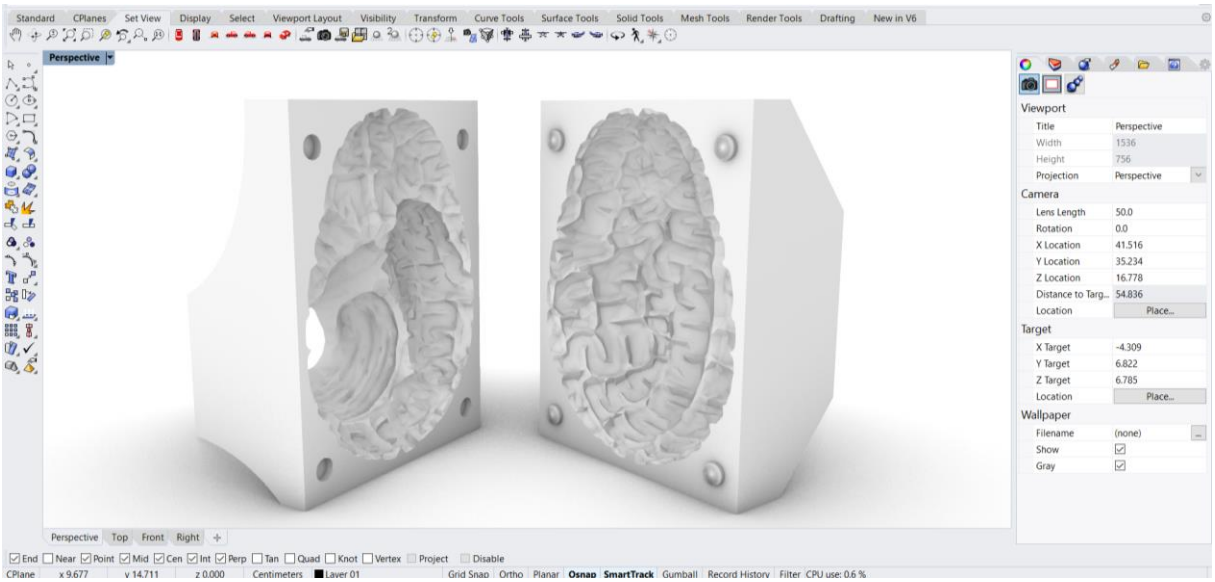

FIGURE 14 -SCREENSHOT FROM RHINO - MOULD B

Pins and holes were added to the moulds in order to make sure they stay in the right position in relation to the two halves. And from the original rectangular shapes surrounding the negative brain space, excess material was removed in order to reduce printing time and reduce material use.

3.3.5. VENTRICLE DEVELOPMENT

The shape of the brain ventricle was based on the predeveloped ventricle shape and was obtained from Sketchfab. This 3D ventricle shape was used for the creation of the hollow spaces in the brain. The link to this 3D ventricle model download can be found in Appendix A. Some adjustments had to be made to the obtained shape in order for it to function of the different production principles of the brain phantom, see figure 15.

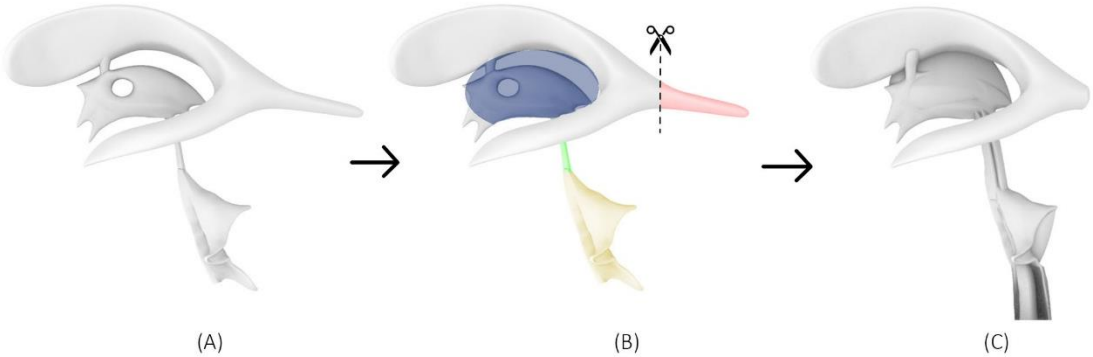

FIGURE 15 - VENTRICLE ADJUSTMENTS (A) ORIGINAL DOWNLOAD SHAPE (B) INDICATION OF CHANGE LOCATIONS (C) ADJUSTED VENTRICLE SHAPE

Some adjustments to the ventricle shape were made in order to be able to use it for the desired application. After the first evaluation, printing the original shape, it was found that the cerebral aqueduct, connection the third to the fourth ventricle, and the channel down the spinal cord were too fragile for 3D printing (highlighted green and yellow in figure 15).
Also, the two the aqueducts connecting lateral ventricles to the third ventricles were simplified in order to be able to use the shapes for the desired fabrication principle, highlighted blue figure 15.

The large 'tails' of the two lateral ventricles, highlighted red in figure 15, were considered to be unnecessarily long as they are not found in all images concerning the ventricles. It was decided to shorten those, simplifying it for the easy removal out of the ventricle.

The fourth ventricle was slightly enlarged to ensure the material to be able to flush out with the 3D PVA printed ventricle.

Two types of ventricles were developed for the creation of the brain phantom. One to be used for the mould A, split in the sagittal plane and one for mould B, split in the transverse plane. The difference is in 'foot' of the ventricle in how they can be assembled, see figure 16.

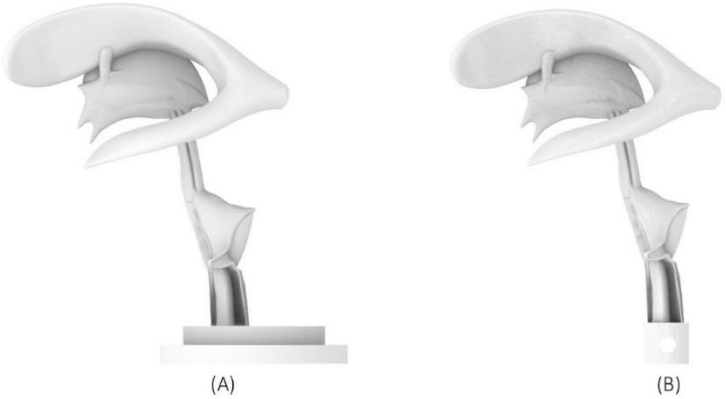

FIGURE 16 - DEVELOPED VENTRICLES (A) VENTRICLE SHAPE TO BE USED FOR MOULD A (B) VENTRICLE SHAPE TO BE USED FOR MOULD B.

Ventricle A will be 3D printed from PVA and PLA and ventricle B will be printed only in PVA as this shape in combination with mould B is not suitable for the production principle in PLA.

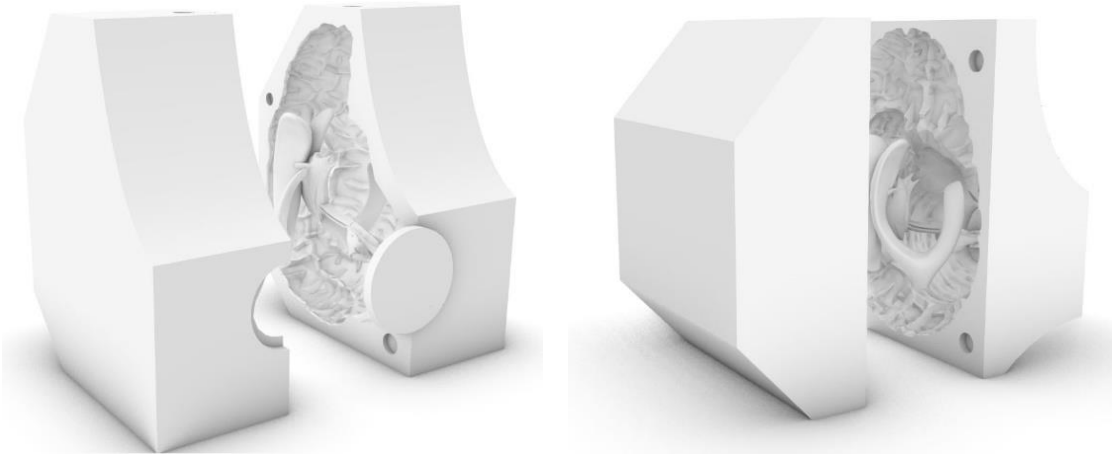

FIGURE 17 - VENTRICLES IN THE MOULDS. MOULD A ON LEFT AND MOULD B ON THE RIGHT

With the modelling of both the moulds and the 'foot' of the ventricles, the location of the ventricles relative to the brain was taken into account by comparing images and positioning the ventricles in the right spot in the moulds, see figure 17. Although all images that were found have slight differences, the gross anatomy was the same. The 'foot' of the modelled ventricle was modelled in such a way that it perfectly fits the mould and the lateral ventricles were positioned at the right height in the brain, see image 18.

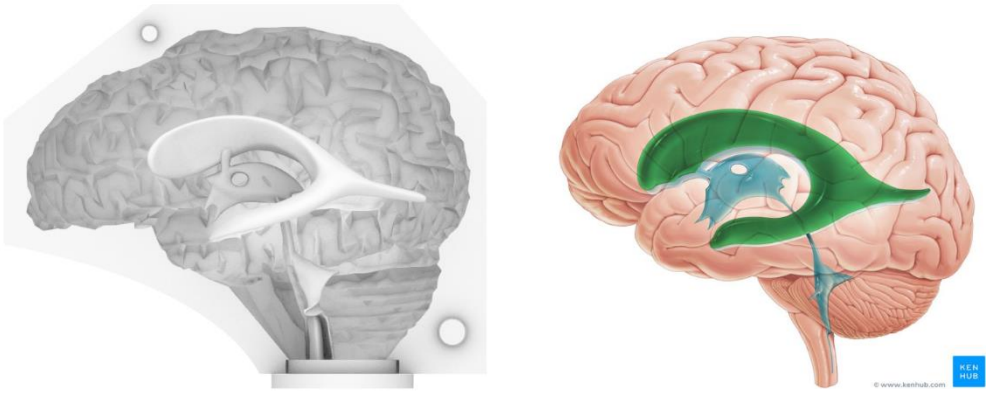

FIGURE 18 - MOULD WITH VENTRICLES POSITIONED AND AN IMAGE FROM THE BRAIN WITH THE LOCATION OF THE VENTRICLES

For the development of the brain phantom, it would be desired to adjust the brain shape as limited as possible. Therefore it was decided not to insert extra air shafts for the removal of the 3D printed PVA ventricles.

3.3.6. PRODUCTION OF THE PARTS

All the different parts are 3D printed. The moulds are 3D printed in PLA and the ventricles are printed either in PLA or PVA, making use of the Ultimaker 3 Extended. More about the settings, the development and the production of the parts can be found in Appendix B.

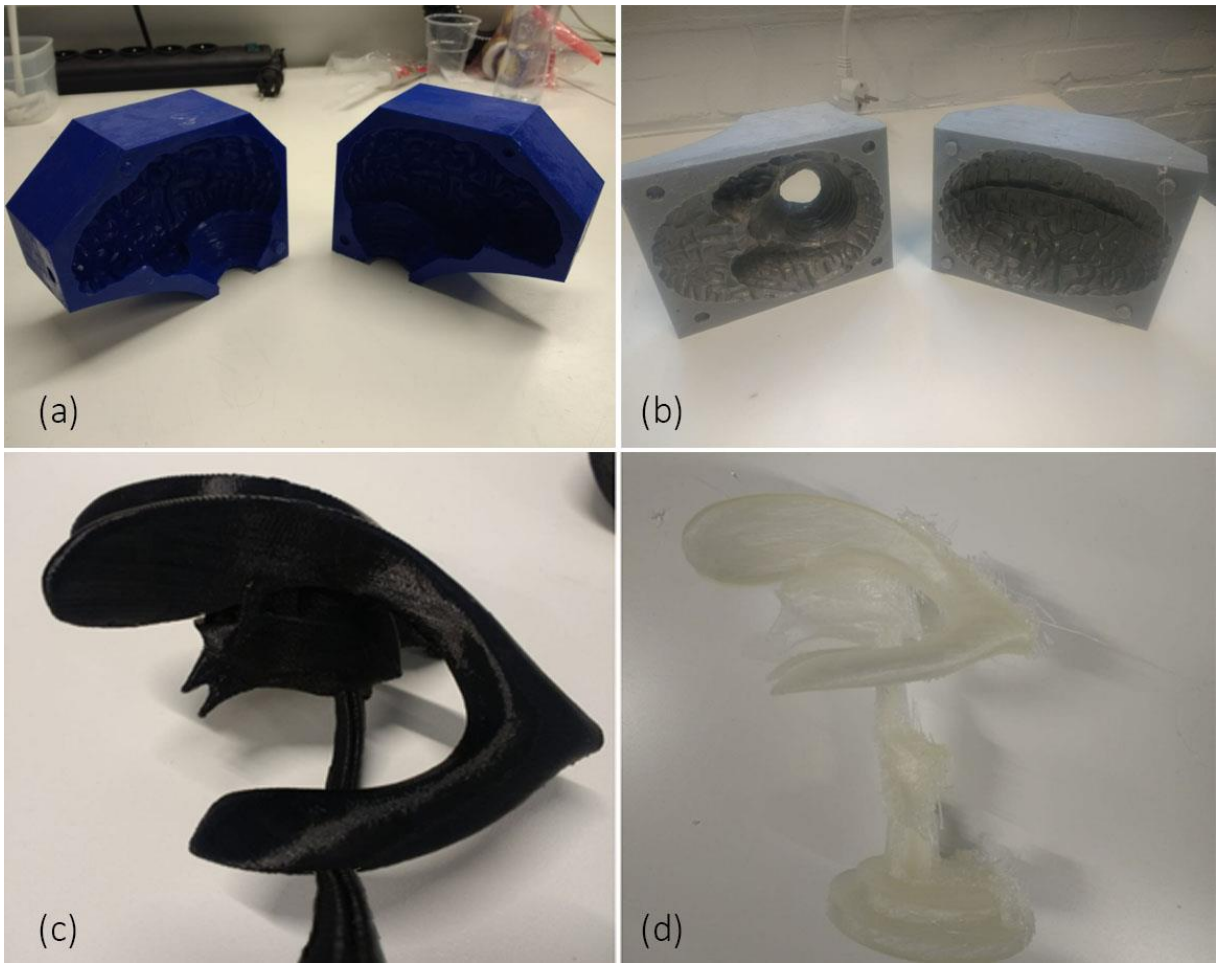

FIGURE 19 - 3D PRINTED PARTS (A) MOULD A (B) MOULD B (C) VENTRICLE FROM PLA (D) VENTRICLE FROM PVA

3.4. MATERIAL SELECTION

TMM's for a phantom should be carefully selected. In terms of mechanical properties, the material should have comparable characteristics as to those of the tissue they resemble, and enough strength and toughness to withstand impact forces that might occur during transportation and usage. For imaging, it should resemble the attenuation characteristics compared to the tissue they resemble.

For this project of the brain, the material should also be suitable for the selected production principles, so the material should be able to be cast into the developed mould shapes. This section describes the material selection.

3.4.1. TMMS IN LITERATURE

In the performed literature study, an overview of brain tissue mimicking materials was given, see section 2.4. Based on the findings in the literature study about TMMs a combination of different TMMs were selected to evaluate for the production of the brain phantom. PVA, PVC, gelatine and agar were described in literature to have promising properties for mimicking brain tissue and were therefore selected to further evaluate for the production of the brain phantom in this study [7], [37], [47], [54], [55], [61]–[63]. Regarding the mechanical properties, these materials are easily adjustable using different concentrations during production. They were assessed on durability and suitability for the selected concepts.

3.4.2. EVALUATION OF SELECTED MATERIALS

The TMMs mentioned in the previous section, section 3.4.1 will be assessed on durability and suitability for the selected concepts. For one the fabrication idea with dissolving the PVA printed ventricle shape out of the casted shape, it is important that the TMM does not dissolve in water. The materials were further investigated and some were found not to be suitable for the production of a brain phantom in this study. Materials excluded from this study, together with the reason for exclusion are listed in table 2.

TABLE 2 - MATERIALS EXCLUDED FOR PHANTOM DEVELOPMENT

Material	Reason for exclusion
PVC	Toxic production process
Agar	Fast degradation and soluble so not applicable for concept 2 and 3
Gelatine	Fast degradation and soluble so not applicable for concept 2 and 3
Polyacrylamide gel	Toxic production process

PVA is a promising material for the development of a brain phantom and was therefore selected for the development of the brain phantom. The following section will provide more information about PVA and its production variables.

3.4.3. PVA

Polyvinyl alcohol (PVA) is a synthetic polymer synthesized from polyvinyl acetate through hydrolysis of the acetate groups [54]. PVA is the world's largest volume, synthetic and water-soluble polymer with a molecular weight ranging from 25,000 to 30,000. When a solution with PVA undergoes a period of freezing cycles and is let to set to slowly thaw to room temperature it is called a freeze-thaw cycle (FTC). During this process of FTC's, the liquid PVA solution forms into an elastic semi-opaque gel known as polyvinyl alcohol hydrogel [8].

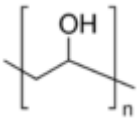

$$[-CH_2CHOH-]_n$$

A paper by Chen et al. investigated PVA hydrogel for the use of brain phantoms. They assessed different concentrations of PVA (4%, 5%, 6%, 7% of 8%) with either 1, 2, or 3 FTCs and concluded that a concentration of 6% PVA solution at 1 FTC was similar to palping the surface of a live brain and had an elastic modulus of 4.6 kPa, which is in the range found from human tissue [64].
This concentration of PVA will be adopted as the right concentration for the development of the brain phantom.

The PVA that will be used for this research is the type that is available at the MISIT lab at the Department of Biomedical Engineering at the TU Delft: Sekisui SELVOL ™ Polyvinyl Alcohol. SELVOL ™ 165. This PVA has a white-to-cream fine granular appearance.

3.4.4. CONCLUSION

Based on the comparison of the characteristics of the different TMMs and the accessibility of them, it was concluded to continue the development of the brain phantom with PVA.
This also because PVA lends itself perfectly for adding contrast material, concerning later development of the phantom for the imaging characteristics. For this research, this concerns CT, but also MRI and ultrasound contrasting additives comply with PVA. The mechanical properties are easily adaptable to the desired characteristics.

As mentioned in section 3.4.3. a 6% PVA solution at 1 FTC will be used for the development of the brain phantom.

3.5. GENERAL PREPARATION AND PRODUCTION

3.5.1. MOULDS

As described in section 3.3.2., two different orientations of brain mould shapes were created in Rhino 3D CAD software. These files were saved as STL file to be able to 3D printed. The moulds were printed in PLA with the Ultimaker 3 Extended 3D printer. The moulds were then coated with XTC-3D brush-on coating for 3D printed parts, in order to make the moulds watertight, so no material could leak through the 3D printed layers while casting. For the exact printing and coating process see appendix B.

To completely prepare the moulds before casting, the edges are brushed with Vaseline, pure petroleum jelly original, to prevent the liquid TMM solution to leaking between the parts. After this, the mould parts were put together and tied together by straps to make sure they stay together after pouring the liquid PVA in.

3.5.2. PVA SOLUTION PREPARATION

The PVA solution used to cast the brain phantom were prepared using SELVOL ™ Polyvinyl Alcohol 165, by Sekisui speciality chemicals, America. A solution of 6% PVA was prepared in a glass beaker by heating water and adding a percentage weight of the PVA to the water. The mixture was constantly stirred and kept to 93°C by using a magnetic stirrer device, IKA C-MAG HS 7 control until all PVA crystals were completely dissolved. The beaker was wrapped in aluminium foil in order to keep a more equally divided heat throughout the mixture. The mixture was constantly stirred at 350 RPM and occasionally additionally stirred to make sure all the PVA crystals dissolved in the solution. More about the production of the PVA and the used concentrations, see Appendix C,

3.5.3. PHANTOM PRODUCTION

When the PVA crystals were completely dissolved, the solution was poured into the moulds. After the mould is filled it was placed into a freezer for the FTC. In this freezer the moulds are frozen at -25°C for at least 24 hours.

After the freezing, the mould was taken out of the fridge and let to rest at room temperature for 12 hours. After this time, the mould was opened to take the brain model out, put in a box filled with water and put into a fridge for storage. More about the production of the phantoms can be found in Appendix C.

3.6. INITIAL RESULTS AND OBSERVATIONS

In this section, the results of the production of the different concepts will be shown along with the observations concerning the models finish and ventricle appearance.

CONCEPT 1:

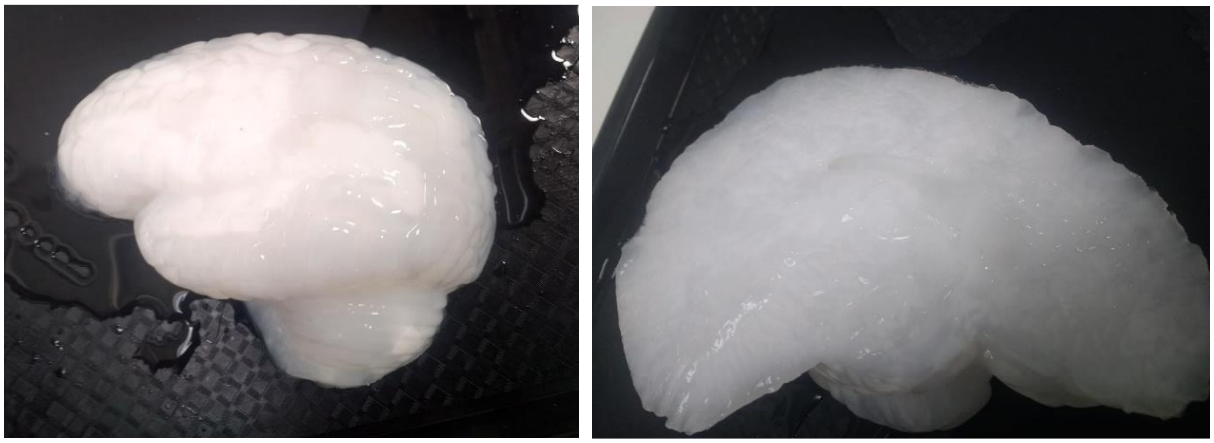

FIGURE 20 - RESULTS CONCEPT 1

This was the first model that was made. During the freeze cycle of the model, the material expanded resulting in the PLA printed mould. For the other models that will be produced, coolant will be added to the solution in order to reduce and control this expansion during freezing.

As can be seen in the picture there is no control over the surface finishing at the point where the material does not touch the mould. It does not have a smooth finish but it is wrinkled after it defrosted. Adding two halves together will result in a strange midline between the two sections and will be hard to fit each other in the right position. Though the use of the solid PLA printed ventricle resulted in a hollow space inside the casted PVA.

CONCEPT 2:

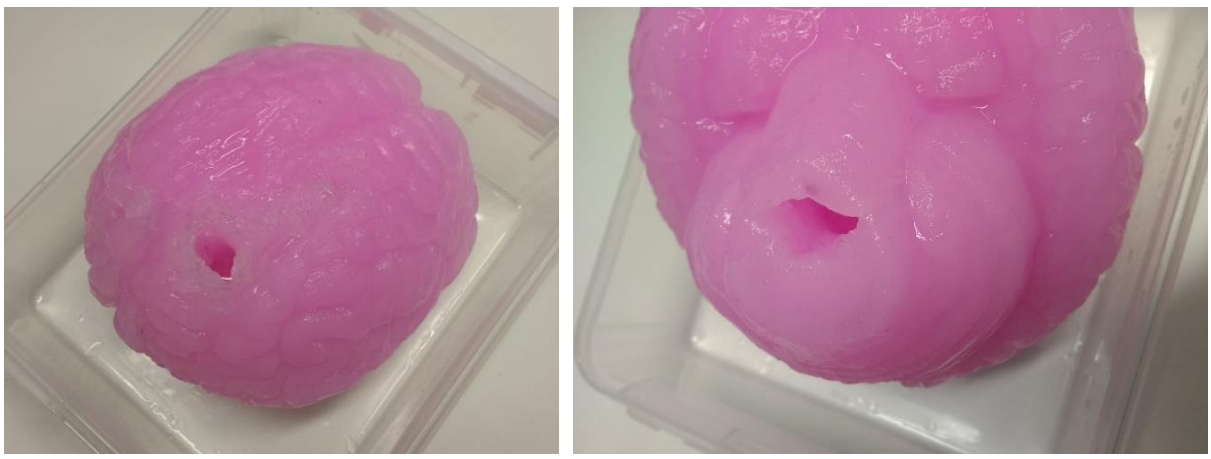

FIGURE 21 - RESULTS CONCEPT 2

Figure 21 shows the results of concept 2, using the PVA printed ventricle. With the first attempt to make the brain phantom with PVA with the sagittal split mould, the PVA solution was poured in while it was not completely cooled down to room temperature. Because of this, the 3D printed ventricles started to dissolve already and changed shape and sank to the bottom of the mould, being the top of the brain, as

you can see on the left in figure 21. Also in this model, the mould leaked so the mould is not completely filled. Altogether it still shows that the 3D printed PVA ventricle can be dissolved out of the PVA brain model, leaving a hollow space This was evaluated by cutting the model in slices. This can be found in Appendix C.

CONCEPT 3:

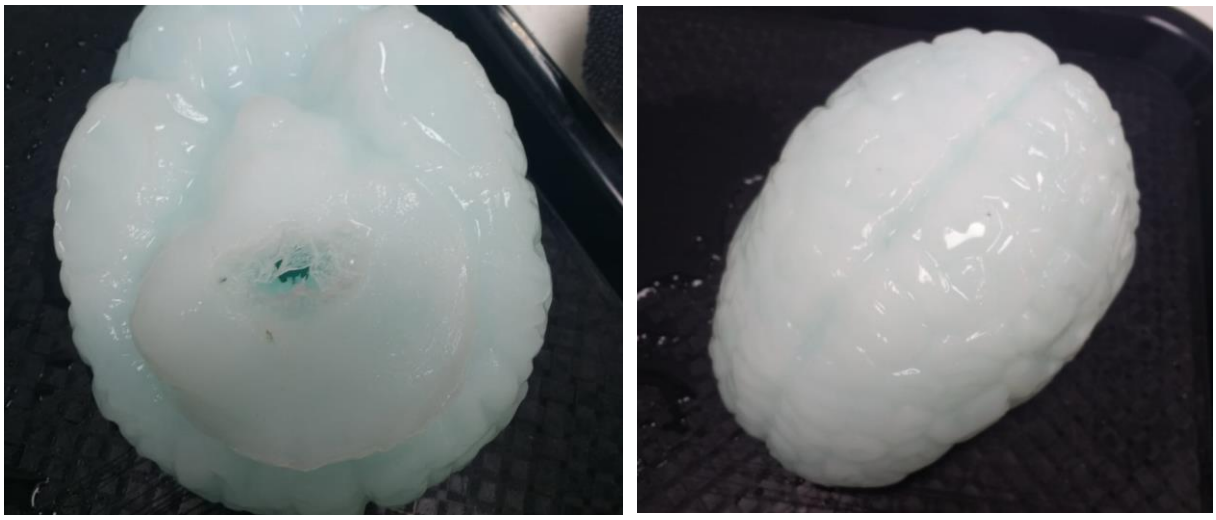

FIGURE 22 - RESULTS CONCEPT 3

The casting of this mould was very easy and no problems with leakage. The difficulties with this concept were the positioning of the PVA ventricles. Also, this model was made from 100% coolant. This model came out smaller than the ones from the other mould. At first, it was expected that this might be due to an error in mould development or production. Later in the process, more experiments with coolant were done and it was concluded that the use of coolant results in shrinking of the material. For more about the use of coolant see chapter 4, section 4.3.

From the results from the concepts it was found that dissolving the PVA printed ventricles out of the TMM brain phantom showed promising results as by touching the model and feeling the inside a hollow space was perceived, and by slicing the model from concept 2 which can be found in Appendix C. For the initial results, to assess this hollow shape on the desired shape of the ventricles it is assessed using ultrasound in the next section, 3.6.1.

3.6.1. ULTRASOUND

The ultrasound machine available at the MISIT lab at the TU Delft was used for the initial evaluation of the models, to check if the hollow spaces were visible and to assess its shape in the models from one part. The ultrasound machine that was used is a Philips HD7 XE.

The figures below show the set up that was used, see figure 23. To use the echo on the brain model, the phantom was placed in a box of water, so the ventricles filled up with liquid, causing it to better visible at the ultrasound images.

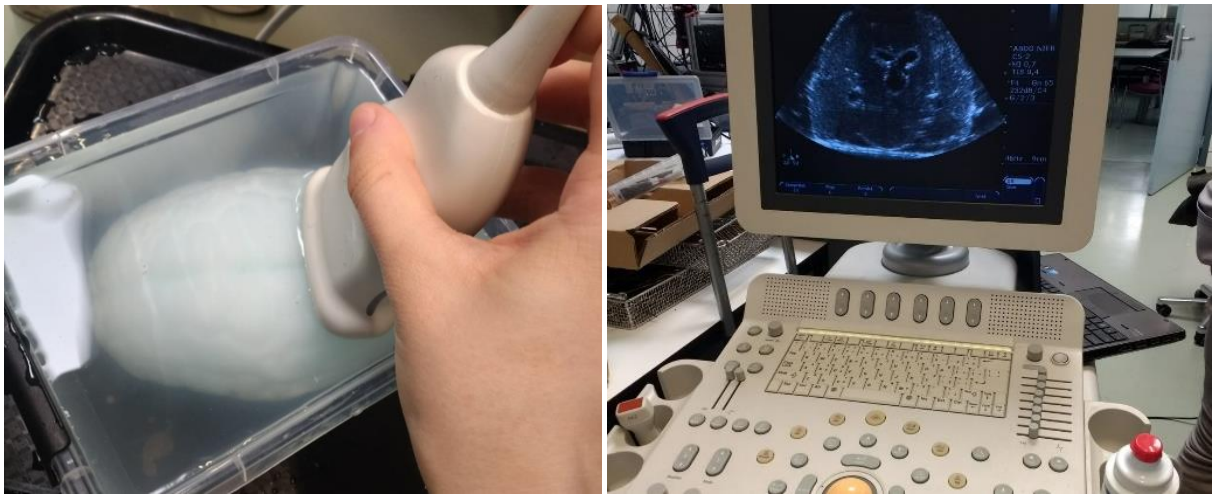

FIGURE 23 - ULTRASOUND IMAGING SET UP

Below, the ultrasound images that were made can be seen, see figure 24. The blue arrow indicates where the lateral ventricles are visible. The shape of the ventricles can be clearly identified. This confirms that there is a hollow space inside the brain model, in the shape of the ventricles.

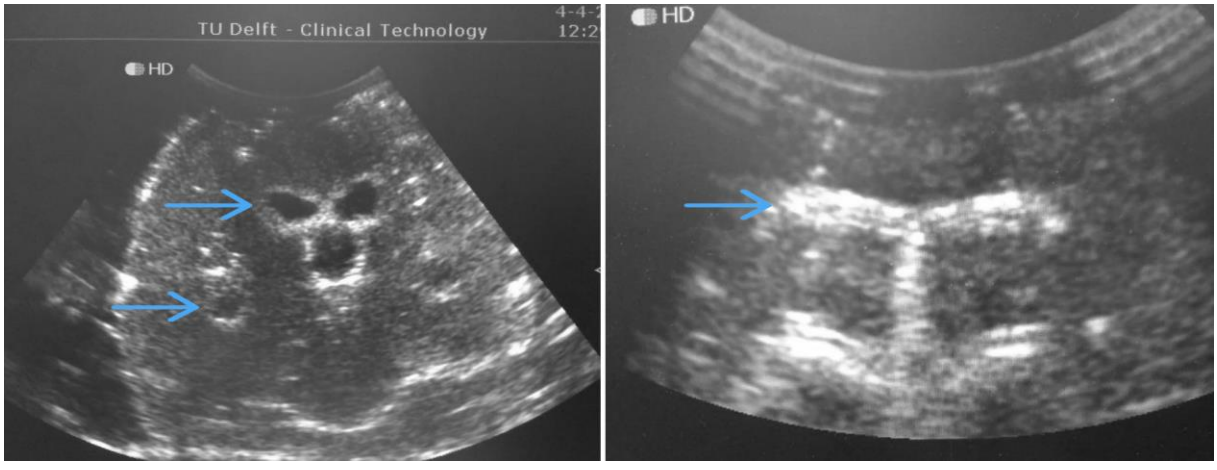

FIGURE 24 - ULTRASOUND IMAGES OF BRAIN PHANTOM FROM CONCEPT 3

3.7. EVALUATION

The different concepts will be evaluated on the basis of a Harris profile, a graphic representation of the strengths and weaknesses of design concepts. Evaluation points were set up with which the concepts must comply. The concepts were assessed on these points, resulting in a clear overview of the potential of the concepts.

EVALUATION POINTS		-2	-1	+1	+2	-2	-1	+1	+2	-2	-1	+1	+2
1.	Control over ventricle position			■	■			■	■		■		
2.	Overall quality		■					■				■	
3.	True to shape		■				■					■	
4.	Finish	■	■					■				■	
5.	Assembly	■	■					■	■			■	■
6.	Ease of fabrication		■					■				■	
7.	Parts		■					■				■	

FIGURE 25 - HARRIS PROFILE

Figure 25 shows the Harris profile assessing the three concepts. The profile clearly shows that concept 1 is not a viable option for the further development of the brain phantom. Concept 2 and 3 both showed promising results, yet concept 2 shows slightly better evaluation based on the Harris profile evaluation points.

3.8. CONCLUSION

Based on the evaluation of the different model described in section 3.6, the fabrication principle of concept 2 was chosen to further investigate the development of the brain phantom.

The model developed with the sagittal split mould and the combination of the 3D printed dissolvable PVA and the PVA as TMM showed promising results. It is the most practical solution as the model can be produced in one part and does not have to be assembled after, creating one smooth brain model. This combination will be used for further evaluation and development for the brain phantom.

4. OPTIMIZATION

The previous chapter describes the initial brainstorm, development and selection of the fabrication principle for a brain phantom. The next chapter will be about the further development and validation the most promising and practical production principle.

4.1. ITERATION

After further development of brain phantoms and further evaluation using the selected mould (see chapter 3, section 3.8.) it was decided to alter from 2 halves to 3 parts. Combining the previously developed mould principles from concept 2 and 3, combining the best of the two concepts, see figure 26.

With the new mould, the original shape of the brain can be used (without the extension of the temporal lobe), while the PVA ventricle can easily be placed in the right position.

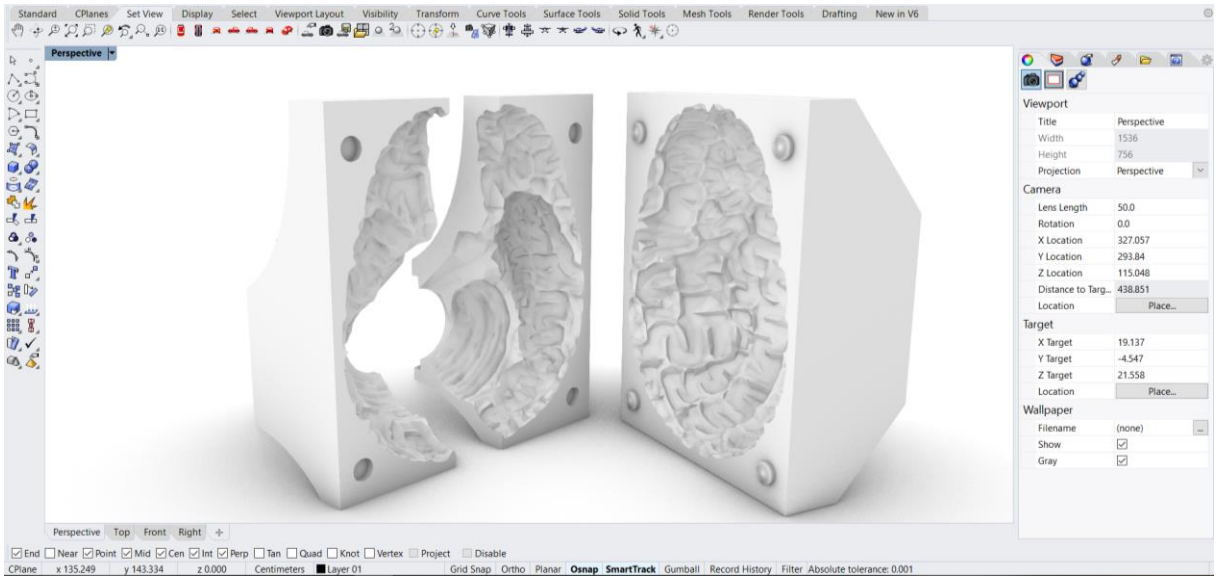

FIGURE 26 - SCREENSHOT FROM RHINO WITH THE IMPROVED MOULD SHAPE

4.2. COMPUTED TOMOGRAPHY

As described in chapter 2 section 2.2.1. Computed Tomography (CT) is a non-invasive technique to create images of structures inside the body with X-rays, a form of electromagnetic radiation. Digital geometry processing can be used to generate 3D images of brain tissue and anatomical structures present inside the brain made from a series of 2D X-ray images [65]. Images are made based on the radiodensity of the different tissues. The radiodensity indicates the ability of the material to electromagnetic radiation to pass through the material. Materials that inhibit the passage of X-rays are called radiodense and the materials that let X-rays pass are called radiolucent. Radiodense materials like bones have a white or light grey appearance on CT scans while radiolucent materials like skin muscles and brain tissue look black or dark grey. Radiodensity can be quantified according to the Hounsfield Scale.

4.2.1. HOUNSFIELD UNITS

The radiodensity of a material can be indicated in Hounsfield Units (HU), which is a linear scale of grey values of voxels. A voxel is a pixel with the thickness of a single slice in the 3D scanned volume). The HU value can be calculated with the following equation:

$$HU = 1000 * \frac{\mu_x - \mu_{water}}{\mu_{water}}$$

In which $\mu_x$it the linear attenuation coefficient of the tissue and μ_{water} is the linear attenuation coefficient of water.

The HU values of the tissue types of the head are listed in the table below, see table 3.

TABLE 3 - TYPICAL HU VALUES OF HUMAN TISSUES IN THE HEAD [56].

Tissue type/TEM	Lowest HU value	Highest HU value
Bone	700	3000
Muscle	10	40
Brain	20	45
Cerebrospinal fluid	5	15

4.2.2. CONTRAST ENHANCING

For this research, the phantom should comply with X-ray and CT imaging. The current material, PVA, is a soft TMM that does not offer enough contrast for the phantom to show the desired characteristics, also see chapter 2 section 2.5.1. Chemicals can be used to change this contrast. The PVA phantom with the previously described PVA concentration and freezing cycles is used as the base solution for dissolving the contrast enhancing chemical. For CT imaging this contrast enhancing chemical is barium sulphate.

$$BaSO_4$$

For this research, SIGMA-ALDRICH ® barium sulphate will be used, which was offered by Philips Healthcare. This barium sulphate comes in white powder shape and is easily dissolvable in a solution.

4.2.3. DIFFERENT CONCENTRATIONS

For the evaluation of what the right concentration of barium sulphate should be, different samples are made to compare the imaging of these samples. Samples of 6% PVA and one FTC as determined in section 3.4.3, where prepared with 0.5%, 1, 1.5%, 2%, 3%, 4% and 5% barium sulphate, see figure 27.

FIGURE 27 - SAMPLES WITH DIFFERENT CONCENTRATIONS OF THE CONTRAST ENHANCING BARIUM SULPHATE

These samples were put in a larger container with water to assess the contrast between the samples and the surrounding water. The container was sent to Phillips Healthcare, Best, The Netherlands to have them scanned with the CT scan so their contrast could be evaluated and to determine the HU of the samples.

4.2.4. SCANS VISUAL

The container containing the samples that were sent to Philips Healthcare was rather large, causing the samples of 5% barium sulphate not to be included in the scans as it did not fit the frame, see figure 28.

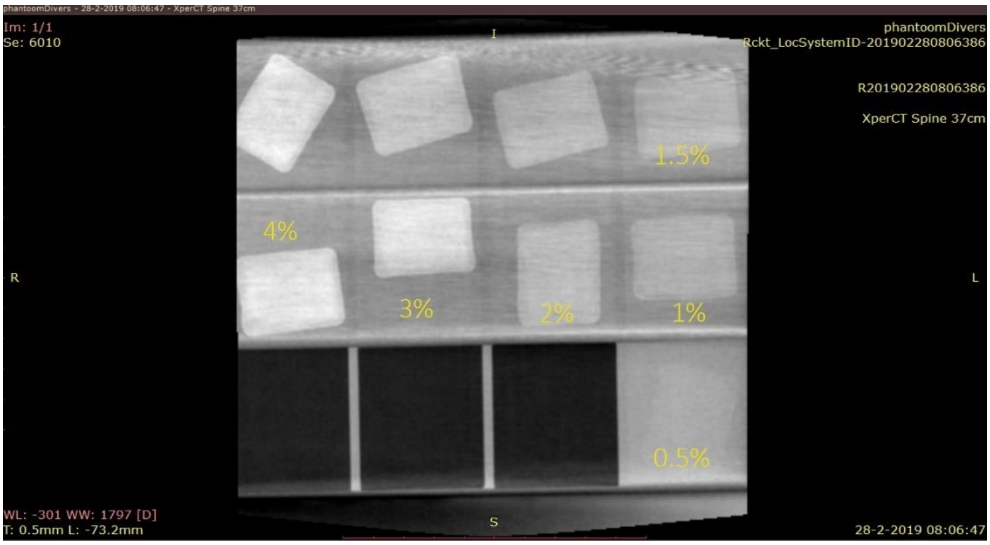

FIGURE 28 - SCAN OF THE SAMPLES WITH DIFFERENT CONCENTRATIONS OF BARIUM SULPHATE

4.2.5. DETERMINATION OF HOUNSFIELD UNITS

From the provided scans of the samples of the previous section, the HU was determined in different ways. As the HU has a linear relation with the grey values ImageJ was used to determine these grey values. ImageJ is an image processing program developed at the National Institutes of Health and the Laboratory for Optical and Computational Instrumentation. As the HU of water and air are known, these values were used to set up an equation to calculate the HU of the samples as a function of their grey value, see Appendix D.

TABLE 4 - DETERMINATION OF HU USING MEAN GREY VALUE FROM IMAGEJ

		Mean Value from ImageJ	Hounsfield Unit (HU)
1	Air	3327	-1000
2	Water	16096	0
3	Sample with 0.5% BaSO4	18766	209
4	Sample with 1% BaSO4	19419	260
5	Sample with 1.5% BaSO4	20012	306
6	Sample with 2% BaSO4	20462	340
7	Sample with 3% BaSO4	24553	662
8	Sample with 4% BaSO4	25077	703

Table 4 shows the mean grey value of the different samples and the calculated value for the HU. These calculated values fall far beyond the expected range and do not match the values described in literature. Therefore these values are assumed false and RadiAnt will be used to inspect the HU of the samples.

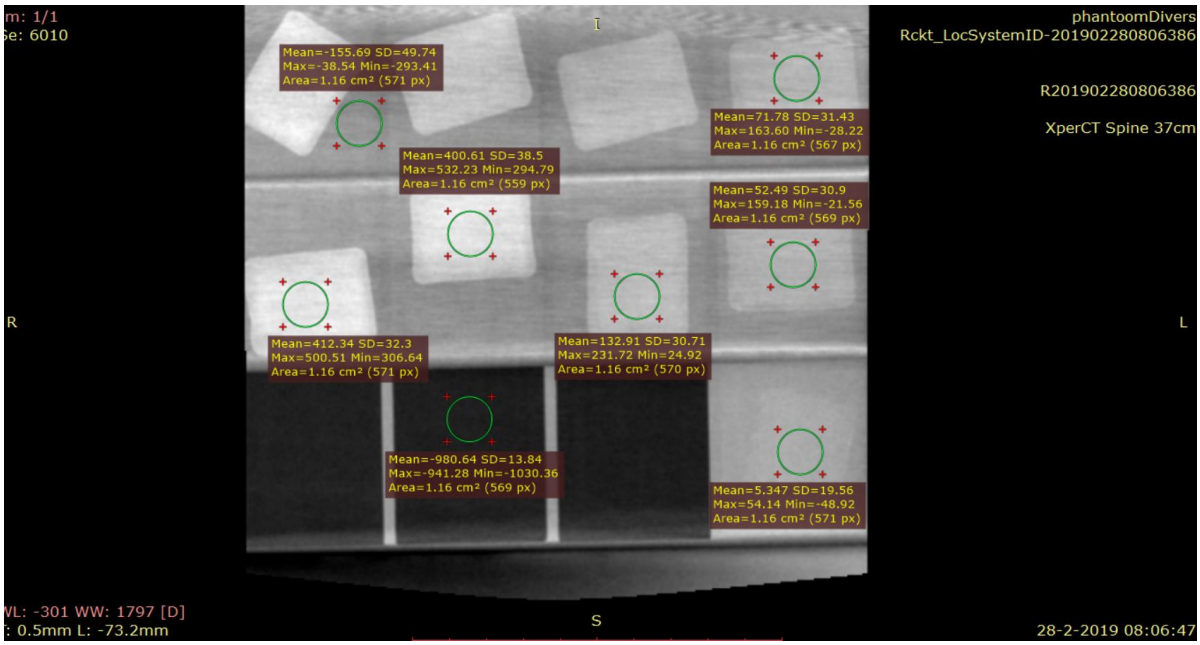

FIGURE 29 - DETERMINING HU OF SAMPLES USING RADIANT

In figure 29 it can be seen which areas were used to determine the HU values from. Air, water and the samples with different concentrations were assessed. Remarkable is the fact that the HU value of air determined with RadiAnt is -980, which is close to the expected value of -1000 stated in literature. However, the mean value of water was found to be -155, which is too low for water. Also, the differences between the samples with different concentrations are found to be inconsistent and do not appear to have a linear relationship, see table 5.

TABLE 5 - DETERMINING THE HU VALUE OF SAMPLES USING RADIANT

		Mean HU determined with RadiAnt
1	Air	-980
2	Water	-155
3	Sample with 0.5% BaSO4	5
4	Sample with 1% BaSO4	52
5	Sample with 1.5% BaSO4	71
6	Sample with 2% BaSO4	132
7	Sample with 3% BaSO4	400
8	Sample with 4% BaSO4	412

The determination of the HU of the samples was considered to be inconsistent so no real conclusions for the development of the brain phantom could be drawn from these values. Based on the determined HU values the samples of 3% and 4% barium sulphate were considered to be definitely too high, and based on the contrast between the sample of 0.5% and the water around it was considered too low. Therefore it was chosen to continue to develop a model from 1% and 2% concentration barium sulphate for further evaluation. Also examples from literature support this [59], [66]. Even though the HU values that were determined with RadiAnt for these concentrations were still too high, as the determining of the HU values were considered not to be truly reliable and needs further evaluation in the brain phantoms.

4.3. COOLANT

For the development of the brain phantom, coolant was used, to reduce expansion during the freeze cycles. The coolant that was used is CareX® long life G12+ coolant. Use of no or too little coolant resulted in cracking of the mould during freezing. To make sure this doesn't happen, coolant was used for the development of the TMM. To check the influence of the coolant on the mechanical and optical characteristics of the brain phantom, a small test was set up using different concentrations of coolant, see figure 30.

FIGURE 30 - SAMPLES WITH DIFFERENT CONCENTRATIONS OF COOLANT PRODUCTION

The use of coolant during the development of a phantom from PVA has some influence on the mechanical properties, in particular, the high concentrations of coolant. An interesting observation is that the sample of 100% coolant is significantly smaller than the other samples with lower concentrations. This is also clearly visible in the scans of the samples, see figure 31 and 32.

FIGURE 31 - SAMPLES WITH DIFFERENT CONCENTRATIONS OF COOLANT RESULTS

Via trial and error, it was concluded that the use of 40% of coolant was sufficient to eliminate the risk of too much expansion of the PVA during freezing, resulting in breaking of the mould. At 40% coolant, it is was assumed that this has a neglectable influence on the mechanical properties of the phantom. The exact influence of the use of coolant on the mechanical characteristics has to be further researched, also at other concentrations of PVA.

Regarding the imaging of the PVA made with different concentrations of coolant, it was found that coolant does not influence the imaging characteristic in CT, see figure 32.

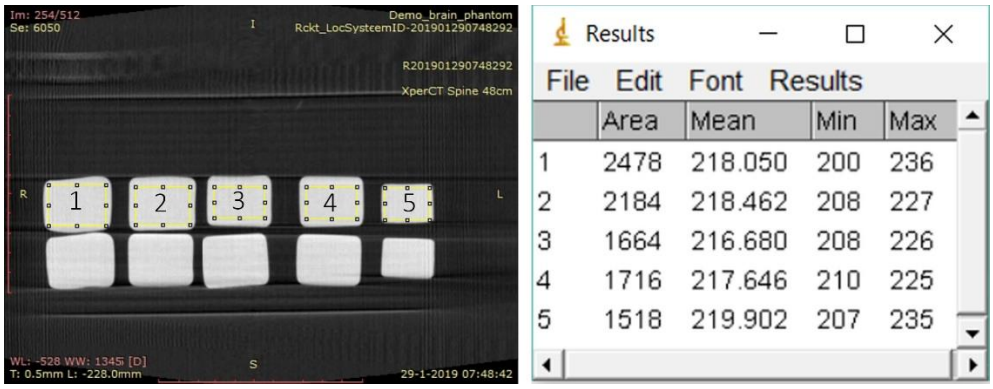

FIGURE 32 - DIFFERENT CONCENTRATIONS OF COOLANT ASSESSED ON INFLUENCE IN GRAYSCALE IN IMAGING WITH CT

The CT images of the samples are analysed using ImageJ. The pixel intensities were assessed at the areas of the samples indicated by the yellow borders in the figure. The values corresponding to the area can be found in the table. In this table, it can be found that the values do not drastically differ so it was concluded that the used coolant does not influence the imaging characteristic in CT.

4.4. PRODUCTION

For increasing phantom contrast in CT imaging, barium sulphate will be added to the solution before it is poured into the brain mould. The process of PVA solution preparation is the same as mentioned in section 3.5.2. except for the addition of barium sulphate. This was added after the PVA crystals were completely dissolved. Solutions were prepared with 1% and 2% weight barium sulphate of the initial base solution. After the barium sulphate was added, the solution continued to be stirred until it was cooled to room temperature, before it was poured into the mould and again put into the freezer at -25°C for 24 hours. More about the preparation of the solution and the used concentrations can be found in Appendix C.

Due to some trial and errors, it was found that the solution had to be cooled down as much as possible before it was poured into the moulds, as the barium sulphate would sink to the bottom during the solidifying process, see Appendix E.

The mechanical properties of the model did not change noticeably with the addition of these quantities of barium sulphate. Although, it should be further investigated what the effect of the barium sulphate is on the mechanical characteristics of the phantom.

4.4.1. RESULTS

The figures below show the physical brain models that were developed using the new and improved mould, see section 4.1.1. Figure 33 shows the model developed with 1% barium sulphate and figure 34 the one with 2% barium sulphate.

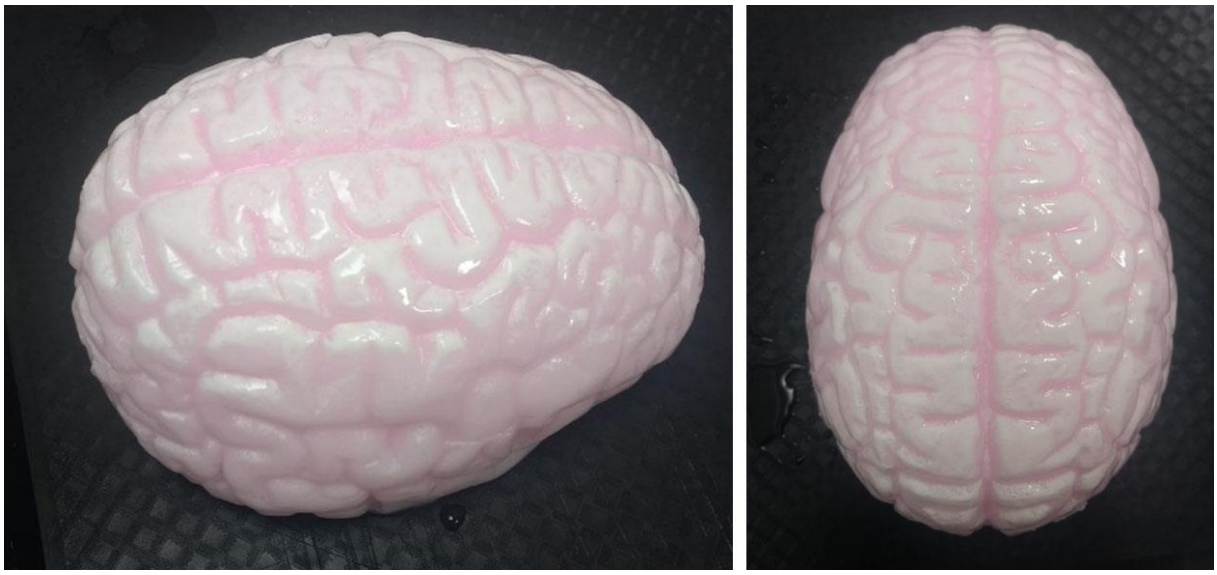

FIGURE 33 - BRAIN PHANTOM 1% BARIUM SULPHATE

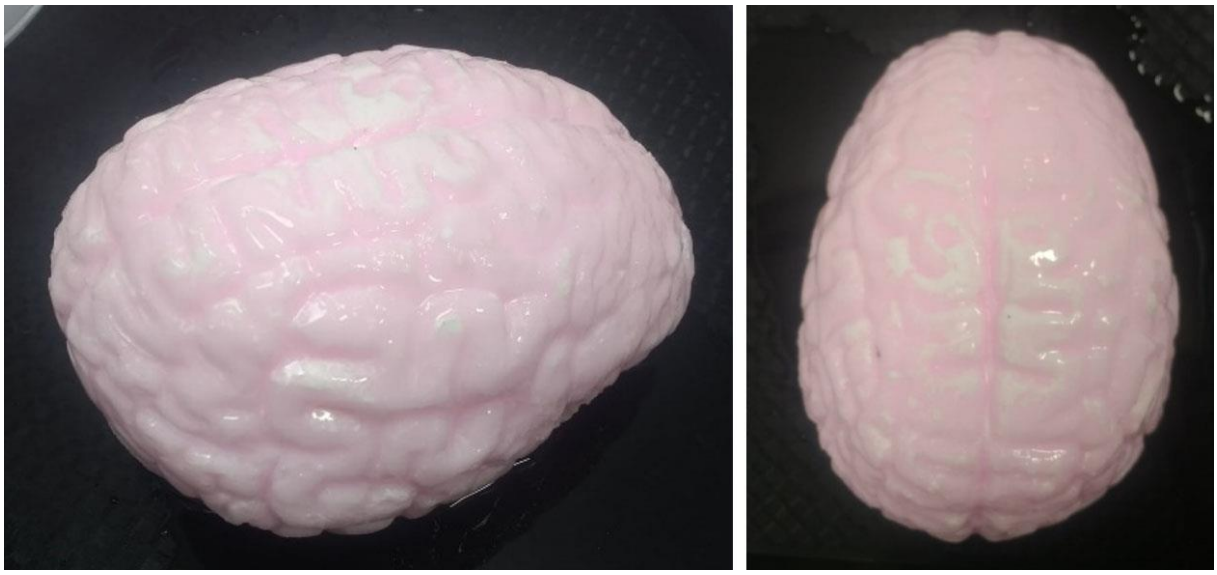

FIGURE 34 - BRAIN PHANTOM 2% BARIUM SULPHATE

Both brain models have a white deposit at the top of the brain where the barium sulphate sedimented during solidifying while freezing. The phantom with 1% barium sulphate has slightly more white deposition than the 2% phantom, as can be seen in the figures above, see figure 33 and 34.

5. EVALUATION AND VALIDATION

To evaluate the developed brain phantoms, the models were scanned at Philips Healthcare, Best, the Netherlands with the XperCT Philips Allura FD20. The data were stored in a DICOM format. To be able to view those files, two software's 3D RadiAnt and 3D slicer were used. RadiAnt is a Windows DICOM viewer for medical images and 3D Slicer is a free and open source software package for image analysis and scientific visualization.

For the evaluation of the brain phantoms, these programs were used to assess the ventricle shape inside from the anterior-posterior, lateral and axial view, as well as segmentation tools that were used to recreate the ventricular shape from the models.

5.1. SCANS VISUAL

This section will display the scans using the used DICOM viewers to evaluate the developed brain phantoms with 1% and 2% barium sulphate.

5.1.1. RADIANT

PHANTOM 1% BARIUM SULPHATE

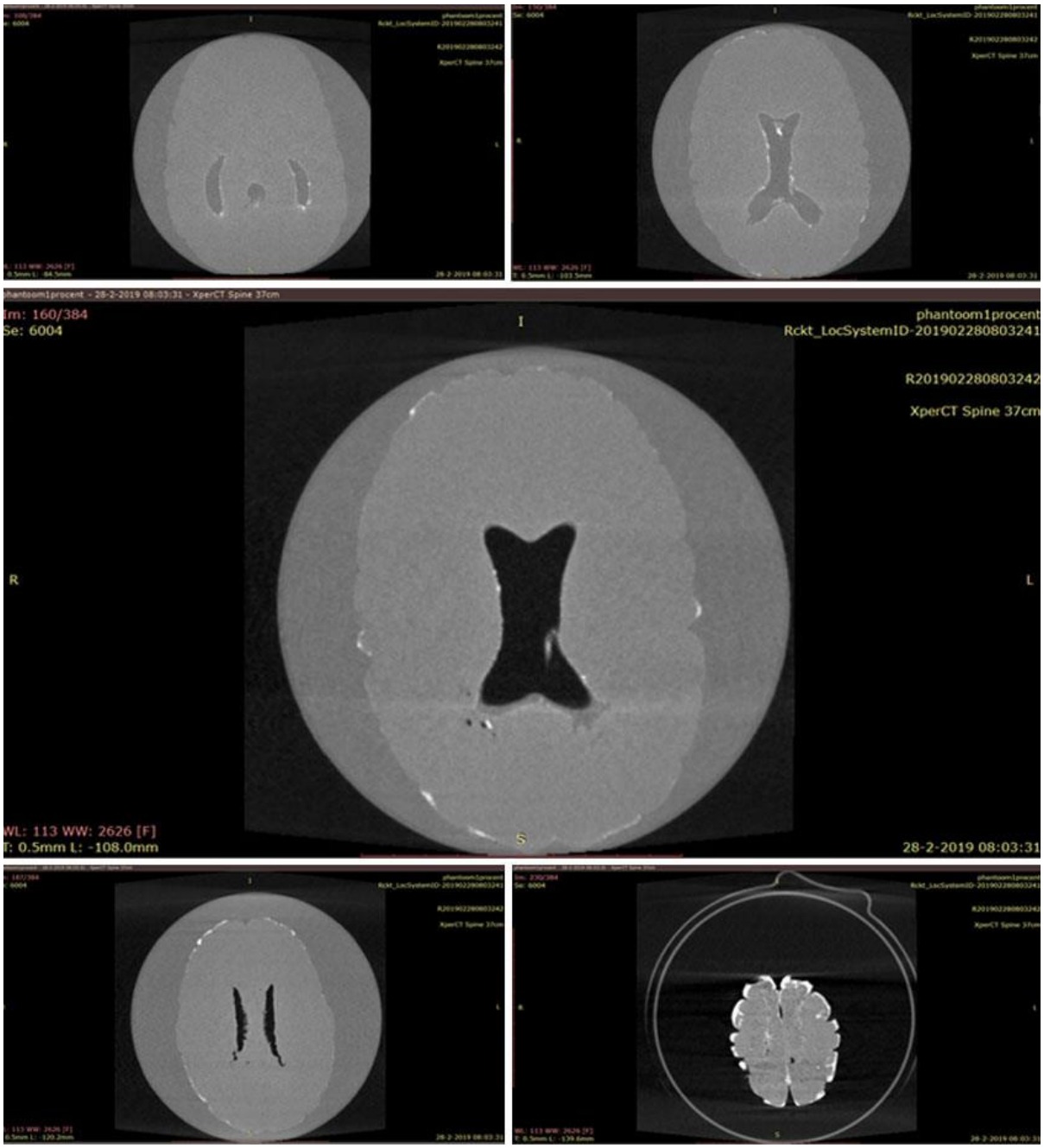

FIGURE 35 - PHANTOM WITH 1% BARIUM SULPHATE VISUALIZED USING RADIANT SHOWING DIFFERENT SLICES

Figure 35 shows the CT scan of the brain phantom made with 1% barium sulphate. The images clearly show the ventricles. They are aligned in the centre and the image is visibly symmetrical. Though as the slices move more to the top of the brain, the ventricles turn up different than the lower slices. This is due to the fact that air got trapped within the ventricles and therefore shows up with different contrast. Though as can be seen in the middle image from figure 35, the two lateral ventricles seem to have

merged together along the longitudinal fissure, the split line between hemispheres of the brain. A small septum should be present, dividing the ventricles into two separate structures.

At some places around the edges of the brain and around the ventricles and especially at the top of the brain, brighter spots can be seen. This is due to the accumulation and sedimentation of barium sulphate, creating a higher concentration in these points. This higher concentration in barium sulphate has a higher radiodensity causing it to light up brighter on the scans.

PHANTOM 2% BARIUM SULPHATE

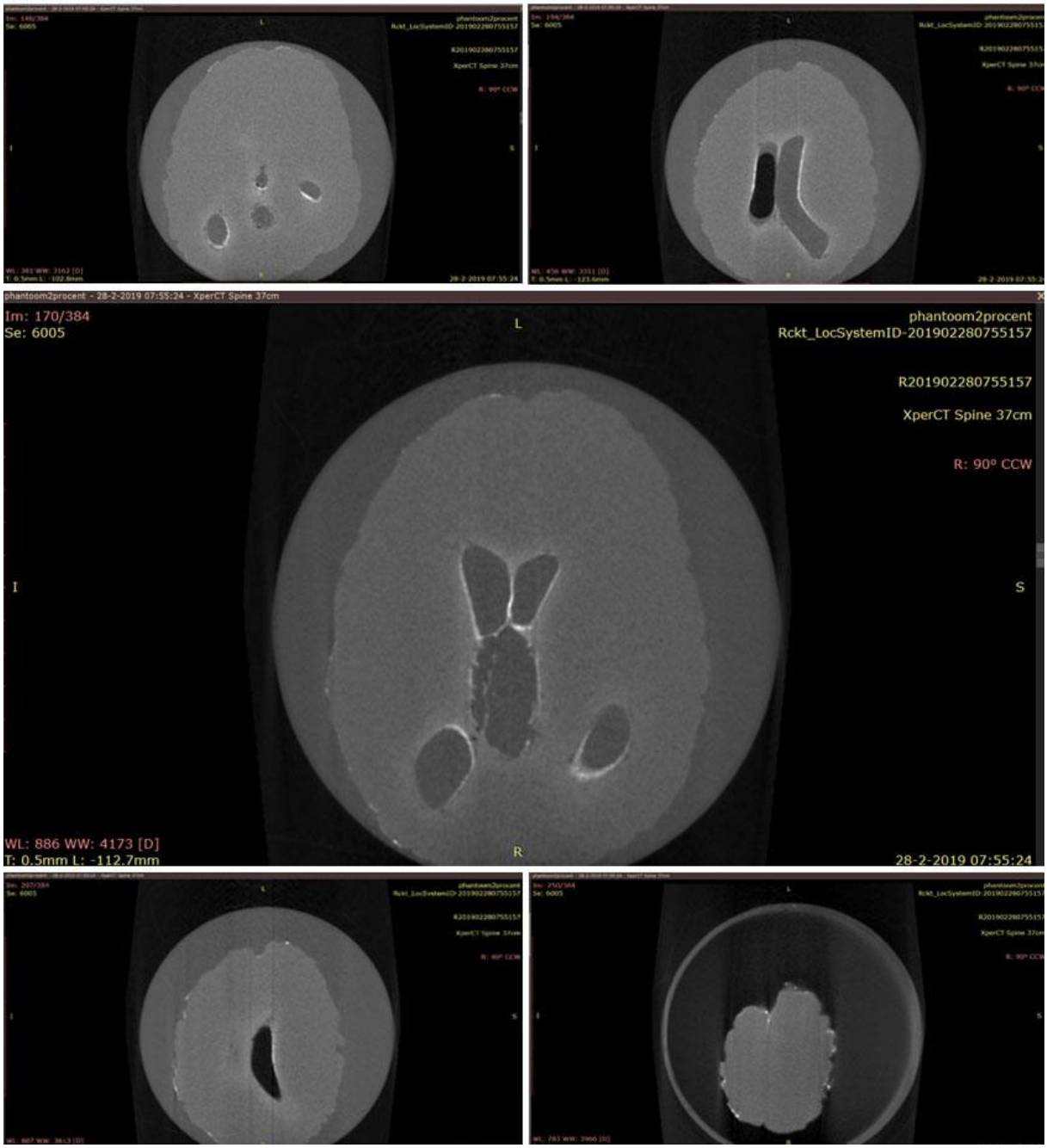

FIGURE 36 - PHANTOM WITH 2% BARIUM SULPHATE VISUALIZED USING RADIANT SHOWING DIFFERENT SLICES

Figure 36 shows the CT scan of the brain phantom made with 2% barium sulphate. Also in this model, the ventricles are clearly visible, yet not as symmetrical as can be seen in figure 35, as the ventricles are not aligned on a clear centreline. By analysing the slices more carefully it was found that this was due to the fact that the phantom model is skewed in the tray at the moment of the CT scan. Compared with figure 34, it can be concluded that the phantom is undoubtedly symmetrical. Though as can be seen in the bottom right picture in figure 36, the right hemisphere seems to be larger than the left side, so it was concluded that phantom is skewed in the tray.

The shape of the third ventricle is considered to be slightly enlarged compared to the originally designed ventricle, see the middle image from figure 36. The two lateral ventricles are also slightly merged but there is still a small sign of a septum dividing the two.

Also in this model, the ventricles have air trapped inside causing them to have a different contrast with the tissue mimicking material around. It seems there is more air present in the ventricle on the left side as is shows up black in lower slices.

Also, the sedimentation of barium sulphate is visible in this model yet less than in the 1% barium sulphate model this was expected as in the figures 33 and 34 from section 4.4.1. there is a clear difference in a white haze on top of the brain phantoms.

5.1.2. 3D SLICER

3D slicer offered 3 views on the scanned phantoms, which are presented below. Also, the build in Volume Rendering tool was used in order to create a 3D rendered shape of the scanned brain model.

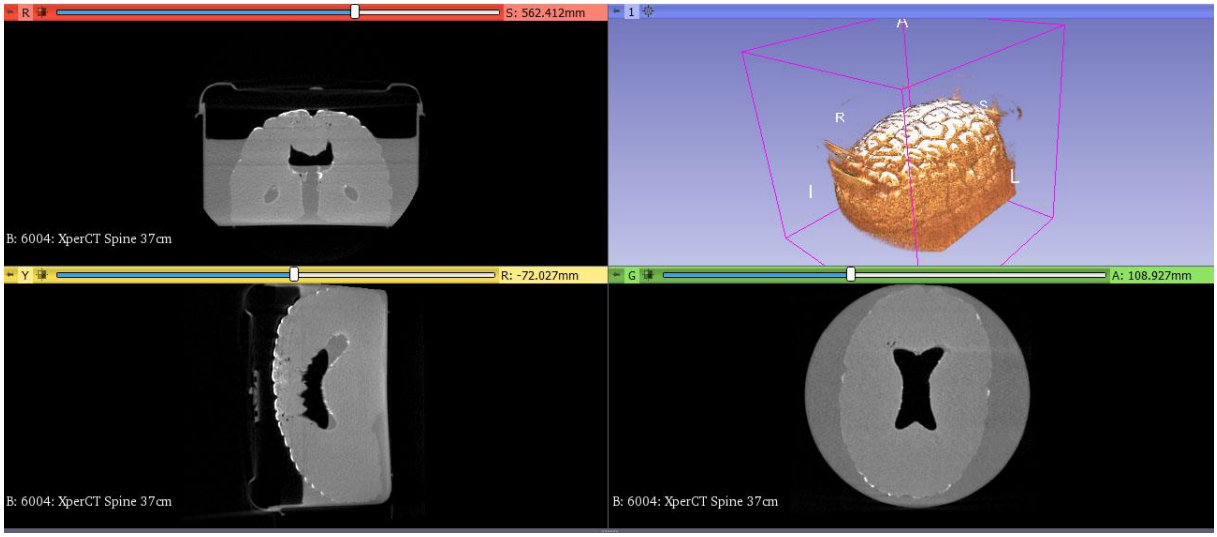

FIGURE 37 - PHANTOM WITH 1% BARIUM SULPHATE VISUALIZED USING 3D SLICER

From these images, it can be seen that there is air trapped in the ventricles as the top part of the lateral ventricles turn up black in the scans. Yet this does indicate that there is a hollow space inside the brain model. 3D slicer provides two extra views that were not assessed with RadiAnt. In two left images in figure 37, it shows that the lateral ventricles have some sort of 'tail' creating a rough finish of the top of the lateral ventricles and don't follow the desired smooth shape. This 'tail' is not visible in two left images in figure 38. The top right images in figure 37 clearly shows the absence of a septum between the lateral ventricles and seem to have merged to one.

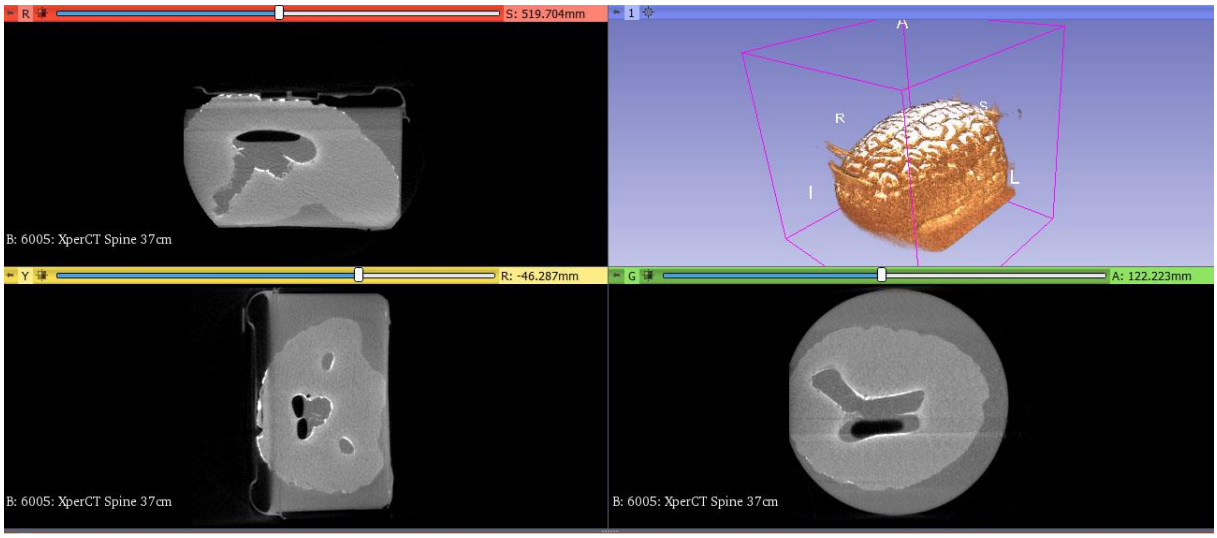

FIGURE 38 - PHANTOM WITH 2% BARIUM SULPHATE VISUALIZED USING 3D SLICER

In figure 38, the phantom with 2% barium sulphate can be seen as shown with 3D slicer. The top left image shows the brain is slightly tilted forward and the bottom left images shows the brain to be tilted to the side, resulting in the distorted images in RadiAnt.

The bottom left image also shows that the third ventricle is enlarged and seems to have merged with the lateral ventricles, yet there still is a small septum visible between the lateral ventricles.

A white glow is visible around the whole ventricle shape caused by the sedimentation of bariumsulphate.

5.1.3. CONTRAST

As can be found in chapter 2, section 2.3.2. the ventricles of the brain, filled with fluid, normally show up darker on a CT. For assessing the scans in the previous sections it was chosen to change the contrast in the images to show only a part of the ventricles in black. This was chosen to clearly show the difference between the part of the ventricle that is filled with fluid and the part of the ventricles that got air trapped inside, as water and air have a different radiodensity.

5.1.4. POSITION OF THE VENTRICLES

To evaluate if the ventricles are in the right position, the modelled mould and ventricle are put next to the scan to compare the results, see figure 39. This was only done for the 1% barium sulphate phantom as the other one was not scanned in the right position.

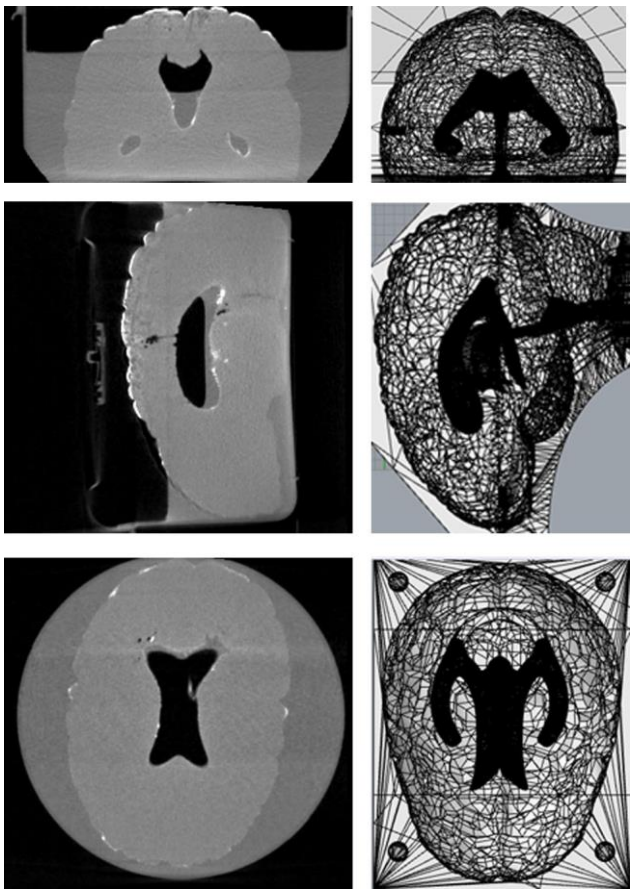

FIGURE 39 - POSITION OF THE VENTRICLES IN THE PHANTOM AND IN THE ORIGINAL MOULD

5.1.5. BRAINS WITH MEMBRANE

In the first scans, the images show that air got trapped inside the ventricles. A second attempt was done, yet this time the brain phantoms were put into plastic bags with water and the brains were put inside the container upside down. It was thought to use the plastic bags as a membrane around the brain to make sure the ventricles were filled with water. However, this idea did not work out the way it was planned and the new images show even more air in the scans. For these images see Appendix F. It was decided to continue with the initial scans.

5.2. SEGMENTATION

3D slicer was used in order to obtain the ventricle shape out of the CT scans by using segmentation tools, segment editor. This segment tool selects areas based on master volume intensity range. The threshold range can be edited in order to segment the right area, see figure 40.

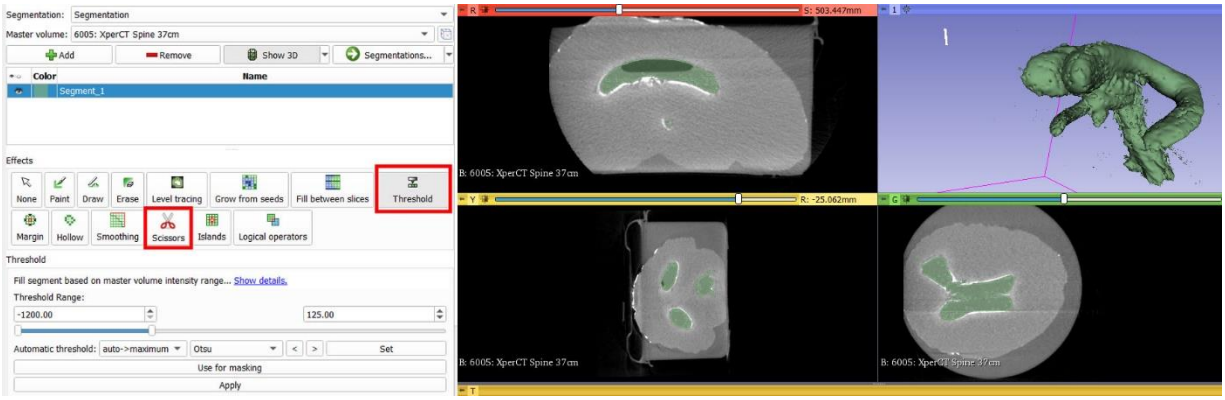

FIGURE 40 – SEGMENTATION PROCESS OF THE VENTRICLE IN 3D SLICER

For the segmentation of the ventricle, the threshold was set on -1200 to 125, to include both the water and the air that was trapped in the ventricle. With this threshold, also the water surrounding the brain was included. This could be excluded by using the scissors tool and cutting around the region of interest, the ventricles, to eliminate excess information. A preview of the segmented element can be seen in the top right corner in 3D slicer, see figure 40. The segmented ventricles were saved as .STL files in order to compare them with the originally designed 3D PVA printed ventricles, see figure 41 and 42. The comparison is done in the next section, 5.2.1.

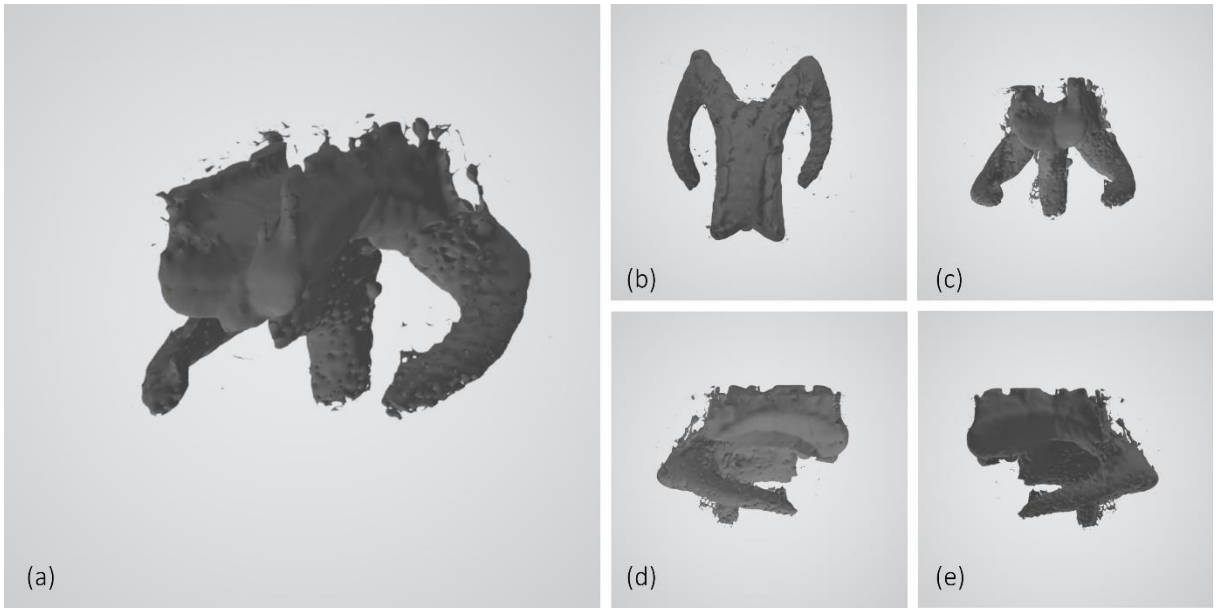

FIGURE 41 - DIFFERENT VIEWS OF THE SEGMENTED VENTRICLE FROM THE 1% BARIUM SULPHATE BRAIN PHANTOM (A) 3D VIEW (B) TOP VIEW (C) FRONT VIEW (D) LEFT VIEW (E) RIGHT VIEW

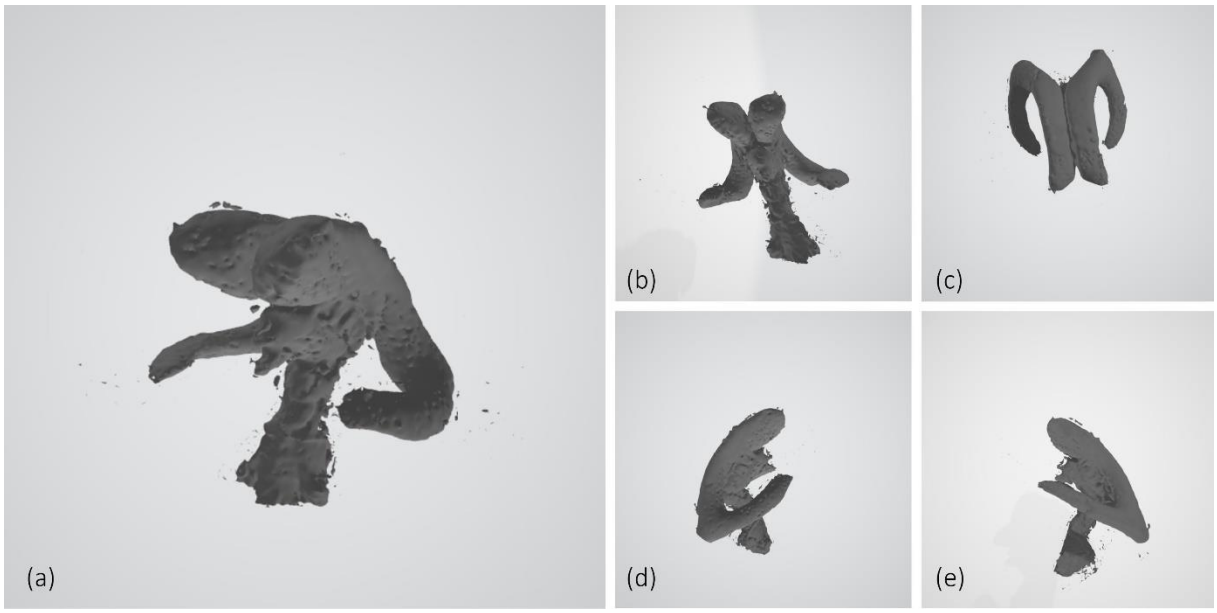

FIGURE 42 - DIFFERENT VIEWS OF THE SEGMENTED VENTRICLE FROM THE 2% BARIUM SULPHATE BRAIN PHANTOM (A) 3D VIEW (B) TOP VIEW (C) FRONT VIEW (D) LEFT VIEW (E) RIGHT VIEW

5.2.1. VENTRICLE COMPARISON

The segmented model from the previous section was compared with the original modelled and the 3D PVA printed ventricle shape in order to evaluate the quality of the ventricle. Generally, it can be said that the originally designed ventricle and the segmented ventricles have the same shape.

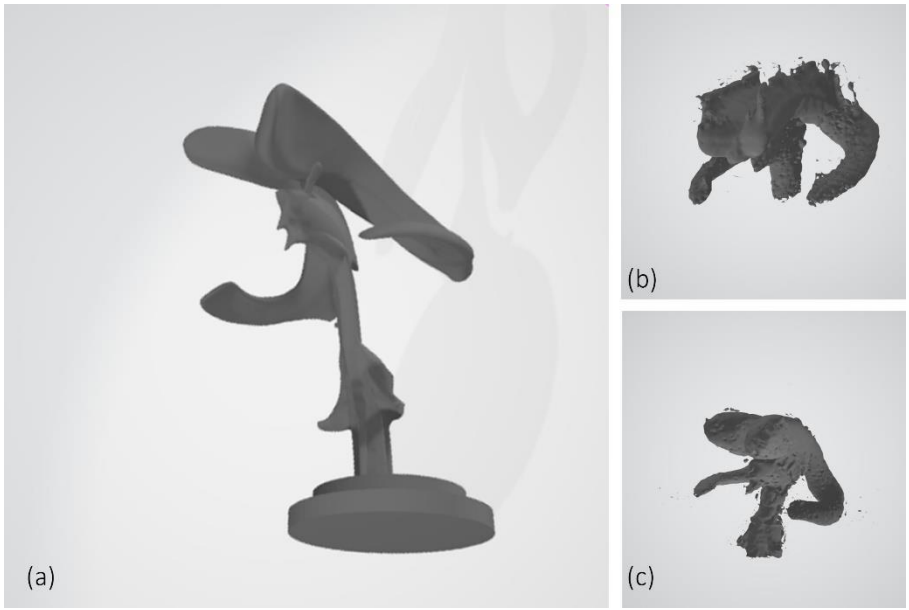

FIGURE 43 - 3D VENTRICLE MODELS (A) ORIGINAL SHAPE (B) VENTRICLE SEGMENTED FROM BRAIN PHANTOM 1% (C) VENTRICLE SEGMENTED FROM BRAIN PHANTOM 2%

It can clearly be seen that the segmented ventricle has a rougher surface finish. This is due to the production process but also the quality of the segmentation tool of 3D slicer. Because the ventricles had to be printed with support material which had to be removed after printing it still shows some remains.

5.3. ENDOSCOPIC EVALUATION

Lastly, to evaluate the surface finish of the ventricles, an endoscope was used to be able to look inside. At first, this was done via the fourth ventricle, as this was the opening already existing in the model, and no new hole had to be made. Though via this technique it was difficult to determine the position and navigate through the ventricles as some angles could not be made with the rigid endoscope. Therefore it was decided to enter the ventricles via the back of the brain, as illustrated in figure 44. For the endoscopic intervention, the 2% barium sulphate model was used.

FIGURE 44 - ENDOSCOPIC INTERVENTION ON BRAIN PHANTOM

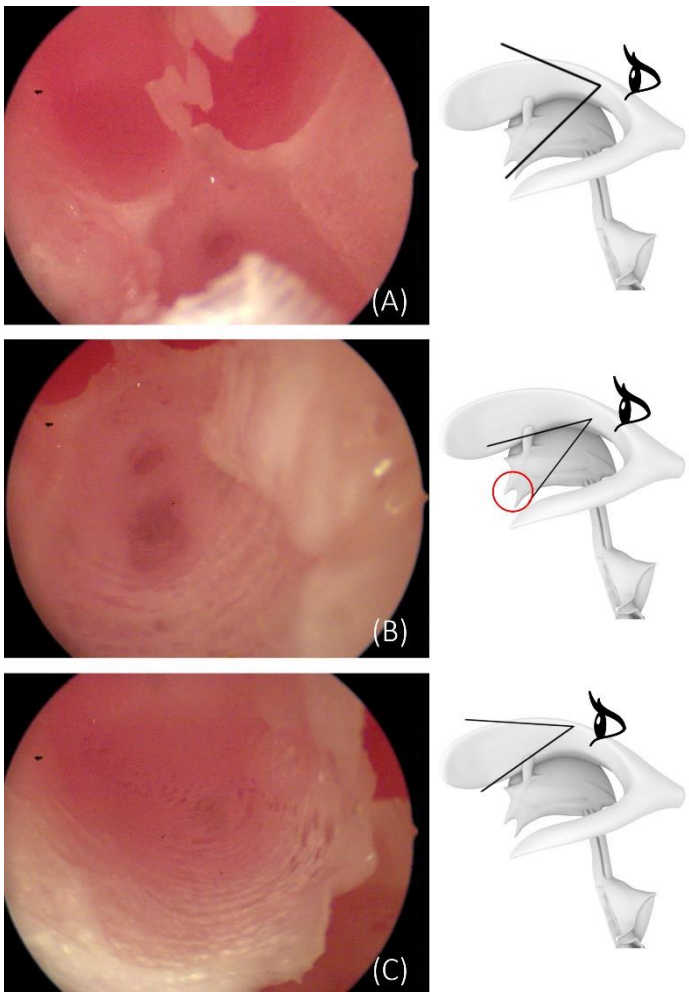

FIGURE 45 - ENDOSCOPIC VIEWS OF THE BRAIN PHANTOM

The images from figure 45 show the endoscopic view inside the ventricles of the brain phantom. The images next to the endoscopic images show what part of the ventricle is visible in the image.

In the image (A) the lateral ventricles are clearly visible, however, there are some unintentional loose films of material between the left and right lateral ventricle. This was identified as a part of the septum that should devide the two lateral ventricles in two separate structures.

(B) shows the third ventricle and two darker sports are visible. This is where the 'spikes' from the third ventricle are located, indicated by the red circle in the image.

Image (C) from figure 45 shows the inside of the left lateral ventricle. It was considered that the ventricle has quite a smooth finish, yet the white sedimentation of barium sulphate can be seen in the ventricle.

5.4. EVALUATION OF THE RADIODENSITY

To assess the radiodensity of the two models of 1% and 2% barium sulphate, a built-in tool from RadiAnt was used to determine the HU of the two phantoms. Notwithstanding that this was considered unreliable during the tests with samples of different concentrations of barium sulphate, it was still done with the two phantom models to get an indication of their radiodensity.

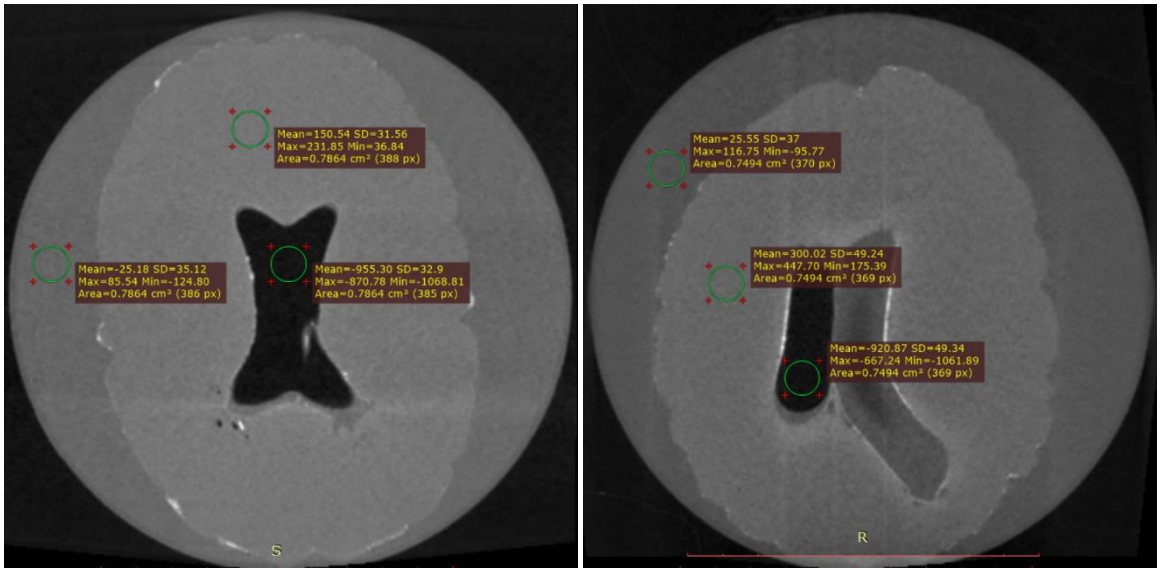

FIGURE 46 -AREAS OF DETERMINING HU WITH RADIANT (LEFT 1% BARIUM SULPHATE PHANTOM, RIGHT 2% BARIUM SULPHATE PHANTOM)

As can be seen in figure 46, different areas were selected to find their average HU. An area of air, water and TMM were selected for their HU values. The figure above shows the mean HU values of the areas but also the maximum and minimum value within the region. Assessing the different HU at different areas of the phantoms, it was found that there is a great variety between within tissue and within the different layers.

The areas of air in the 1% and the 2% barium sulphate phantom give a HU of -955 and -920 respectively. This is somewhat close to the anticipated -1000 of air. Both the areas of water in the phantoms give a HU value of -25, which of water is normally expected to be 0.

The HU of the 1% barium sulphate as determined by RadiAnt is 150 and the phantom of 2% barium sulphate has a HU of 300. These values are too high to be representing real brain tissue.

5.5. CLINICAL VALIDATION

To conclude on the validation and to gain more insight into a clinical opinion on the phantoms, the scans were evaluated by a radiologist and a neuroradiologist.

The scans of both the 1% and 2% barium sulphate phantoms were evaluated by Dr T.P.W. de Rooij and Dr R.E. Hagenbeek, two radiologists from Haaglanden Medical Centre in The Hague, specialized in neuroradiology. They provided a brief evaluation of the models.

About the 1% model, they concluded it was a very decent model. The overall remark was that the ventricles were too much to the dorsal side of the brain, meaning that the ventricles are positioned too much to the back of the brain. The lateral ventricles were considered to be on the bigger range than desired and also too much to the dorsal side, together with the rest of the interconnected system.

About the 2% model, not much feedback was given as it was concluded that this phantom was far from reality with quite a few artefacts.

6. DISCUSSION

The goal of this study was to develop an anthropomorphic brain phantom that contains the hollow space of the ventricles of the brain. The important criteria for this development of the phantom were: a realistic representation of the ventricles, suitability for X-ray/CT imaging and that the phantom can be developed using simple production principles to allow for 'home-made' fabrication.

To reach this goal, first, an extensive and structured brainstorm session was done to find possible design ideas. After the concepts were made, a 3D shape of the brain was developed into 3D printable moulds for the production of the phantom. 3D models of the ventricles were developed to go with the moulds to make the hollow space in the model. The shapes of the shape of the ventricles were adjusted in order to make it suitable for 3D printing and the desired phantom development. PVA as TMM for the production of the phantom was selected from the literature based on the desired properties and the ease of production. The use of a 3D printed soluble ventricle from PVA was chosen for the production of the phantom. After optimization and adjustments for the desired optical characteristics in CT scanning, prototypes were developed and assessed in their quality and imaging characteristics. Altogether the use of soluble PVA for the development of a hollow space in a casted model is a novelty in this field of application and shows promising results for the future.

6.1.1. INTERPRETATION OF THE RESULTS

This study was performed to find an acceptable production principle for a brain phantom containing hollow spaces. For this, different production principles were considered to find one concept that worked. Even though the use of the Harris profile is a way to assess the concepts in an objective way, it is still in some way subjective as some requirements don't allow for a 100% objective rating.

For the evaluation of the developed prototypes, DICOM viewers were used assessing the models. This assessment was only done based on expectations and compared with images that were found online. This part of the study could not be performed in-depth due to the inexperience of the observer. It was only briefly evaluated by a radiologist and a neuroradiologist, but the majority of the results are based on knowledge from literature and expectations. Though it still provided some interesting observations and results.

6.1.2. QUALITY OF THE MODEL

The development of the brain phantom with the designed moulds is considered to have a good and realistic shape. Though the overall volume of the brain model might shrink over time due to the addition of coolant during production.

Assessing the position of the ventricles relative to the brain, it is considered to be in great control when the PVA solution is not poured into the mould at a too hot temperature, but as cool as possible. The ventricles stay in place as they were originally modelled which means that there is great control over their position.

Quality of the shape of the ventricles can, however, be improved. For the phantom development, the shapes of the ventricles were slightly adjusted, resulting in a not 100% anatomically correct ventricle shape in the model. Also in the developed prototypes, the two lateral ventricles seem to have fused together along the longitudinal fissure, the split line between hemispheres of the brain.

They are supposed to be two distinct ventricles, separated by a thin membrane of tissue material. The third ventricle in the prototypes were slightly enlarged. This was already done during the development of the 3D model of the ventricles, in order to make it suitable for 3D printing and to ensure the removal of the material. Yet in the scans, it appears to be even larger, which might be due to the removal of the 3D printed material and evaluating the hollow spaces by touching the insides of the model.

The segmented 3D shapes out of the designed prototypes showed to be very accurately resembling the initially modelled ventricle structure and shape. Regarding the surface finish, it can be seen that the shapes have a very rough surface, but the overall shape is correct. This rough surface finish is partially due to the segmentation process and the threshold settings. Also the presence of support material during 3D printing of the ventricles has left its marks on the surface as it was not completely removable. A solution to this might be to dip the 3D printed ventricle in water, after the majority of the support material is removed by hand, and let is set and dry again. This might cause the small lose strings of support material to dissolve, leaving a smooth surface. Yet this is just a principle of thought and needs further investigation if it works as expected.

The scans showed bright spots around the edges and around the ventricles, especially at the bottom of the mould due to the sedimentation of the barium sulphate. There already had been a great improvement regarding this when the PVA solution was cooled off below 10°C before pouring the solution into the mould, but still, these spots are undesired in a brain phantom. It might be possible to decrease this sedimentation by even cooling the solution down more, just before it solidifies, before pouring it into the mould.

One of the biggest errors of the developed prototypes it that the ventricles got air stuck inside. In an attempt to solve this, a kind of membrane was made around the phantoms made from a plastic bag. This, unfortunately, did not result in the desired outcome as there was still air trapped and the scans did not improve. There has to be another solution to make sure the ventricles are completely filled with fluid to have a useful brain model. A membrane or other method to do that should be explored.

6.1.3. PRACTICAL ASPECTS

In the end, the tests with samples with different concentrations barium sulphate are not reliable enough to draw any conclusions on. A different test should be set up with more samples to really asses the radiodensity of the samples with different concentrations of barium sulphate. The errors in the current samples might be due to manual mistakes in the measurements of barium sulphate as small fluctuations in measurements will have a big influence on concentration when working with small volumes.

Concerning the right contrast characteristics, more research is needed. The right amount of barium sulphate concentration to match the desired HU of the TMM was not found. The samples that were made to assess this turned out to be unfeasible for the determination of the right contrast resolution in the images as the calculated values were too high and exceeded realistic expectations. During the preparation of the samples with different concentrations barium sulphate, very small amounts of materials where used. Because of this, small deviations in measurements can have a large impact on the eventual outcome. Also in the samples, a small part of the barium sulphate sedimented to the bottom, this might have also influenced the results of the different barium sulphate evaluations.

The concentration of barium sulphate for the imaging of the brain phantom should be further evaluated. Based on findings in literature and the findings with the scans in this study it can be said that the concentration should be somewhere between 0.5% and 1,5%. However before this can be implemented, more research is needed. Also towards the influence on the mechanical properties of the material. Although it can be expected that the very small concentrations that were used should only have a small impact if any at all.

During transport to Philips for testing, the phantoms sometimes spend a day outside a refrigerator. There is no knowledge yet about if and how this influences the phantom characteristics and stability. For this research, it was just neglected but it should be further investigated how this would affect the phantom.

6.1.4. LIMITATIONS OF THIS STUDY

During the brainstorm session, other interesting production principles for the development of a brain phantom containing ventricles were identified, that were excluded during the brainstorming phase of this project as they were beyond the feasibility in the time frame and possibilities of this project.

Currently casting is the preferred method of phantom fabrication. However, technology in 3D printing is improving at a fast rate. Although the printing of soft tissue is not the main area of interest for 3D printing, it might evolve at some point. Developments in other areas of 3D printing could result in the ability to print soft tissues as well. Full-sized 3D printed phantoms can have great beneficial value as internal structures can be very easily included.

About the mechanical properties of the brain phantom, no conclusions could be drawn during this study, due to lack of usable data about the properties of brain tissue characteristics and comparison material. The concentration of PVA as TMM was only based on findings literature and could not be evaluated and confirmed in this study. So it is unclear to say if the used concentration of 6% PVA for the TMM is correct as there are differences in preparation, types and brands of PVA that is used and these researches are conducted by different people, thereby inter-operator differences are possible.

Furthermore, many of the researches looking into the mechanical properties of brain tissue did not only look at human brains but also porcine brain was examined. These are considered to be highly similar to human brain tissue. Additionally, data about the brains were usually collected ex-vivo which influences the properties of the tissue.

6.1.5. RECOMMENDATIONS FOR FURTHER RESEARCH

Regarding the development of phantoms from PVA with the FTC, there are a few aspects that need further investigation on their influence on the properties and characteristics of the phantom. There are many variables in the freezing aspect that have a lot of unknown influences on the material properties. Such influences are the freezing temperature and freezing time in relation to the amount of PVA.

For the development of the models in this study, coolant was used in order to reduce the expansion during freezing which might cause the mould to break. During this study, a small test was already set up to get an indication of the influence of coolant on the phantom, but for further development, this should be deeper investigated.

With 3D slicer, an open source software platform for medical image informatics, image processing, and three-dimensional visualization, CT images can be transformed into three-dimensional shapes. This can be done for the ventricle with the segmentation tool, of which the digital 3D shape can be saved as an STL file for 3D printing. This way, customizable ventricles are possible for the development of a patient-specific brain phantom. Though this should first be further investigated before it can be applied but has great potential for the future.

Furthermore, it would be very interesting to look at the incorporation of different brain tumours in the model. As TMM PVA can be very easily adjusted to the desired properties by using different concentrations and FTC's so incorporating the desired characteristics of brain tumours would offer a great area of research.

Altogether the use of soluble PVA for the development of a hollow space in a casted model is a novelty in this field of application. It is a very promising approach and this research serves as a proof of concept for further development. This method can also be used in a wider area when hollow spaces are required in a model.

7. CONCLUSION

The goal of this study was to develop an anthropomorphic brain phantom containing the ventricles of the brain, with the correct mechanical and optical characteristics. An addition to this goal was to use TMMs and production principles that allowed simple 'homemade' phantom fabrication to make the design affordable and accessible for researchers, as commercial phantoms are rather expensive.

The goal was divided into two subgoals which will be '*Evaluate different production principles and materials to produce a hollow space of the ventricles in a brain model*' and '*Evaluate the models by assessing the X-ray characteristics of the material to validate for X-ray/CT use*'. '

Regarding the first subgoal, de design of the brain phantom containing a hollow space in the shape of the ventricles, it can be concluded that creating of such a phantom can be considered achieved. The use of soluble PVA printing is a very promising fabrication technique to have a phantom created in one part. Images show the ventricles are clearly visible in the images and are considered to be in the right and desired position. Although at this point this concept is still just a proof of concept as the CT images clearly showed the ventricular shapes, there is a lot that can be improved in order to increase the quality of the models.

The second subgoal can be concluded to be less achieved. The used concentrations of barium sulphate in the production of the phantoms did not match the desired optical results in the obtained CT scans yet it did show potential but just has to be used at different concentrations.

Altogether the use of soluble PVA for the development of a hollow space in a casted model is a novelty in this field of application. The overall evaluation of the prototypes has shown that this technique is promising for the development of a brain phantom, using PVA and 'homemade' fabrication techniques. This makes the design affordable and easy to adjust to patient-specific cases as personalized models can be made.

There is still a lot to be further developed, yet this research serves as proof of concept that soluble PVA can be used to develop a hollow space representing the ventricles in a brain phantom. The use of PVA as TMM and 3D printed PVA for dissolving the ventricles shows promising results for the future.

REFERENCES

[1] N. Abolhassani, R. Patel, and M. Moallem, "Needle insertion into soft tissue: A survey," *Med. Eng. Phys.*, vol. 29, no. 4, pp. 413–431, May 2007.

[2] J. P. Holland, L. Waugh, A. Horgan, V. Paleri, and D. J. Deehan, "Cadaveric Hands-on Training for Surgical Specialties: Is This Back to the Future for Surgical Skills Development?," *J. Surg. Educ.*, vol. 68, no. 2, pp. 110–116, Mar. 2011.

[3] J. J. H. Leong *et al.*, "Validation of orthopaedic bench models for trauma surgery," *J. Bone Joint Surg. Br.*, vol. 90–B, no. 7, pp. 958–965, Jul. 2008.

[4] V. Waran *et al.*, "Neurosurgical Endoscopic Training via a Realistic 3-Dimensional Model With Pathology," *Simul. Healthc. J. Soc. Simul. Healthc.*, vol. 10, no. 1, pp. 43–48, Feb. 2015.

[5] G. Breimer, F. Haji, … V. B.-O., and undefined 2016, "Simulation-based education for endoscopic third ventriculostomy: a comparison between virtual and physical training models," *academic.oup.com*.

[6] T. Lange, D. Indelicato, J. R.-S. oncology clinics of North, and undefined 2000, "Virtual reality in surgical training," *Elsevier*.

[7] P. Li, Z. Yang, and S. Jiang, "Materials Science & Engineering C Tissue mimicking materials in image-guided needle-based interventions : A review," *Mater. Sci. Eng. C*, vol. 93, no. September, pp. 1116–1131, 2018.

[8] S. J.-S. Chen, P. Hellier, J.-Y. Gauvrit, M. Marchal, X. Morandi, and D. L. Collins, "An Anthropomorphic Polyvinyl Alcohol Triple-Modality Brain Phantom Based on Colin27," Springer, Berlin, Heidelberg, 2010, pp. 92–100.

[9] J. L. Hellier, *The Brain, the Nervous System, and Their Diseases [3 volumes]*. 2014.

[10] J. E. (John E. Hall and A. C. Guyton, *Guyton and Hall textbook of medical physiology*. Saunders Elsevier, 2011.

[11] J. S. Allen, H. Damasio, and T. J. Grabowski, "Normal neuroanatomical variation in the human brain: An MRI-volumetric study," *Am. J. Phys. Anthropol.*, vol. 118, no. 4, pp. 341–358, Aug. 2002.

[12] K. L. Bigos, A. R. Hariri, and D. R. Weinberger, Eds., *Neuroimaging Genetics*. Oxford University Press, 2016.

[13] F. A. C. Azevedo *et al.*, "Equal numbers of neuronal and nonneuronal cells make the human brain an isometrically scaled-up primate brain," *J. Comp. Neurol.*, vol. 513, no. 5, pp. 532–541, Apr. 2009.

[14] M. J. T. FitzGerald, G. Gruener, and E. Mtui, *Clinical neuroanatomy and neuroscience*. Saunders/Elsevier, 2012.

[15] S. G. Waxman, *Correlative neuroanatomy*. Appleton & Lange, 1996.

[16] E. N. Marieb and K. Hoehn, *Human anatomy & physiology*, 9th ed. Boston: Pearson, 2013.

[17] T. Salgueiro, “Robot assisted needle interventions for brain surgery,” no. December, 2014.

[18] C. W. Schmidt, “CT scans: balancing health risks and medical benefits.,” *Environ. Health Perspect.*, vol. 120, no. 3, pp. A118-21, Mar. 2012.

[19] K. R. Fink and J. R. Fink, “Imaging of brain metastases.,” *Surg. Neurol. Int.*, vol. 4, no. Suppl 4, pp. S209-19, 2013.

[20] K.-D. Merboldt, W. Hanicke, and J. Frahm, “Self-diffusion NMR imaging using stimulated echoes,” *J. Magn. Reson.*, vol. 64, no. 3, pp. 479–486, Oct. 1985.

[21] M. Mascalchi, M. Filippi, R. Floris, C. Fonda, R. Gasparotti, and N. Villari, “Diffusion-weighted MR of the brain: methodology and clinical application.,” *Radiol. Med.*, vol. 109, no. 3, pp. 155–97, Mar. 2005.

[22] R. N. Sener, “Diffusion MRI: apparent diffusion coefficient (ADC) values in the normal brain and a classification of brain disorders based on ADC values,” *Comput. Med. Imaging Graph.*, vol. 25, no. 4, pp. 299–326, Jul. 2001.

[23] T. Ebisu *et al.*, “Discrimination of brain abscess from necrotic or cystic tumors by diffusion-weighted echo planar imaging,” *Magn. Reson. Imaging*, vol. 14, no. 9, pp. 1113–1116, Jan. 1996.

[24] S. Lu, D. Ahn, G. Johnson, and S. Cha, “Peritumoral diffusion tensor imaging of high-grade gliomas and metastatic brain tumors.,” *AJNR. Am. J. Neuroradiol.*, vol. 24, no. 5, pp. 937–41, May 2003.

[25] M. O. Irfanoglu, C. G. Koay, S. Pajevic, R. Machiraju, and P. J. Basser, “Diffusion Tensor Field Registration in the Presence of Uncertainty,” Springer, Berlin, Heidelberg, 2009, pp. 181–189.

[26] N. Bulakbasi, M. Kocaoglu, F. Ors, C. Tayfun, and T. Uçöz, “Combination of single-voxel proton MR spectroscopy and apparent diffusion coefficient calculation in the evaluation of common brain tumors.,” *AJNR. Am. J. Neuroradiol.*, vol. 24, no. 2, pp. 225–33, Feb. 2003.

[27] L. E. Ginsberg, G. N. Fuller, M. Hashmi, N. E. Leeds, and D. F. Schomer, “The Significance of Lack of MR Contrast Enhancement of Supratentorial Brain Tumors in Adults: Histopathological Evaluation of a Series,” *Surg. Neurol.*, vol. 49, no. 4, pp. 436–440, Apr. 1998.

[28] A. Valencia, B. Blas, and J. H. Ortega, “Modeling of Brain Shift Phenomenon for Different Craniotomies and Solid Models,” vol. 2012, 2012.

[29] U. Mezger, C. Jendrewski, and M. Bartels, “Navigation in surgery,” *Langenbeck’s Arch. Surg.*, vol. 398, no. 4, pp. 501–514, Apr. 2013.

[30] I. J. Gerard, M. Kersten-Oertel, K. Petrecca, D. Sirhan, J. A. Hall, and D. L. Collins, “Brain shift in neuronavigation of brain tumors: A review,” *Med. Image Anal.*, vol. 35, pp. 403–420, Jan. 2017.

[31] T. Pringsheim, K. Fiest, and N. Jette, “The international incidence and prevalence of neurologic conditions: how common are they?,” *Neurology*, vol. 83, no. 18, pp. 1661–4, Oct. 2014.

[32] M. C. Dewan *et al.*, “Global neurosurgery: the current capacity and deficit in the provision of

essential neurosurgical care. Executive Summary of the Global Neurosurgery Initiative at the Program in Global Surgery and Social Change," *J. Neurosurg.*, pp. 1–10, Apr. 2018.

[33] T. Munch, K. Rostgaard, M. Rasmussen, J. W.- Brain, and undefined 2012, "Familial aggregation of congenital hydrocephalus in a nationwide cohort," *academic.oup.com*.

[34] S. Sunder and R. Prasad, "Minimally Invasive Endoscopic Brain and Spine Surgery," *Apollo Med.*, vol. 3, no. 4, pp. 399–403, Dec. 2006.

[35] A. Neubauer, S. W.- Neurosurgery, and undefined 2013, "Virtual endoscopy in neurosurgery: a review," *academic.oup.com*.

[36] M. Randazzo, J. Pisapia, … N. S.-S. neurology, and undefined 2016, "3D printing in neurosurgery: a systematic review," *ncbi.nlm.nih.gov*.

[37] Z. Tan, D. Dini, F. y Baena, A. F.-M. & Design, and undefined 2018, "Composite hydrogel: A high fidelity soft tissue mimic for surgery," *Elsevier*.

[38] A. Goriely *et al.*, "Mechanics of the brain: perspectives, challenges, and opportunities," *Biomech. Model. Mechanobiol.*, vol. 14, no. 5, pp. 931–965, Oct. 2015.

[39] B. Rashid, M. Destrade, and M. D. Gilchrist, "Mechanical characterization of brain tissue in simple shear at dynamic strain rates," *J. Mech. Behav. Biomed. Mater.*, vol. 28, pp. 71–85, 2013.

[40] M. Hrapko, J. Van Dommelen, … G. P.-, and undefined 2006, "The mechanical behaviour of brain tissue: large strain response and constitutive modelling," *content.iospress.com*.

[41] A. Tamura, S. Hayashi, K. Nagayama, and A. T. Matsumoto, "Mechanical Characterization of Brain Tissue in High-Rate Extension," *J. Biomech. Sci. Eng.*, vol. 3, no. 2, pp. 263–274, 2008.

[42] A. Tamura, S. Hayashi, … K. N.-J. of, and undefined 2008, "Mechanical characterization of brain tissue in high-rate extension," *jstage.jst.go.jp*.

[43] S. Cheng, L. B.-J. of biomechanics, and undefined 2007, "Unconfined compression of white matter," *Elsevier*.

[44] S. Budday, R. Nay, R. de Rooij, … P. S.-… of the mechanical, and undefined 2015, "Mechanical properties of gray and white matter brain tissue by indentation," *Elsevier*.

[45] K. Miller, A. Wittek, and G. Joldes, "Biomechanical Modeling of the Brain for Computer-Assisted Neurosurgery," 2011, pp. 111–136.

[46] G. Franceschini, D. Bigoni, … P. R.-J. of the M., and undefined 2006, "Brain tissue deforms similarly to filled elastomers and follows consolidation theory," *Elsevier*.

[47] A. E. Forte, S. Galvan, F. Manieri, F. Rodriguez y Baena, and D. Dini, "A composite hydrogel for brain tissue phantoms," *Mater. Des.*, vol. 112, pp. 227–238, Dec. 2016.

[48] Y. Jamin *et al.*, "Exploring the biomechanical properties of brain malignancies and their pathologic determinants in vivo with magnetic resonance elastography," *Cancer Res.*, vol. 75, no. 7, pp. 1216–1224, 2015.

[49] A. W. Toga and J. C. Mazziotta, *Brain mapping : the methods*. Academic Press, 2002.

[50] R. Bibb, D. Eggbeer, and A. Paterson, *Medical modelling : the application of advanced design and rapid prototyping techniques in medicine*. .

[51] K. Pal, A. K. Banthia, and D. K. Majumdar, "Polymeric Hydrogels: Characterization and Biomedical Applications," *Des. Monomers Polym.*, vol. 12, no. 3, pp. 197–220, Jan. 2009.

[52] W. Callister and D. Rethwisch, *Materials science and engineering: an introduction*. 2007.

[53] J. Maitra, V. S.-A. J. P. Sci, and undefined 2014, "Cross-linking in hydrogels-a review," *pdfs.semanticscholar.org*.

[54] K. J. M. Surry, H. J. B. Austin, A. Fenster, and T. M. Peters, "Poly(vinyl alcohol) cryogel phantoms for use in ultrasound and MR imaging," *Phys. Med. Biol.*, vol. 49, no. 24, pp. 5529–5546, Dec. 2004.

[55] Y. Cao, G. Li, X. Zhang, and Y. Liu, "Tissue-mimicking materials for elastography phantoms : A review," *Extrem. Mech. Lett.*, vol. 17, pp. 62–70, 2017.

[56] M. A. O. C. Uljat, D. A. G. Oldenberg, P. R. T. Ewari, and R. A. S. S. Ingh, "A review of tissue substitutes for ultrasound imaging m," vol. 36, no. 6, pp. 861–873, 2010.

[57] J. Kuß *et al.*, "A head phantom prototype to verify subdural electrode localization tools in epilepsy surgery," *Neuroimage*, vol. 54, no. SUPPL. 1, pp. S256–S262, Jan. 2011.

[58] A. Hellerbach, V. Schuster, A. Jansen, and J. Sommer, "MRI Phantoms – Are There Alternatives to Agar?," *PLoS One*, vol. 8, no. 8, p. e70343, Aug. 2013.

[59] S. J.-S. Chen *et al.*, "An anthropomorphic polyvinyl alcohol brain phantom based on Colin27 for use in multimodal imaging," *Med. Phys.*, vol. 39, no. 1, pp. 554–561, Jan. 2012.

[60] C. P. Sales *et al.*, "Evaluation of different magnetic resonance imaging contrast materials to be used as dummy markers in image-guided brachytherapy for gynecologic malignancies.," *Radiol. Bras.*, vol. 49, no. 3, pp. 165–9, 2016.

[61] M. O. Culjat, D. Goldenberg, P. Tewari, and R. S. Singh, "A review of tissue substitutes for ultrasound imaging," *Ultrasound Med. Biol.*, vol. 36, no. 6, pp. 861–873, 2010.

[62] M. Lazebnik, E. L. Madsen, and G. R. Frank, "Physics in Medicine & Biology Tissue-mimicking phantom materials for narrowband and ultrawideband microwave applications Tissue-mimicking phantom materials for narrowband and ultrawideband microwave applications," 2005.

[63] I. Reinertsen and L. Collins, "A realistic phantom for brain-shift simulations A realistic phantom for brain-shift simulations," no. October, pp. 1–8, 2006.

[64] R. K. Chen and A. J. Shih, "Multi-modality gellan gum-based tissue-mimicking phantom with targeted mechanical, electrical, and thermal properties," *Phys. Med. Biol.*, vol. 58, no. 16, pp. 5511–5525, Aug. 2013.

[65] E. D. Seleþchi and O. G. Duliu, “IMAGE PROCESSING AND DATA ANALYSIS IN COMPUTED TOMOGRAPHY.”

[66] “Comparison of Various Low Hounsfield-Unit-Value Barium Sulphate Oral Contrast Agents for Abdominal CT: From VOLUMEN to READI-CAT.” [Online]. Available: http://archive.rsna.org/2007/5014305.html. [Accessed: 09-Apr-2019].

APPENDIX

APPENDIX A – BRAIN AND VENTRICLE DOWNLOADS

Brain download: https://sketchfab.com/models/735ca31a3b22433281e6fa9606792faa?ref=related

Ventricles:https://sketchfab.com/models/35e035e2065a431b9476ecdc5c81f144

APPENDIX B – MOULD AND VENTRICLE FABRICATION AND PREPARATION

BRAIN

The mould for the brain phantom was based on a predeveloped, polygonal surface mesh, digital brain model. This 3D model was obtained from Sketchfab and used to create the different mould designs from. This mesh shape was used to subtract from a rectangular shape, creating a 'negative' shape of the brain in a square shape. This process is visualized in the figure below. Starting with the positive brain shape, going to a square with a negative brain shape.

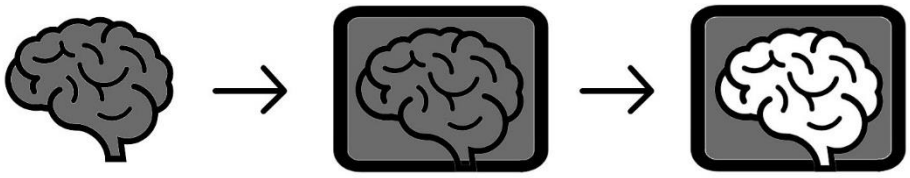

Two moulds were developed in Rhino. Rhinoceros is a commercial 3D computer graphics and computer-aided design application software developed by Robert McNeel & Associate. For describing the fabrication and preparation only one mould will be shown as the process for both the moulds was identical.

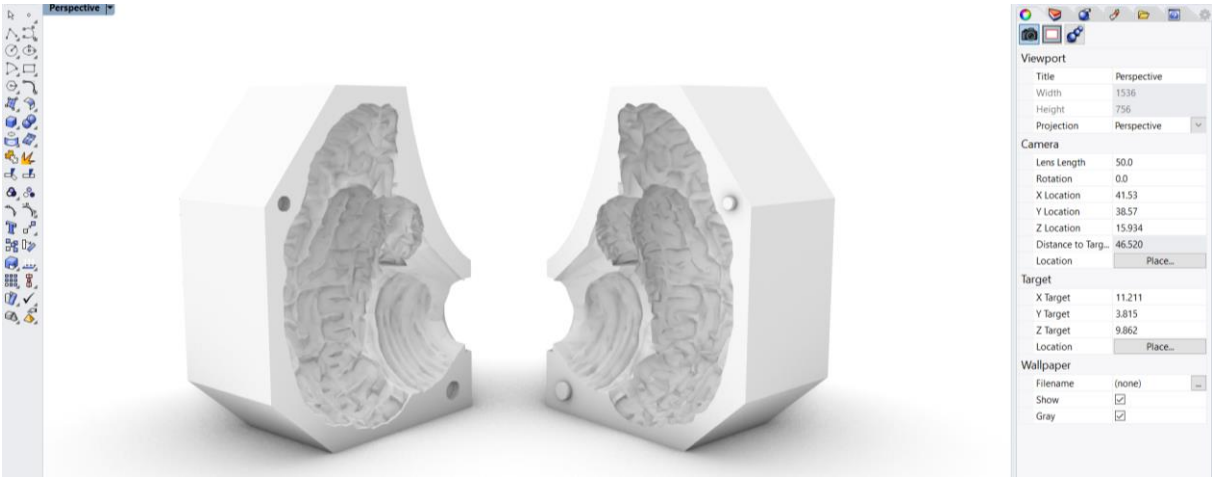

After the moulds were designed they were saved as .STL files for 3D printing. Preparation for printing with the Ultimaker was done with Cura, an open source 3D printer slicing application.
Settings like printing speed and infill density where determined. The moulds were printed in PLA.

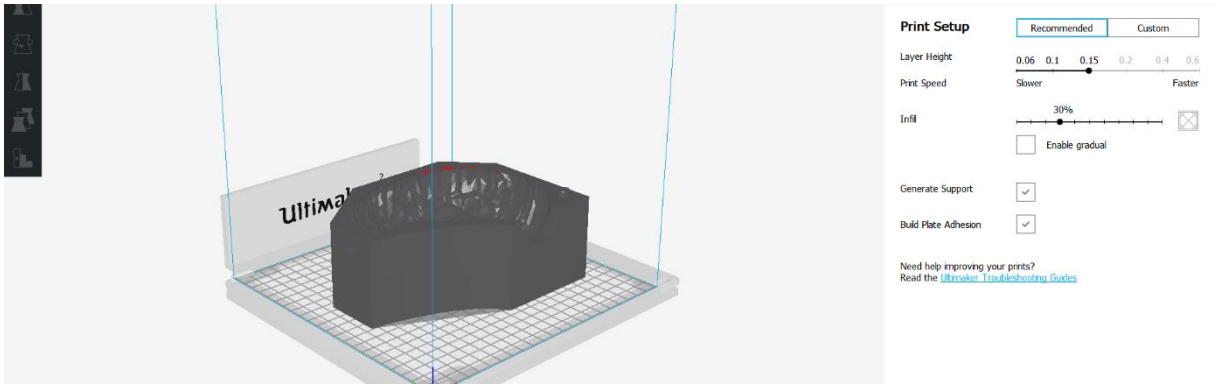

The image below shows the 3D printed mould halves of mould A. After prints were done, they were coated using XTC-3D Smooth-On Coating in order to make the mould water tight so no TMM would leak out between the layers.

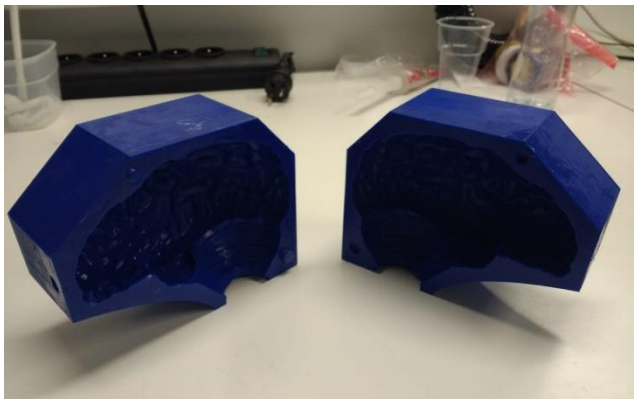

VENTRICLE

For the printing of the ventricles, an Ultimaker 3 Extended was used. This printer can print two materials, the first nozzle printing PLA, the second nozzle printing the support from PVA. For the ventricles, both the 'body' and the support were both printed from PVA. Different positions and angles of the ventricles on the building plate were evaluated for minimizing support material, to ensure easier removal of the support.

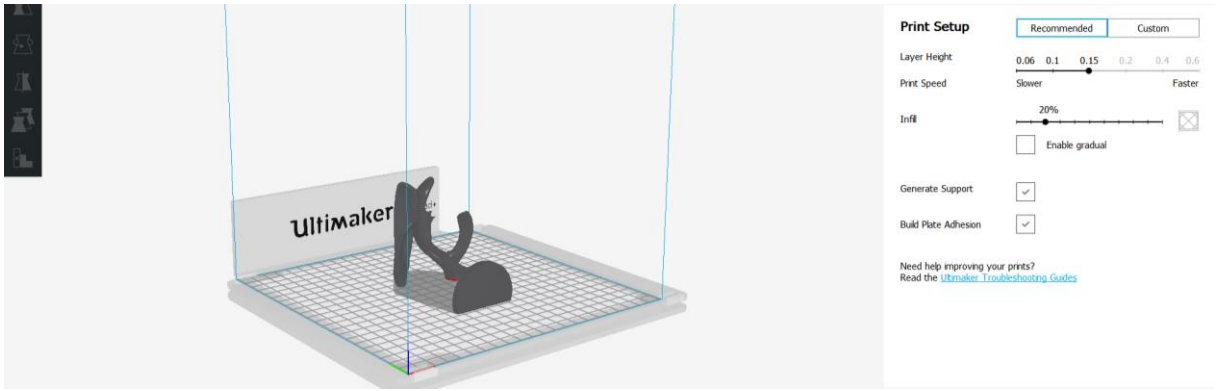

Support

Also, different types of support structures, lines, triangles, were assessed to find that lines are the easiest to remove, at a support density of 30% to assure support but easily removed. After printing this support material had to be removed by using a small cutting device. The images below show the different support structures and ventricles with the support removed, side and back view

PVA Solution - For Brain Phantom

Polyvinyl alcohol (PVA) is a synthetic polymer synthesized from polyvinyl acetate through hydrolysis of the acetate group. PVA is the world's largest volume, synthetic and water-soluble polymer with a molecular weight ranging from 25,000 to 30,000. When a solution with PVA undergoes a period of freezing cycles and is let to set to slowly thaw to room temperature it is called a freeze-thaw cycle (FTC). During this process of FTC's, the liquid PVA solution forms into an elastic semi-opaque gel known as polyvinyl alcohol hydrogel

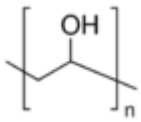

$$[-CH2CHOH-]n$$

Preparation of PVA Solution

For the development of a brain phantom, it was found that a concentration of 6% PVA with one FTC was similar to palping the surface of a live brain and had an elastic modulus of 4.6 kPa, which is in the range found from human tissue.

Additives
Contrast Enhancing

PVA is a soft TMM that does not offer enough contrast for the phantom to show the desired characteristics. Chemicals can be used to change this contrast. For CT imaging this contrast enhancing chemical is barium sulphate.

$$BaSO_4$$

Coolant

For the development of a phantom, it is recommended to use coolant in the solution to reduce expansion during the freeze cycles, which can result in breaking of the mould. The use of 40% coolant has shown to reduce the expansion and has only minimal effect on the mechanical properties of the material.

Procedure

The production of PVA requires a lot of attention in order to make a good solution. The behaviour of the polymer is tricky and the preparation requires patience. It is recommended to use an automatic stirrer as the solution requires to be stirred continuously to prevent burning of the PVA.

1. Preheat the desired amount of tap water to 88-90 °C, or just below boiling point, add to a glass beaker and place on the magnetic stirrer/hot plate).

2. Set hot plate temperature to 93 °C and have the magnetic stirrer stir as fast as possible (depending on the amount of solution). Recommended RPM is between 350-500.

3. Add the coolant to the glass beaker and let it heat up of a few minutes.

4. Slowly add in the PVA grains to the solution, while still constantly stirring.

5. Stir constantly until all the PVA grains are solved and the whole solution is clear. To speed up this process, the glass beaker can be wrapped in aluminium foil. This will keep the heat inside the solution and makes a more evenly distributed temperature throughout the solution.

6. When PVA is completely solved, barium sulphate can be added to the solution. Turn off the hot plate but have the magnetic stirrer continuing stirring and wait till the solution is completely cooled off before pouring it in the mould.

7. When the solution is cooled down as much as possible, pour it in the mould and place it in a freezer at -20°C for at least 24 hours (depending on the amount of solution). After this 24 hours, remove from the freezer and let thaw to room temperature.

(For a brain phantom at 6% PVA, one FTC was enough to mimic the brain tissue. If more FTC is required, remove the model from the freezer, let it thaw to room temperature. Then repeat the freezing process as many times as desired).

Storage

After the phantom is finished, store the model in a container filled with water in a refrigerator. It can be stored in the fridge for a couple of months. It is recommended to check on the phantom every once in a while to make sure no bacteria are growing on the model.

CAUTION! Never leave the hot plate/magnetic stirrer unattended.

CAUTION! Stir constantly with a magnetic stirrer and additionally stir with stick or spoon every once in a while to prevent burning. If the PVA does burn to the bottom of the glass beaker, make sure to clean it right away. Tip: empty the glass beaker and add water. Put on the hot plate and stir constantly until you can remove the burned PVA.

CAUTION! When the model is removed from the freezer too soon and the PVA did not have enough time to make enough connections, the model will not be stable and fall apart.

IMAGES OF THE PHANTOM DEVELOPMENT

The images below serve as an impression of the production of the phantoms. The PVA solution on the heating and stirring plate, the PLA ventricles and how the mould leaked when applying too little Vaseline on the edges of the moulds.

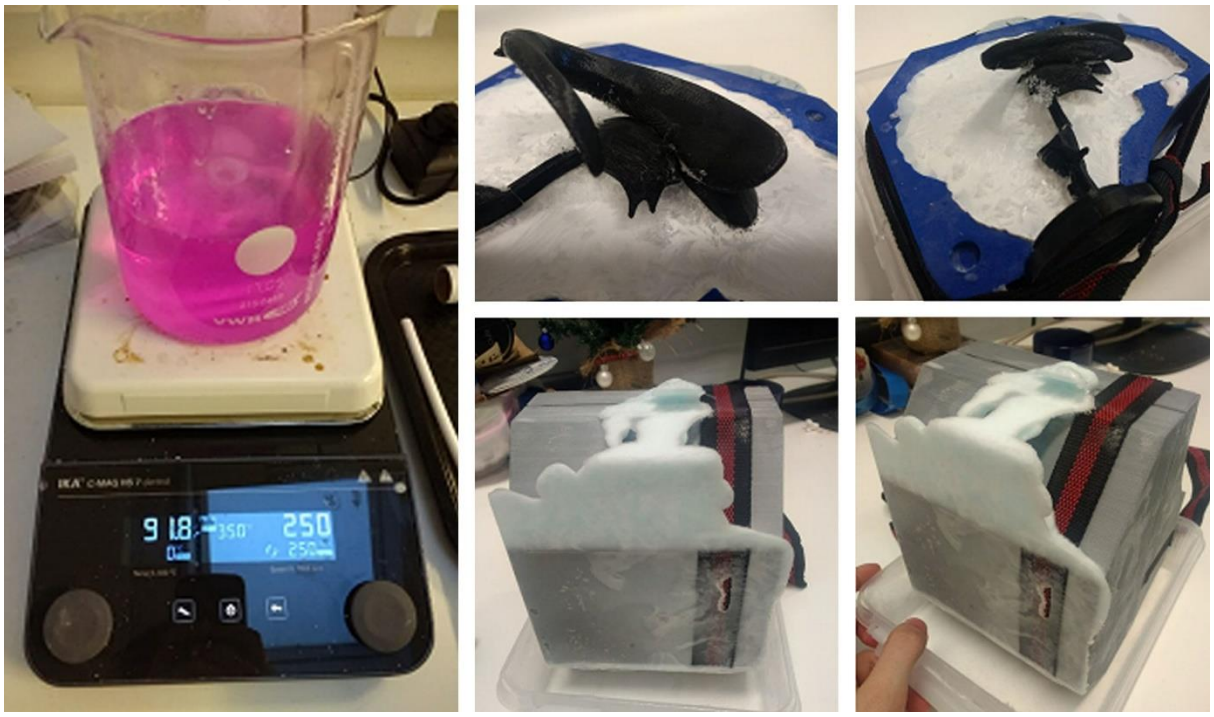

The images in the top right that are shown above, show the result first concept after freezing. Before freezing the ventricle shape as in the correct position, but due to the freezing process and the expanding of the PVA solution, the ventricles did not stay in the desired position, resulting in less accuracy and loss in control over the ventricle position.

With the brain model from concept 2, the PVA solution was cast in the model when it was still too hot, causing the PVA printed ventricle to dissolve and float around. Yet this still showed that the use of soluble PVA is promising to leave a hollow space in a model. The model was cut into slices as shown I the figure below. The ventricle shape was not recognisable anymore and the position was not accurate, yet it shows the hollow spaces.

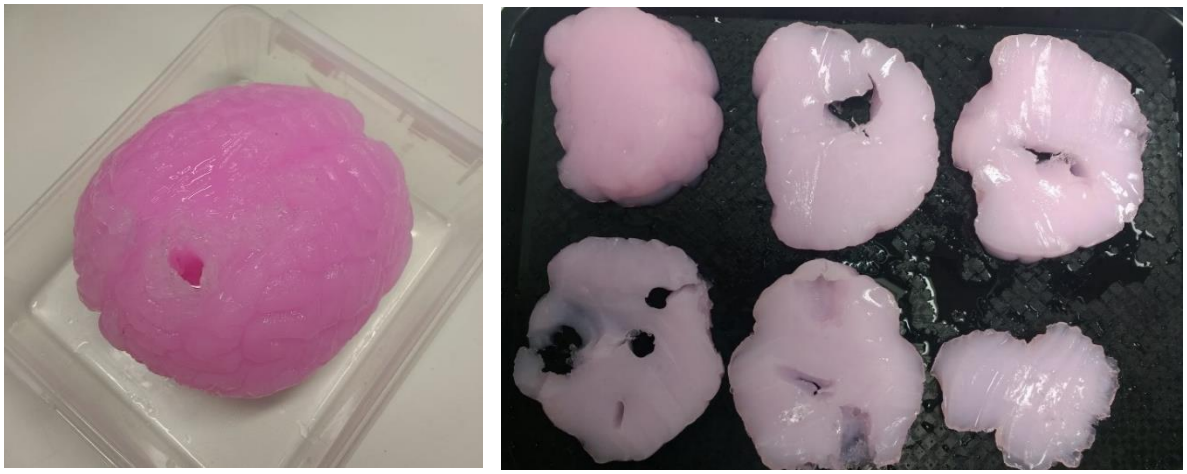

CONCENTRATIONS OF THE SOLUTION

For the prototypes of the brain phantom, two types were made. One with 1 % barium sulphate and one with 2% barium sulphate. For those solutions, the same base solution was made twice, after which the desired amount of barium sulphate was added.

For the brain phantom a complete volume 1.1 liter was needed (1100 ml).

6% mass percentage was used to create the solution, and 94% liquid. Of this liquid part is composed of 60% water and 40% coolant.

Percentages		Ingredient	Used volume
94%	60%	Water	660 ml
	40%	Coolant	440 ml
6%		PVA	70 gram

Phantom 1% barium sulphate: 11 gram was added to the total solution.
Phantom 2% barium sulphate: 22 gram was added to the total solution

APPENDIX D – DETERMINING HU VALUE

To be able to determine the right HU value of the samples with different barium sulphate concentrations, the image was analysed using ImageJ, an image processing program developed at the National Institutes of Health and the Laboratory for Optical and Computational Instrumentation. There is a linear relationship between the grey values of a CT image and the HU values. To determine the grey values, ImageJ was used to find the pixel values. This was done by selecting the area of interest and the program gave the mean, min and max value of that area, out of one of the slices of the provided CT scan. Slice I00145 was used as it was found that this slice best showed all the samples. To determine the values of the samples, first, the pixel values of air and water were determined, as the HU values of air and water, are known, see chapter 2 section 2.3.2. optical characteristics.

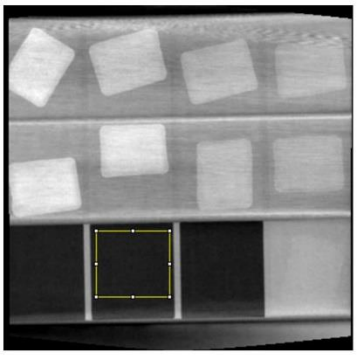

1) Area of air value

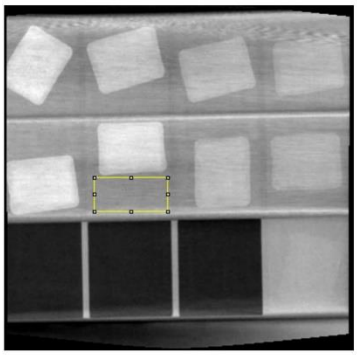

2) Water

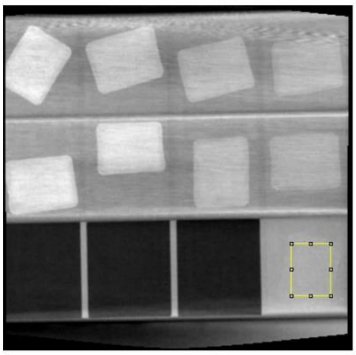

3) Sample with 0.5% BaSO4

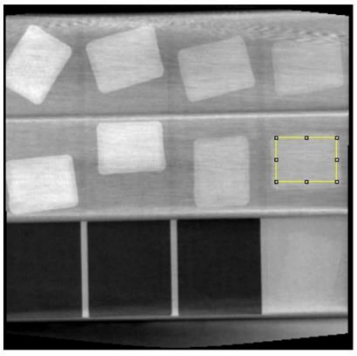

4) Sample with 1% BaSO4

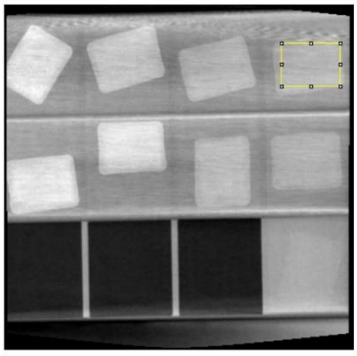

5) Sample with 1.5% BaSO4

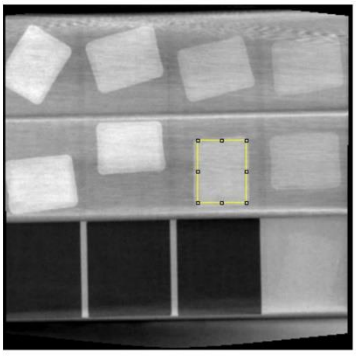

6) Sample with 2% BaSO4

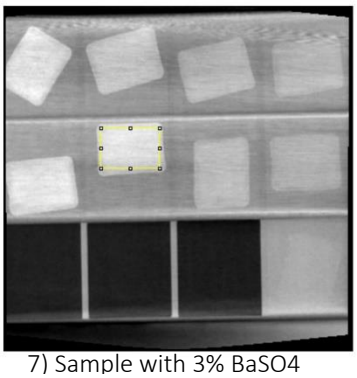

7) Sample with 3% BaSO4

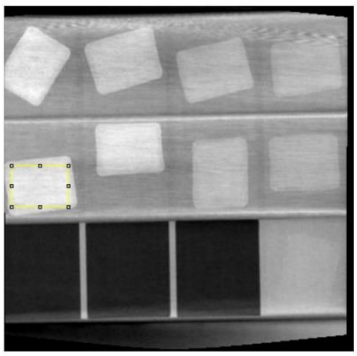

8) Sample with 4% BaSO4

The previous images show the areas of the air, water and different samples where the values where determined. These values were put into a table, from where the HU values can be determined. The first column of numbers in the table corresponds with the numbers of the images above.

Results

File Edit Font Results

	Area	Mean	Min	Max
1	1174.624	3327.982	2416	4222
2	603.626	16096.610	14205	20083
3	499.827	18766.007	17639	19997
4	646.043	19418.968	17737	21208
5	613.415	20012.420	17786	22345
6	734.956	20461.520	17877	22349
7	574.261	24552.871	20042	27139
8	568.959	25077.070	22245	27205

		Mean Value from ImageJ	Hounsfield Unit (HU)
1	Air	3327	-1000
2	Water	16096	0
3	Sample with 0.5% BaSO4	18766	209
4	Sample with 1% BaSO4	19419	260
5	Sample with 1.5% BaSO4	20012	306
6	Sample with 2% BaSO4	20462	340
7	Sample with 3% BaSO4	24553	662
8	Sample with 4% BaSO4	25077	703

Based on the measured values for air and water in ImageJ and the know HU for air and water, and the fact that is known that there is a linear relationship between the grey values and HU, the following equation was set up:

$HU(x)=0.0783x-1260$
with as x the mean value from ImageJ.

With this equation, the HU for the samples was calculated as can be found in the table above. The calculated HU via this method are exceeding realistic values yet it is not clear why this method does not provide the expected values.

APPENDIX E – FAILED MODELS

Throughout the project, there have been a few brain models that not turned out the way it was expected. Two of those models will be presented here.

FAILED MODEL 1


The figures above show the first model that was made with the new improved mould as described in chapter 4, and with the addition of barium sulphate to the PVA solution. This model was made with a different kind of PVA from Sigma Aldrich. After the FTC when the model was removed from the mould it immediately fell apart, as the images illustrate. Though it remains unclear why this exactly happened, it is thought to be due to the use of the different PVA which might have a different way to correctly produce the solution. Though this model still provided valuable information on the use of barium sulphate as it can be clearly seen that the barium sulphate sank to the bottom of the mould during the freezing process. To make sure this does not happen again, the PVA solution should be cooled off as much as possible before pouring it into the mould to minimize this sedimentation of barium sulphate.

FAILED MODEL 2

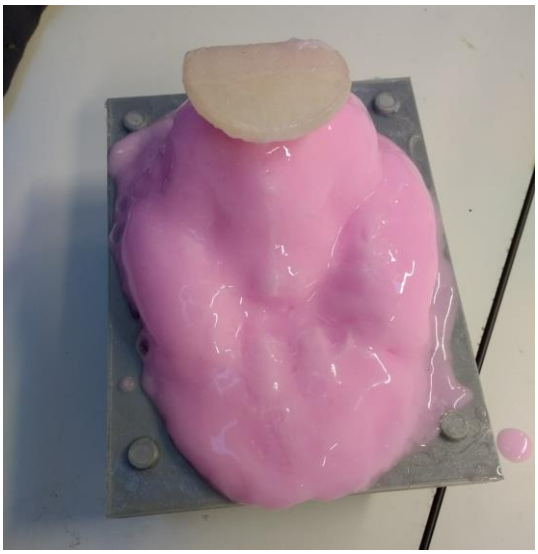
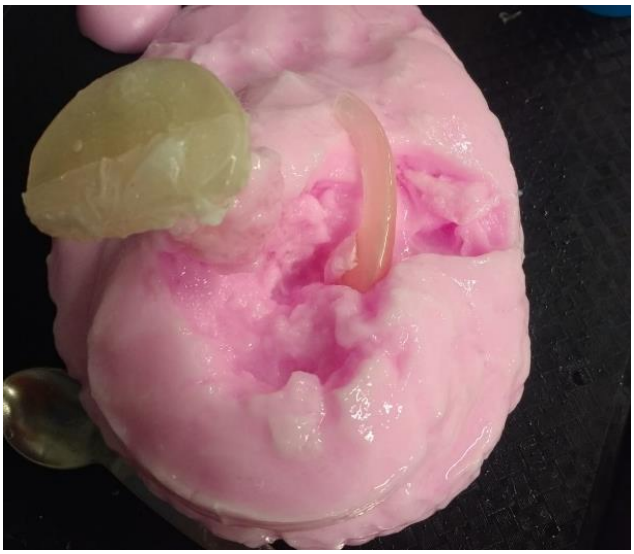

The images above show a new attempt, a new model with barium sulphate. For this model, the original Selvol™ PVA was used again. For this model, the knowledge about the barium sulphate from the previous failed model was taken into account for the production. After the preparation of the PVA solution with barium sulphate the solution was cooled down, first to room temperature and after to under 10 °C in a fridge and stirred every 10 minutes. This process took about an hour. When the solution was cooled down it was poured into the mould and put into the freezer. Though also this model fell apart immediately after removal from the mould, yet not as bad as the previous one. Also with this model, it remains unclear why this happened. It might be due to the removal from the freezer sooner than should.

APPENDIX F – SCANS BRAIN MODEL WITH MEMBRANE

After the first CT scan images of the developed brain phantoms, it was concluded that there was air present in the ventricles. A second attempt was done, yet this time the brain phantoms were put into plastic bags with water and the brains were put inside the container upside down, see figures below.

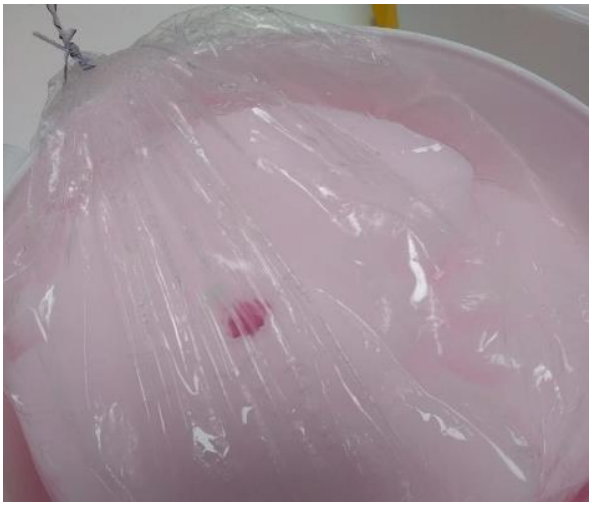

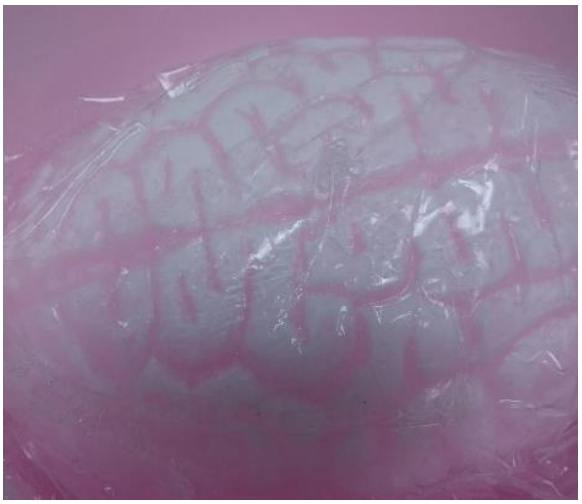

It was thought to use the plastic bags as a membrane around the brain to make sure the ventricles were filled with water. However, this idea did not work out the way it was planned and the new images show even more air in the scans. See images below.

Phantom 1%

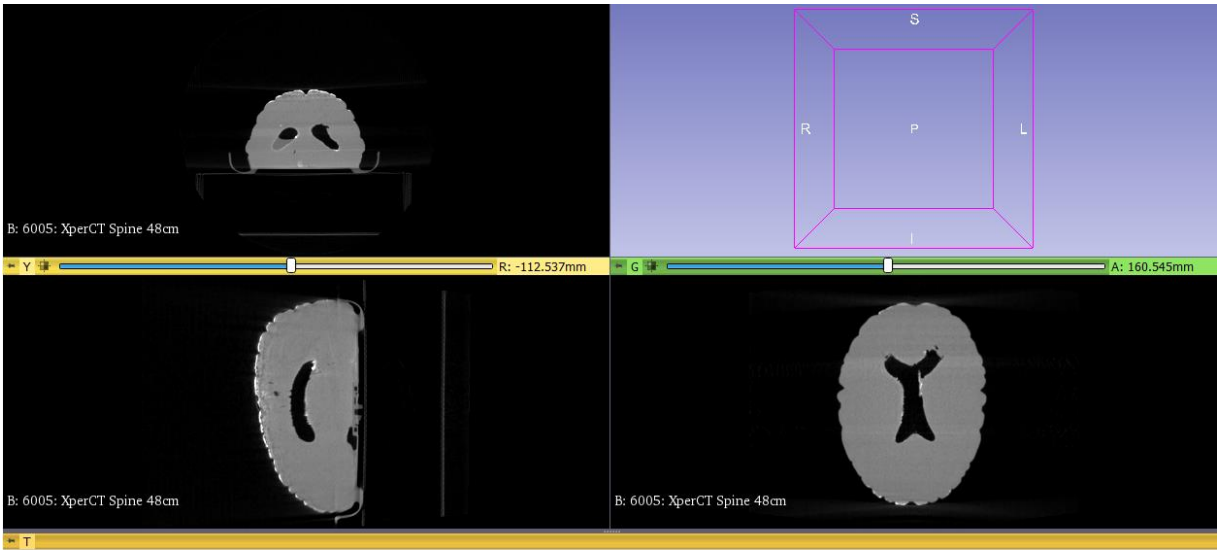

These images show the DICOM files viewed with 3D slicer. The ventricles show up black. The shape of the ventricles can clearly be seen. Only in the left top image, some grey can be seen where there is liquid in the ventricle.

Phantom 2%

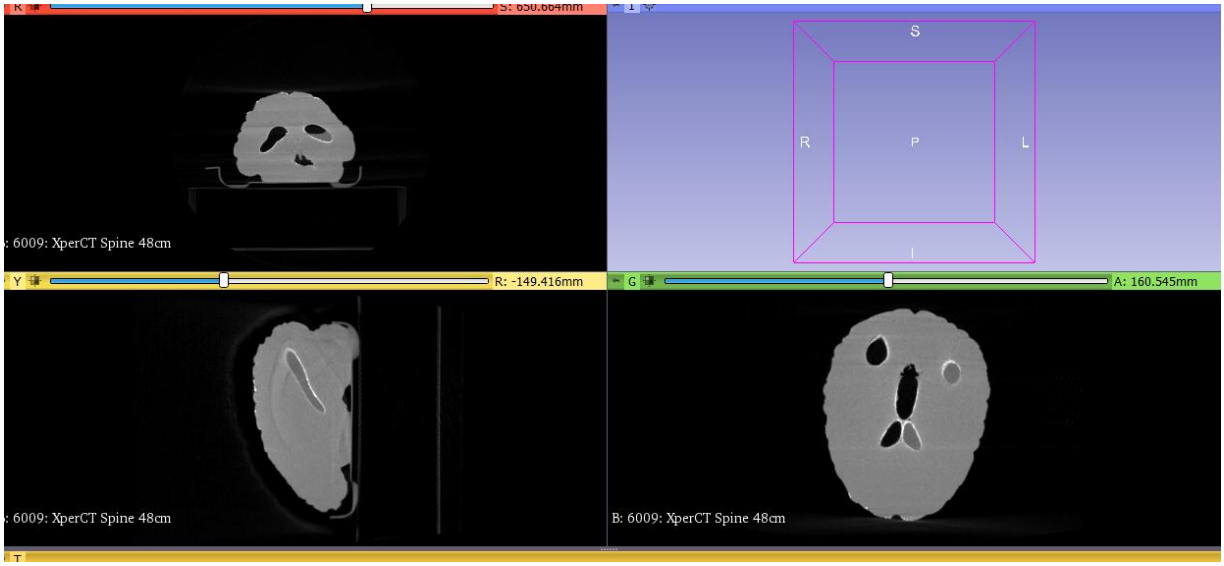

These images also show the ventricles to show up black, meaning that there is air inside. The right bottom images show only one of the ventricles contains water.

So the use of a plastic bag functioning as a membrane to make sure the ventricles are filled with water did not work out the way it was expected.